UNIVERSIDADE ESTADUAL DE CAMPINAS
FACULDADE DE ENGENHARIA QUÍMICA

ÁREA DE CONCENTRAÇÃO
DESENVOLVIMENTO DE PROCESSOS QUÍMICOS

Modelagem, Simulação e Análise de Reatores Contínuos Para a Hidrólise Enzimática de Bagaço de Cana

AUTOR: ARTURO GONZÁLEZ QUIROGA
ORIENTADOR: Prf. Dr. RUBENS MACIEL FILHO
COORIENTADOR: Prf. Dra. ALINE CARVALHO DA COSTA

Dissertação de Mestrado apresentada à Faculdade de Engenharia Química como parte dos requisitos exigidos para obtenção do título de Mestre em Engenharia Química

Campinas, São Paulo
Dezembro de 2009

FICHA CATALOGRÁFICA ELABORADA PELA
BIBLIOTECA DA ÁREA DE ENGENHARIA E ARQUITETURA - BAE - UNICAMP

G589m	González Quiroga, Arturo Modelagem, simulação e análise de reatores contínuos para a hidrólise enzimática de bagaço de cana / Arturo González Quiroga. --Campinas, SP: [s.n.], 2009. Orientadores: Rubens Maciel Filho, Aline Carvalho da Costa. Dissertação de Mestrado - Universidade Estadual de Campinas, Faculdade de Engenharia Química. 1. Hidrólise. 2. Fluidodinâmica. 3. Bagaço de cana. 4. Reatores químicos - Modelos matemáticos. I. Maciel Filho, Rubens. II. Costa, Aline Carvalho da. III. Universidade Estadual de Campinas. Faculdade de Engenharia Química. IV. Título.

Título em Inglês: Modeling, simulation and analyze of continuous reactors for enzymatic hydrolysis of sugar cane bagasse
Palavras-chave em Inglês: Hydrolysis, Fluid dynamics, Sugarcane bagasse, Chemical reactors - models
Área de concentração: Desenvolvimento de Processos Químicos
Titulação: Mestre em Engenharia Química
Banca examinadora: Carlos Eduardo Vaz Rossell, Antonio Maria Francisco Luiz José Bonomi
Data da defesa: 10/12/2009
Programa de Pós Graduação: Engenharia Química

Dissertação de Mestrado defendida por Arturo González Quiroga e aprovada em 10 de dezembro de 2009 pela banca examinadora constituída pelos doutores:

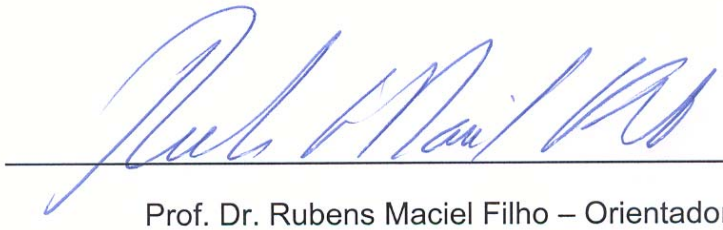

Prof. Dr. Rubens Maciel Filho – Orientador

Prof. Dr. Carlos Eduardo Vaz Rossell

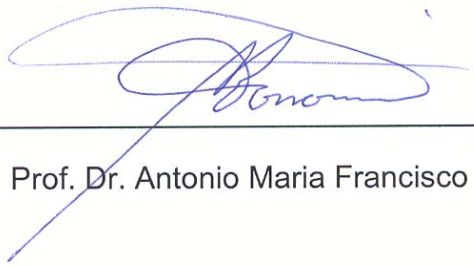

Prof. Dr. Antonio Maria Francisco Luiz José Bonomi

Este exemplar corresponde à versão final da Dissertação de Mestrado em Engenharia Química.

Prof. Dr. Rubens Maciel Filho - Orientador

Para minha querida mãe *Hermelinda*,

minha amada esposa *Gloria*

e minha adorada filha *Isabella*.

Agradecimentos

A minha esposa e minha filha pela paciência e amor a pesar da distancia.

A minha mãe e aos meus irmãos pelo apoio e carinho.

A minhas tias Tilsia e Teresa, e aos meus primos Andrés, Claudia e Sandra pelo apoio incondicional.

Aos colegas do LOPCA pela amizade e soporte acadêmico; especialmente Laurita, Oscar, Jeffrey, Leonardo, Melvin e Aulus.

Aos meus colegas de moradia, Germano, Roger, Gabriel, Marcelo, Tiago, Hugo, Luis e Alexandre pela amizade e confiança.

Aos meus orientadores Prf. Dra. Aline Carvalho da Costa e Rubens Maciel Filho pelo incentivo, orientação e valiosas sugestões.

Por fim, gostaria de registrar o meu agradecimento à UNICAMP pela oportunidade, à FAPESP pelo apoio financeiro, ao BRASIL pela acolhida e a UIS (da Colômbia) pela minha formação como engenheiro.

Conteúdo

Nomenclatura

C	Concentração de cellulose (g/L)
CBH	Concentração das enzimas celobiohidrolase (g proteína/L)
C_S	Consistência da polpa (adimensional)
$CSTR$	Reator contínuo de tanque agitado
C_V	Fração de volume de sólidos (adimensional)
C_D	Coeficiente de arraste
d	Diâmetro de partícula (m)
D	Diâmetro de tubulação (m)
E	Função de distribuição de tempos de residência (adimensional)
EG	Concentração das enzimas endoglicanase (g proteína/L)
E_{1b}	Concentração de EG/CBH adsorvida no substrato prétratado (g proteína/S)
E_{2b}	Concentração de β-glicosidase adsorvida no substrato (g proteína/S)
E_{1bC}	Concentração de EG/CBH adsorvida na fração celulósica do substrato prétratado (g proteína/L)
E_{1bL}	Concentração de EG/CBH adsorvida na lignina (g proteína/L)
E_{2bL}	Concentração de β-glicosidase adsorvida na lignina (g proteína/L)
E_{2fL}	Concentração de β-glicosidase em solução quando o substrato tem lignina
E_{1max}	Massa máxima de EG/CBH que pode ser adsorvida numa unidade de massa de substrato prétratado (mg proteína/g lignina)
E_{1maxL}	Massa máxima de EG/CBH que pode ser adsorvida numa unidade de massa de lignina (mg proteína/g lignina)

E_{2maxL}	Massa maxima de β-glicosidase que pode ser adsorvida numa unidade de massa de lignina (mg proteína/g lignina)
F_G	Função objetivo (adimensional)
G	Aceleração gravitacional (m/s^2)
G	Concentração de glicose (g/L)
G_2	Concentração de celobiose (g/L)
i	Subíndice
j	Subíndice
K	Coeficiente de intercambio interfacial (Adimensional)
K_{1ad}	Constante de dissociação para a adsorção/desorção da EB/CBH em substrato prétratado (L/g proteína)
K_{1adL}	Constante de dissociação para a adsorção/desorção da EB/CBH na lignina (L/g proteína)
K_{2adL}	Constante de dissociação para a adsorção/desorção da β-glicosidase na lignina (L/g proteína)
k_{1r}	Constante de reação para celulose → celobiose (L/gh)
k_{2r}	Constante de reação para celulose → glicose (L/gh)
k_{3r}	Constante de reação para celobiose → glicose (h^{-1})
K_{1IG}	Constante de inibição da glicose nas enzimas na reação celulose → celobiose (g/L)
K_{2IG}	Constante de inibição da glicose nas enzimas na reação celulose → glicose (g/L)
K_{3IG}	Constante de inibição da glicose nas enzimas na reação celobiose → glicose (g/L)
K_{1IG2}	Constante de inibição da celobiose nas enzimas na reação celulose → celobiose (g/L)
K_{2IG2}	Constante de inibição da celobiose nas enzimas na reação celulose → glicose (g/L)
K_{3M}	Constante de saturação do substrato (celobiose) (g/L)
K_{rec}	Constante de recalcitrância (adimensional)

k_{D1bC}	Constante de desativação de enzimas (h^{-1})
k_{mG}	Constante de Micahelis aparente
k_{inh}	Constante de inibição aparente
k_{Xy}	Constante de velocidade aparente xilana-xilose (adimensional)
L	Concentração de lignina (g/L)
l	Comprimento da tubulação (m)
l_m	Comprimento do defletor
mv	Velocidade média da lama
Ma	Macrofluido
Mi	Microfluido
nr	Número de reatores
P	Pressão (Pa)
PFR	Reator tubular
R	Reator
Re	Número de Reynolds (Adimensional)
rpm	Revoluções por minuto
r_j	Taxa da reação j (g/Lh)
R_S	Reatividade do substrato (adimensional)
S	Concentração de substrato prétratado (g/L)
S^h	Substrato hipotético
sd	Desvio padrão
T	Temperatura (ºC)
t	Tempo de reação (h)
v	Atividade da EG/CBH (FPU/L)
VR	Volume de reação (m^3)

v_{mG}	Constante de velocidade de reação aparente celulose→glicose (g/Lh)
v_{Xy}	Parâmetro de ajuste xilana→xilose (adimensional)
v_T	Velocidade de transição (m/s)
v_C	Velocidade crítica para lamas com tendência à sedimentação (m/s)
WRV	Volume de retenção de água (adimensional)
Xy	Concentração de xilose (g/L)
X_C	Conversão de celulose
X_{Xyn}	Conversão de xilana
α	Constante (adimensional)
τ	Tempo de residência (h)
η	Constante (adimensional)
Δ	Constante (adimensional)
ξ	Constante (adimensional)
θ	Constante (adimensional)
ρ	Densidade (kg/m^3)
μ	Viscosidade (Pa.s)
$\overline{\overline{\tau}}$	Tensor de estresse (Pa)
λ	Viscosidade aparente da lama
φ	Angulo de separação dos defletores

Resumo

Por mais de um século, a principal fonte de combustível e produtos químicos para a sociedade humana tem vindo a partir de recursos fósseis, os quais são limitados e estão concentrados em poucas regiões do mundo. Biomassa, como a única fonte de carbono renovável, mostra-se promissora para a produção de combustíveis e produtos químicos em grande escala. Na última década, a produção de bioetanol a partir de biomassa lignocelulósica através de hidrólise enzimática tem sido estudada intensamente a nível de bancada. Reatores contínuos, nos quais a fração celulósica e a hemicelulósica de substratos lignocelulósicos são convertidos em açúcares redutores (para serem fermentados a bioetanol), são o tema desta dissertação. As principais questões consideradas aqui são: a cinética, o padrão de contato sólido-líquido, o comportamento fluidodinâmico da lama durante a hidrólise, configurações alternativas de reatores contínuos, e estratégias de operação contínua com relação ao substrato e a enzima.

Foram revisados os modelos cinéticos mais recentes para a hidrólise enzimática de substratos lignocelulósicos, dando especial atenção aos modelos úteis para projeto de reatores. Foi proposto um esquema de classificação de modelos cinéticos baseado no número de reações consideradas. Com respeito à utilidade de um modelo cinético na otimização do sistema de reação, é desejável que este inclua a adsorção das enzimas na fração celulósica do substrato e na lignina, a inibição das enzimas por produto final, a reatividade do substrato e a desativação das enzimas. Neste trabalho, um modelo de uma reação foi ajustado a perfis experimentais de glicose e xilose obtidos na hidrólise enzimática de bagaço de cana prétratado com peróxido de hidrogênio alcalino. O modelo cinético apresentado difere de outros modelos em que este inclui a predição do perfil de xilose por meio de uma relação algébrica que faz uso do perfil de glicose, e é especialmente útil na ausência de dados experimentais de adsorção e reatividade do substrato.

O comportamento fluidodinâmico da lama de biomassa durante a hidrólise enzimática é complexo devido à ampla distribuição de tamanhos de partícula, às formas incomuns das partículas de biomassa e às mudanças na reología que experimenta o material ao longo da reação. Neste trabalho é apresentado um levantamento detalhado da

fluidodinâmica de suspensões de polpas fibrosas e lamas com tendência à sedimentação, devido a que o comportamento fluidodinâmico de lamas de biomassa pode ser entendido a partir dessas duas situações limite. Além disso, foi desenvolvido um modelo fluidodinâmico com balanços microscópicos e solucionado com um software de fluidodinâmica computacional para estudar o escoamento de lamas de biomassa em reatores tubulares com e sem defletores angulares internos. Por outro lado, a micromixtura do material dentro dos reatores foi considerada em duas situações limite: um material que é fracionado em cúmulos discretos que reagem como reatores batch durante o tempo que estejam no sistema de reação, e um material que imediatamente ingressa no sistema de reação entra em contato íntimo com outros elementos de fluido ao nível molecular. As conversões em reatores continuous para as anteriores situações limite de micromistura foram obtidas.

Os reatores contínuos considerados foram reatores de tanque agitado em serie, reatores tubulares e combinação entre eles. Devido a que a biomassa adsorve água, no começo da reação de hidrólise a fase móvel pode desaparecer a concentrações de substrato maiores de 10% w/w, aproximadamente. A alimentação distribuída de substrato numa serie de reatores de tanque agitado foi uma alternativa proposta neste trabalho para incrementar a produtividade volumétrica dos reatores. Consequentemente, uma série de reatores de tanque agitado com alimentação distribuída, seguida de um reator tubular, foi a melhor alternativa para incrementar a reatividade volumétrica dos reatores e diminuir o volume de reação.

O presente trabalho é em grande parte exploratório sendo que não há procedimentos detalhados de projeto e escalonamento de reatores de hidrólise enzimática de biomassa lignocelulósica na literatura científica atual. Consequentemente, reatores contínuos alternativos assim como procedimentos de modelagem mais detalhados são brevemente discutidos ao final do trabalho. De vital importância são experimentos para elucidar aspectos tais como a reutilização de enzimas por recirculação ou re-adsorção em substrato fresco, adsorção de enzimas a altas concentrações iniciais de substrato (>10% w/w), e a relação entre as propriedades reológicas da lama e a extensão da reação de hidrólise.

Palavras chaves: *Hidrólise enzimática, reatores contínuos, modelagem cinética, fluidodinâmica.*

Abstract

For ever a century, the main source of fuel and chemicals for human society has come from fossil resources, which are limited and concentrated in a few regions of the world. Biomass, as the only source of renewable carbon, shows great promise for large-scale economical production of renewable transportation and fuel chemicals. In the last decade the bioethanol production from lignocellulosic biomass via, enzymatic hydrolysis, has been intensively studied at laboratory level. Continuous reactors in which the cellulose and hemicellulose fractions of lignocellulosic substrates convert to reducing sugars (which are fermented to bioethanol) are the theme of this dissertation. The main issues considered are kinetics, contacting pattern and fluid dynamics, alternative configurations of continuous reactors, and continuous operating strategies with respect to substrate and enzyme.

The most recent kinetic models for the enzymatic hydrolysis of lignocellulosic biomass, useful for reactor design, were reviewed and classified based on the number of reaction considered. Regarding to reactor design, the main factors that should be include a kinetic model are adsorption of enzymes on cellulose and lignin, inhibition of enzyme by glucose and cellobiose, substrate reactivity and enzyme deactivation. A kinetic model of a single reaction was fitted to experimental profiles of glucose and xylose obtained by the enzymatic hydrolysis of pretreated of sugarcane bagasse. This kinetic model differs of previous models in that it predicts xylose concentration based on glucose concentration. This kinetic model is a useful in the absence of experimental data on enzyme adsorption and substrate features others than concentration.

The fluid dynamic behavior of biomass slurries during enzymatic hydrolysis is very complex due to the wide particle size distribution, the extremes shapes of particles and the significant rheological changes of the slurry with the progress of the enzymatic hydrolysis. This works reviewed the fluid dynamic behavior of fiber pulp suspensions and settling slurries because the fluid dynamic behavior of biomass through continuous reactors can be framed between these two limiting situations. In addition, a computational fluid dynamic model was developed to asses the fluid dynamic behavior of biomass slurries in tubular and baffled tubular reactors, motivated by the benefits of tubular reactors to carry

out the enzymatic hydrolysis in terms of lower reaction volume and lower agitation requirements. On the other hand, the micromixing behavior of the flowing material was framed between two limiting situations: an incoming material that is broken up into discrete clumps in which the reaction proceed independently as in a batch reactor, and an incoming material that immediately comes into intimate contact with other fluid elements at molecular level. Conversions in continuous reactors corresponding to the above extreme states of micromixing were obtained.

The continuous reactor considered were stirred tanks reactors in series, tubular reactors, and combination between them. As biomass adsorbs water, this may cause the bulk to become unsaturated at initial substrate concentration higher than 10% w/w, approximately. Operating the enzymatic hydrolysis in a distributed feeding mode by adding fresh substrate and enzyme at subsequent stirred tank reactors was proposed as an alternative to increase the volumetric productivity of reactors. A reactors configuration consisting of stirred tank reactors in series with continuous distributed feeding of substrate and enzyme, followed by a tubular reactor allow increasing the volumetric productivity of the reaction system overcoming mixing limitations and lowering the required reaction volume.

It should be noted that this work is exploratory and that there are not major reports in open literature about the design and scale-up of continuous reactors for enzymatic hydrolysis. Some alternative continuous reactors, as well as modeling approaches for reactor design, are suggested. Of paramount importance are experiments to elucidate relevant aspects as reutilization of enzymes by recirculation of readsorption, adsorption of enzymes at high substrate concentrations (>10% w/w), and the relation between rheological properties of slurries with the extent of saccharification.

Keywords: *Enzymatic hydrolysis, Continuous reactors, Kinetics models, Fluid dynamics.*

Capítulo 1 – Síntese da Investigação

1.1. Introdução

O Brasil atualmente se defronta com a perspectiva de um significativo aumento na demanda por etanol combustível. Esta previsão se sustenta em certas realidades de mercado como: (*i*) aumento do consumo interno de álcool hidratado devido ao sucesso dos *flex-fuel* no mercado de veículos automotivos leves; (*ii*) expansão das exportações brasileiras de etanol em função do crescente interesse mundial pela mistura deste à gasolina, como forma de diminuir as emissões de gases de efeito estufa; (*iii*) oscilações no preço do barril de petróleo, fonte não renovável de energia.

O acréscimo na demanda por etanol exige, respectivamente, que a produção seja ampliada em igual proporção. Para evitar a expansão de fronteiras agrícolas para a cana de açúcar, é necessário aumentar a produtividade de litros de álcool por hectare-ano de cana plantada. Duas rotas tecnológicas complementares possibilitariam atingir esse objetivo. Uma envolve a introdução de novas variedades de cana enquanto a outra busca desenvolver tecnologias que aproveitem integralmente a biomassa da planta (bagaço e palha) para produzir etanol. Essa última recebe o nome de etanol lignocelulósico ou de 2ª geração.

O uso do bagaço apresenta uma série de vantagens: já vem processado das moendas; está disponível em grandes quantidades; tem custo mínimo; está pronto para uso no local, evitando aumento de custo devido ao transporte. O que vai definir se o bagaço excedente produzido na moenda da cana será destinado à queima para gerar bioeletricidade ou à produção de etanol lignocelulósico será o mercado.

Para obter etanol lignocelulósico são necessários, basicamente, dois processos: a hidrólise dos polissacarídeos em açúcares e a fermentação destes em etanol. A hidrólise pode ser realizada por processos que utilizam ácidos, solventes orgânicos ou enzimas. Dentre estes, a rota enzimática tem sido amplamente estudada nos últimos anos devido a sua potencialidade em proporcionar maiores rendimentos por ser realizada a pressão

ambiente e temperaturas moderadas – entre 50^{o} e 60^{o}C e não formar subprodutos indesejáveis. A fermentação é uma técnica bem conhecida e dominada. Já a hidrólise enzimática possui uma série de gargalos que impedem sua reprodução em escala industrial. Dentre eles, os mais importantes são: a lenta velocidade de reação (>72 h para atingir conversões da celulose acima de 90%); o alto custo das enzimas; e a dificuldade para operar a hidrólise enzimática com concentrações de substrato maiores de 10% w/w (base seca).

1.2. Objetivos

O objetivo desta tese é apresentar um estudo detalhado da hidrólise enzimática, com abrangência sobre as etapas de modelagem cinética e modelagem de reatores. Dentre os objetivos destacam-se:

- Levantamento dos modelos cinéticos da hidrólise enzimática, com considerações relativas aos seus principais aspectos positivos e negativos, fundamentalmente quando esses modelos cinéticos são aplicados à hidrólise enzimática de substratos lignocelulósicos.
- Ajuste de um modelo cinético a dados experimentais de hidrólise enzimática de bagaço de cana gerados no Laboratório de Engenharia de Processos Fermentativos e Enzimáticos (LEPFE) da Faculdade de Engenharia Química da Universidade Estadual de Campinas (UNICAMP).
- Modelar e simular o desempenho de uma serie de reatores de tanque agitado e de um reator tubular para a hidrólise enzimática de bagaço de cana.
- Desenvolver e simular um modelo para uma serie de reatores de tanque agitado para a hidrólise enzimática de bagaço de cana com alimentação distribuída de substrato e enzima. Avaliar o desempenho de alimentação distribuída de substrato e enzima em dois ou três reatores seguida de uma serie de reatores de tanque agitado ou de um reator tubular.
- Desenvolver e simular um modelo para o comportamento fluidodinâmico de misturas bagaço de cana-água em tubulações horizontais com e sem defletores

angulares internos. Avaliar o desempenho de um reator tubular com defletores angulares internos para a hidrólise enzimática de bagaço de cana.

- Comparar o desempenho dos diferentes tipos de reatores simulados ao longo do trabalho.

1.3 Organização desta dissertação

O capítulo 2 apresenta a modelagem cinética da reação de hidrólise enzimática e discute tópicos relativos às principais características dos modelos propostos na literatura. Fazem parte ainda do capítulo considerações acerca de como incorporar a reatividade do substrato e a desativação das enzimas nos modelos já existentes.

A modelagem e o ajuste de parâmetros cinéticos para a hidrólise enzimática de bagaço de cana pré-tratado com peróxido de hidrogênio alcalino são apresentados no capítulo 3. Um algoritmo genético é utilizado para gerar o valor inicial dos parâmetros cinéticos que servem como estimativa inicial num algoritmo Levenberg-Maquard para finalizar o procedimento de ajuste. Os alcances e limitações do modelo cinético são discutidos em detalhe.

No capítulo 4, a modelagem e simulação de reatores de tanque agitado em serie e um reator tubular para a hidrólise enzimática de bagaço de cana, são apresentadas. O fluxo da mistura bagaço-água é considerado como tendo comportamento equivalente a macrofluido e microfluido a fim de encontrar a conversão máxima e mínima que pode ser atingida neste tipo de reatores. O modelo cinético foi ajustado com dados da literatura por meio de métodos de otimização determinísticos. Isso se justifica, pois a modelagem e a simulação foram realizadas antes dos dados experimentais referidos no capítulo 3 estiverem prontos.

O capítulo 5 apresenta a proposta de alimentação distribuída de substrato e enzima em reatores de tanque agitado em serie. Fazem parte ainda do capítulo um levantamento completo de hidrólise enzimática de substratos lignocelulósicos a altas concentrações de substrato (> 10% w/w, base seca), a simulação de combinação de reatores com alimentação distribuída de substrato e enzima e tanques agitados em serie ou um reator tubular, e considerações acerca da utilidade do modelo proposto. Neste capítulo foi usado o modelo

cinético ajustado no capítulo três. O mesmo procedimento para o projeto de reatores, realizado com um modelo cinético apresentado e ajustado na literatura é reportado no apêndice A desta dissertação. A justificação desta extensão do trabalho é que o modelo cinético é o mais completo dos que têm sido proposto e ajustado até agora, permite obter conclusões adicionais às obtidas no capítulo e se constitui num modelo candidato para ser ajustado a dados da hidrólise enzimática de bagaço de cana em próximos trabalhos.

O levantamento do comportamento fluidodinâmico sólido-líquido em tubulações horizontais é então considerado no Capítulo 6, com ênfase nas velocidades de transição entre os diferentes padrões de fluxo a fim de avaliar o desempenho do reator tubular.

O capítulo 6 mostrou a importância de manter as partículas de bagaço suspendidas na menor velocidade de fluxo possível para reduzir o volume de reação num reator tubular. Portanto, no capítulo 7, é apresentada a modelagem e simulação do fluxo da mistura bagaço de cana-água numa tubulação com defletores angulares internos. Foi avaliada a velocidade média de fluxo, assim como a localização dos defletores. È discutida a utilidade de um reator tubular com defletores angulares internos. As simulações foram feitas em estado estacionário e em estado transiente utilizando o software de fluidodinâmica computacional ANSYS-CFX 11.0 (de Ansys Inc., EUROPE).

No capítulo 8 são comparadas as diferentes opções de reatores para a hidrólise enzimática. Tomando como base de cálculo um fluxo mássico no primeiro reator de uma series de reatores de tanque agitado ou de um reator tubular e com os perfis de conversão obtidos no capítulo 5, é possível obter uma primeira aproximação dos volumes de reação necessários para atingir uma determinada conversão de celulose e hemicelulose. Embora não se façam considerações detalhadas de agitação e mistura, o estudo visa o aumento da produtividade volumétrica do sistema de reação e é um marco de referência para trabalhos posteriores. Fazem parte ainda do capítulo considerações acerca da concentração de uma corrente diluída de glicose em evaporadores de múltiplo efeito com o intuito de mostrar o impacto da concentração de glicose na saída dos reatores no consumo de vapor e na área de troca térmica dos evaporadores.

Finalmente, o capítulo 9 apresenta as conclusões deste trabalho e sugestões para trabalhos futuros. São apresentados brevemente sistemas de reação alternativos que têm a potencialidade de operar com concentrações de substrato maiores do que as concentrações

que podem ser hidrolisadas em reatores de tanque agitado e/ou tubular convencionais. Fazem-se sugestões acerca da cinética da reação de hidrólise e o projeto de reatores tanto na experimentação como na modelagem. Procurou-se justificar cada uma das sugestões com literatura recente na área e com os resultados desta dissertação.

O fluxograma da Figura 1.1 ilustra de que forma a tese está organizada com as inter-relações entres capítulos.

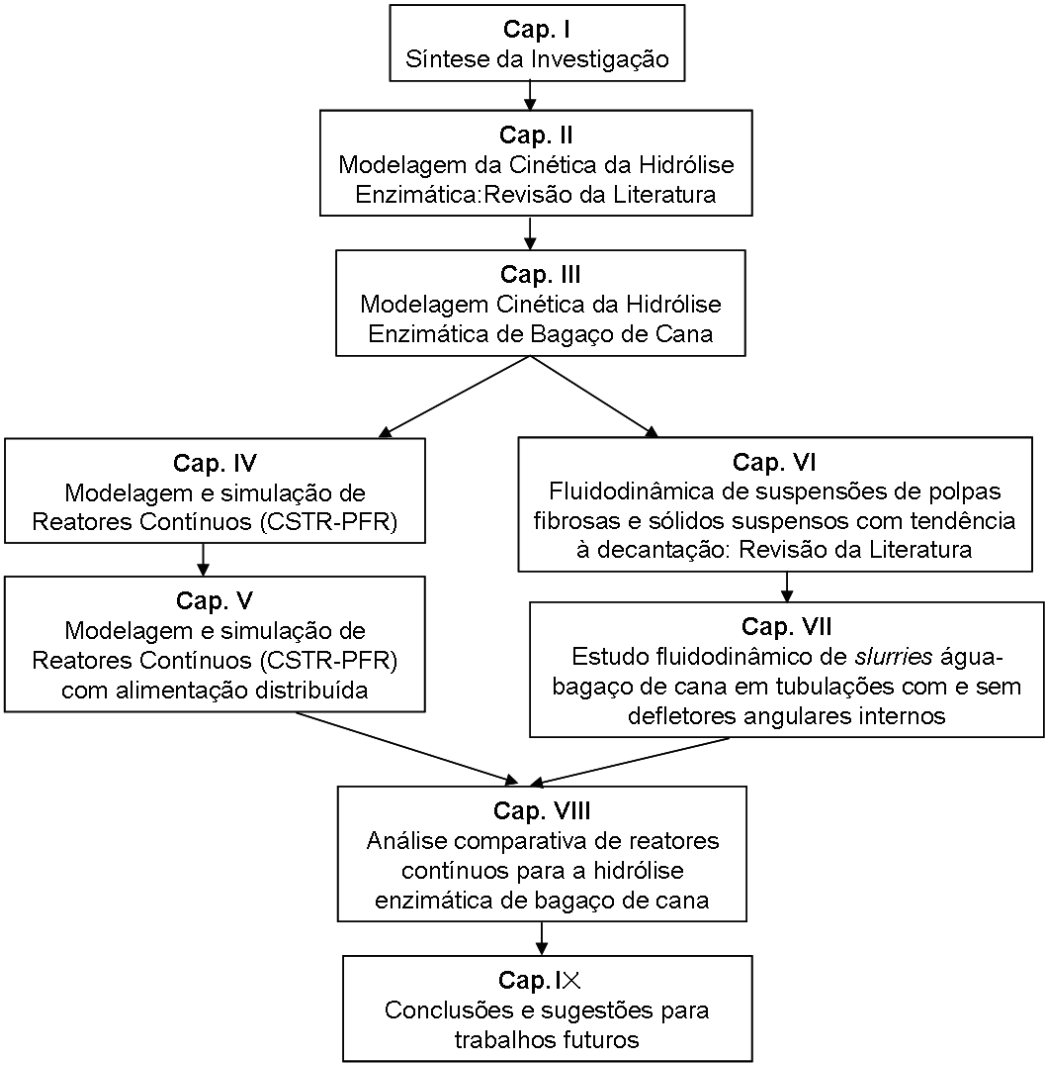

Figura 1. Organização da dissertação.

Capítulo 2 – Modelagem Cinética da Reação de Hidrólise Enzimática de Substratos Lignocelulósicos

2.1. Introdução

A descrição quantitativa da reação de hidrólise enzimática é de grande potencial em dois contextos: na estruturação e validação de conhecimento fundamental do mecanismo de reação, e na otimização do processo. Alguns dos modelos cinéticos reportados na literatura são utilizados para correlação de dados experimentais e não podem ser usados em condições que não sejam aquelas nas quais foram ajustados. Outros modelos têm uma base mecanística, mas incluem a informação mínima necessária para a descrição do processo e são potencialmente úteis na otimização do processo de hidrólise enzimática. Também há modelos bem detalhados particularmente úteis no conhecimento ao nível de outras propriedades do substrato além da concentração e múltiplas atividades enzimáticas. Neste capítulo a ênfase é nos modelos cinéticos potencialmente úteis no projeto de reatores.

A revisão aqui abordada engloba a modelagem da adsorção das enzimas celulase e β-glicosidase na celulose e na lignina, da liberação de glicose e celobiose a partir da hidrólise de celulose, da produção de glicose a partir da hidrólise de celobiose, assim como diferentes formas usadas na literatura para modelar a reatividade do substrato e a desativação das enzimas. Contudo, a consideração de todos os aspectos anteriores aumenta significantemente o número de parâmetros que devem ser ajustados e consequentemente o número de experimentos a serem feitos a fim de se obter um modelo cinético robusto. A revisão mostra que os conceitos de "reatividade do substrato" e "desativação de enzimas", uma vez incorporadas em equações cinéticas propostas na literatura, podem melhorar os modelos cinéticos atuais.

2.2. Desenvolvimento

O desenvolvimento deste capítulo é apresentado a seguir, no manuscrito intitulado: *Kinetic Modeling of the Enzymatic Hydrolysis of Lignocellulosic Substrates: A Review.*.

Kinetic Modeling of the Enzymatic Hydrolysis of Lignocellulosic Substrates: A Review

Abstract

Enzymatic hydrolysis of lignocellulose is one attractive process option for production of reducing sugars which serve as a raw material for ethanol production or other chemical products. Published works pertaining to kinetic modeling of enzymatic hydrolysis of lignocellulosic substrates are reviewed with a particular emphasis on semimechanistic kinetic models useful for reactor design. Topics considered were reaction schemes based on products and modeling of enzyme adsorption, substrate reactivity, and enzyme deactivation. Despite the enzymatic reaction is very complex with many enzymatic and substrate properties impacting reaction rates, it is important highlights that there is consensus regarded to the main factors that must be incorporated and the general structure of a representative kinetic model. This review provides a solid foundation for future model refinements.

Keywords: *kinetic model; reactor design; enzymes adsorption; substrate reactivity*

Review Outline

1. Introduction

Quantitative description of cellulose enzymatic hydrolysis is of potential value in two contexts: for structuring and testing fundamental understanding and for designing and evaluating engineered systems. Some kinetic models are used for correlating data and are unlikely to be reliable under conditions different from those for which the correlation was developed. Some kinetic models have a mechanistic base but include the minimal information necessary for descriptive purposes and are potentially useful for optimization, economic evaluation and design of industrial systems. Finally, there are detailed models particularly useful for developing and testing understanding at the level of substrate features and multiple enzyme activities. Enzymatic hydrolysis of lignocellulosic biomass is exceedingly complex, whit many enzymatic and substrate properties impacting reaction rates (Zhang and Lynd, 2004), therefore the full extent of this complexity is not represented in any quantitative model proposed to date (Shao et al., 2009). In this study, the emphasis is

put on models formulated for the enzymatic hydrolysis of lignocellulosic biomass that are potentially useful for optimization, economic evaluation and design of industrial systems. The most relevant modeling efforts in reported research are summarized in this paper. For the reader interested in a detailed description of kinetic models for pure cellulosic and lignocellulosic substrates hydrolysis it is suggested to examine the following review publications: Mansfield et al. (1999); Mosier et al. (1999); Lynd et al. 2002; Zhang and Lynd, (2004); Gan et al. (2003); Jørgensen et al. 2007; Zhu et al. (2008) Himmel (2008) and Bansal et al. (2009).

2. Lignocellulosic substrates

2.1 Native substrates

Natural cellulose molecules occur in elementary fibrils closely associated with hemicellulose and lignin. The chemical composition on dry basis of some lignocellulosic materials is shown in Table 1. The interactions among cellulose, hemicellulose and lignin vary with the plant cell type and with plant maturity and are a dominant structural feature limiting the rate and extent of utilization of whole untreated biomass materials (Lynd et al., 2002).

Table 1. Composition of some lignocellulosic materials

Lignocellulosic substrates	**Lignin (%)**	**Hemicellulose (%)**	**Cellulose (%)**	**Reference**
Hardwood stems	18-25	24-40	40-55	Howard et al. (2003)
Softwood stems	25-35	25-35	45-50	
Nut shells	30-40	25-30	25-30	
Corn Cobs	15	35	45	
Rice straw	18	24	32.1	
Coastal Bermuda grass	6.4	35.7	25	
Switch grass	12.0	31.4	45	
Rye grass (early leaf)	2.7	15.8	21.3	
Rye grass (seed leaf)	7.3	25.7	26.7	
Sugar cane bagasse	19-24	27-32	32-44	Rowell (1992)
Wheat straw	16-21	26-32	29-35	

Barley straw	14-15	24-29	31-34	
Grass Elephant	23.9	24	22	

Cellulose is a linear condensation polymer consisting of D-glucose subunits, linked together by β-1,4-glycosidic bonds (Fengel and Weneger, 1984). The cellulose in a plant consists of parts with a crystalline structure, and parts with an amorphous structure. The cellulose chains are "bundled" together and form the so called cellulose fibrils or cellulose bundles. These cellulose fibrils are mostly independent and weakly bound through hydrogen bonding (Laureano-Perez et al., 2005). Hemicellulose is a complex carbohydrate structure that consists of different polymers such as pentoses (xylose and arabinose), hexoses (mannose, glucose and galactose), and sugar acids. Hemicellulose has a lower molecular weight than cellulose, and branches with short lateral chains that consists of different sugars (Fengel and Wegener, 1984). Hemicellulose serves as a connection between the lignin and cellulose fibers and gives the whole cellulose-hemicellulose-lignin network more rigidity (Laureano-Perez et al., 2005). Lignin is an amorphous heteropolymer consisting of three different phenylpropane units (p-coumaryl, coniferyl and sinapyl alcohol) that are held together by different types of linkages. The main purpose of lignin is to give the plant structural support, impermeability, and resistance against microbial attack and oxidative stress (Fengel and Wegener, 1984).

Bunches of elementary cellulose fibrils are embedded in a matrix of hemicellulose with a thickness of 7-30 nm (Figure 1). The lignification process occurs late in the process of synthesizing natural fibers, so lignin is located primarily on the exterior of microfibrils where it covalently bonds to hemicellulose. Most of the β-1,4-glucosidic bonds in naturally occurring lignocellulosic materials are inaccessible to enzymes by virtue of the small size of the pores in the multicomponent spatially heterogeneous biomass matrix. Because enzymatic hydrolysis of native lignocellulose usually results in solubilization of ≤20% of the originally present glucan, some form of pretreatment to increase susceptibility to enzymatic hydrolysis is included in most process concepts for biological conversion of lignocellulose (Zhang and Lynd, 2004).

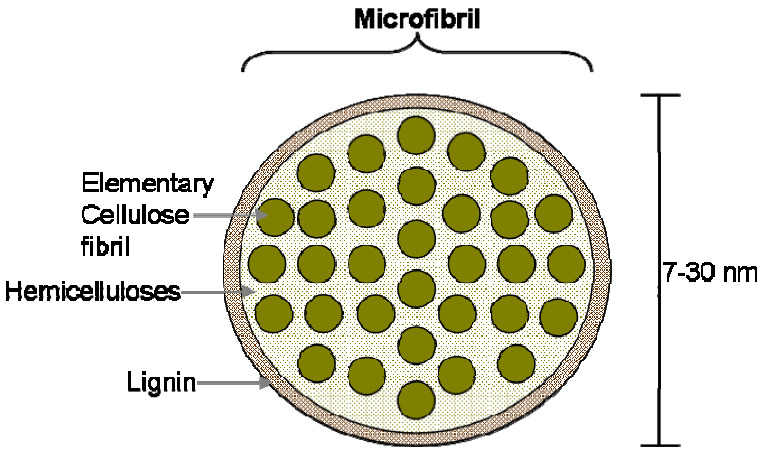

Figure 1. Organization of lignocellulose into elementary fibrils and microfibrils (Adapted from Klein and Snodgrass, 1993)

2.2 Pretreated substrates

During the pretreatment step lignocellulosic biomass is converted from its native form, in which it is recalcitrant to enzymes, into a form for which enzymatic hydrolysis is effective. Rendering lignocellulosic materials susceptible to enzymatic hydrolysis involves overcoming both physical and chemical barriers. Lignin and hemicellulose extraction from lignocellulosic materials expose weak spots on the surface of cellulose fibers open to cellulase attack. A key factor for successful enzymatic conversion of biomass to fermentable sugars is the accessibility of the β-1,4-glucosidic bonds in cellulose to enzymes. Although no particular pretreatment process can presently be viewed as the "ideal" for all lignocellulosic materials or for all process circumstances, a list of the desired properties of an ideal pretreatment process has been generated (Mosier et al., 2005). Such an ideal pretreatment process:

- Produces a highly digestible pretreated solid
- Does not significantly degrade pentoses
- Does not significantly degrade cellulose
- Requires little or no size reduction of biomass feedstock
- Can work in reactors of reasonable size and moderate cost

- Has a high degree of simplicity
- Is effective at low moisture content

Table 2 shows the effect of various pretreatment methods on the structure of lignocellulosic biomass (Mosier et al., 2005).

Table 2. Effect of various pretreatment methods on the chemical composition and chemical/physical structure of lignocellulosic biomass (Mosier et al., 2005)

Pretreatment	Increases accessible surface area	De-crystallizes cellulose	Removes hemicellulose	Removes lignin	Alters lignin structure
Uncatalyzed steam explosion	Xx		xx		x
Liquid hot water	Xx	nd	xx		x
pH controlled hot water	Xx	nd	xx	x	x
Flow trough liquid hot water	Xx	nd	xx	x	x
Dilute acid	xx		xx		xx
Flow through acid	Xx		xx	x	xx
AFEX*	Xx	xx	x	xx	xx
ARP**	Xx	xx	x	xx	xx
Lime	Xx	nd	x	xx	xx

Note: xx, strong effect; x, moderate effect; nd, not determined

*Ammonia fiber expansion

**Ammonia-recycled percolation

3. The enzyme system

Cellulose can be depolymerized by enzymes called cellulases, which catalyze the hydrolysis of β-1-1 bonds present in cellulose. Three major types of enzymatic activities are found in the cellulase complex: (*i*) endoglucanases or 1,4-β-D-glucan-4-glucanohydrolases (EC 3.2.1.4), (*ii*) exoglucanases, including 1,4-β-D-glucan glucanohydrolases (also known

as cellodextrinases) (EC 3.2.1.74) and 1,4-β-D-glucan cellobiohydrolases (cellobiohydrolases) (EC 3.2.1.91), and (*iii*) β-glucosidases or β-glucoside glucohydrolases (EC 3.2.1.21). Endoglucanases cut randomly internal amorphous sites in the cellulose polysaccharide chain, generating oligosaccharides of various lengths and consequently new chain ends. Exoglucanases act in a progressive manner on the reducing or nonreducing ends of the cellulose polysaccharide chains, liberating either glucose (glucanohydrolases) or cellobiose (cellobiohydrolase) as major products. Exoglucanases can also act on microcrystalline cellulose, presumably peeling cellulose chains from microcrystalline structure. β-glucosidases hydrolyze soluble cellodextrins and cellobiose to glucose (Lynd et al., 2002). Holtzapple et al. (1990) defined "cellulase" as the *endo*- (EG) and *exo*-cellulases (CBH) and do not include β-glucosidase (BG).

4. The reaction of enzymatic hydrolysis of lignocellulosic substrates

The enzymatic hydrolysis of lignocellulosic biomass is characterized by an insoluble reactant (cellulose) and soluble catalysts (enzymes). The overall reaction rate is determined by the rates of three events in sequence: (*i*) the external enzyme mass transfer rate through the stagnant liquid film layer adjacent to the solid substrate, (*ii*) the rate of enzyme adsorption on the substrate surface, and (*iii*) the rate of cellulase catalysis. Continuing hydrolysis after the initial phase of fast reaction depends on further enzyme penetration and diffusion inside the solid substrate as it undergoes structural change after the first layer of cellulose was hydrolyzed (Gan et al., 2004).

4.1 Enzyme adsorption

Enzyme adsorption and the formation of the enzyme-substrate complex are considered to be the critical steps in the enzymatic hydrolysis of cellulose. Cellulase adsorption is rapid compared to the time required for hydrolysis, with many studies concluding that adsorption reaches steady-sate within half an hour (Lynd et al., 2002). It has been suggested that cellulase adsorbs on the surface of cellulose and performs a number of catalytic actions while it is moving along the substrate (Sinitsyn et al., 1989). Other authors suggested that the enzyme, having carried out its catalytic action, would desorb

from the substrate and adsorb on another part of the substrate (Money et al., 1999). Medve et al. (1997) observed that adsorption to the residue after hydrolysis leads to loss of the enzymes, while Boussaid and Saddler (1999) noted that complete hydrolysis of the substrate is required to achieve effective release and reuse of the active enzymes. Lignin has been implicated as a competitive cellulase adsorbent which reduces the amount of cellulase available to catalyze cellulose hydrolysis (Ooshima et al., 1990). In addition, it has been suggested that residual lignin blocks the progress of cellulose breakdown (Mansfield et al., 1999). Ramos et al. (1993) postulated that the optimum release of adsorbed enzymes depends on the lignin content of the substrate and of the achievement of complete hydrolysis.

4.2 Substrate reactivity

It has been suggested that the drop in the rate of continuous enzymatic hydrolysis of cellulosic and lignocellulosic substrates could be explained by declining substrate reactivity (Lee and Fan, 1983; Zhang et al., 1999). In studies with pure cellulose, amorphous cellulose is degraded 5-10 times more rapidly when compared to highly crystalline cellulose (Lynd et al., 2002). Jackson et al. (1993) proposed that the high initial hydrolysis rate is due to preferential hydrolysis of the more easily digestible amorphous regions and that the rate decreases later as the enzymes encounter the more recalcitrant crystalline regions. However, several researches found no substantial change in crystallinity as the saccharification progresses (Ohmine et al., 1983; Lenz et al., 1990; Puls and Wood, 1991). In addition to the degree of crystallinity, the reactivity of pretreated lignocellulosic substrates is influenced by surface area, degree of polymerization, pore volume, particle size, lignin content and distribution, and hemicellulose content (Zhu et al., 2008). Actually, it is rather difficult to measure those structural features (Zhang and Lynd, 2004). For instance, the lignin and other non-cellulose contents greatly impact the measurement of crystallinity. Recent studies (Kadam et al., 2004; Drissen et al., 2007; Zhen et al., 2009) investigated the contribution of substrate reactivity change to the nonlinearity of enzymatic hydrolysis of lignocellulosic substrates by feeding fresh enzyme to spent substrate to restart experiments. Because enzymes are fresh, and product inhibition is absent at restart, comparison of the restart rate with the uninterrupted initial rate provides a direct measure of

substrate reactivity. Thus, for lignocellulosic substrates, the change of substrate reactivity obtained restarting hydrolysis of spent substrates may be a more appropriate way to study the reactivity of the substrate during the reaction than resorting to an assumed dichotomy between amorphous and crystalline regions (Kadam et al., 2004).

4.3 Enzyme inactivation

4.3.1 Inhibition by cellobiose and glucose

β-glucosidase is a well-studied enzyme which exhibit competitive or mixed inhibition by glucose (Holtzapple et al., 1990). The type of inhibition exhibited by cellulase is the subject of much confusion. Competitive inhibition of cellulase by cellobiose is the most common mechanism in the literature, but other uncompetitive and noncompetitive mechanisms have also been proposed (Holtzapple et al., 1990; Zhang et al., 2004). Zhang et al. (2004) concluded that the mechanistic basis for this phenomenon is incompletely understood. Gregg and Saddler (1996) and Kadam et al. (2004) suggested that competitive inhibition (inhibitor sugars are substrate analogues and bind to the active site of the enzyme, thereby retarding the formation of the enzyme substrate complex) was dominant. Holtzapple et al. (1984) argued that non-competitive inhibition (inhibitors sugars bind at remote positions of the active site of the enzyme causing the specific reaction rate to diminish) was observed, while some reported a combination of both (Gusakov and Sinitsyn, 1992). Depending on the enzyme/substrate concentration ratio for cellulase and β-glucosidase, different product inhibition patterns may be observed (Gan et al., 2003). Tanaka et al. (1986) performed an experiment by removing where they removed or added glucose and cellobiose to the bulk solution and concluded that product inhibition is not the major cause for the nonlinearity of the enzymatic hydrolysis rate. These results are similar to the obtained by Eriksson et al. (2002), which ran experiments using lignocellulosic substrates.

4.3.2 Deactivation by thermal and mechanical effects

It has been generally accepted that cellulase enzymes are susceptible to inactivation when exposed to temperature and shear stress in the reaction zone (Drissen et

al., 2007). Mukataka et al. (1983) have found that the reduction in activity was lower in substrate free systems then when substrate was present. Ganesh et al. (2000) have shown that when cellulase enzymes were subjected to fluid agitation shear stress, deactivation increased with an increase in the agitation speed. Zheng et al. (2009) found that the enzyme activity decreased less than 10% in an enzymatic hydrolysis system under thermal and mechanical agitation stress after 1-4 days. Adsorbed and free enzymes in solution can be inactivated by thermal and shear stress, but there are no reports about the extension of inactivation in each phase.

4.3.3 Loss of mobility of adsorbed enzyme

Enzymes, as well as proteins, adsorb by attaching various segments of their molecule to the surface. The fraction of amino acid residues in direct contact with the surface is typically 5-20% (Brash and Wojciechowski, 1996). In addition to inhibition by glucose, cellulase enzymes adsorbed on the cellulose fraction of the substrate can lose their activity by tight adsorption and consequently loss of mobility (Gusakov and Sinitsyn, 1985; Gusakov et al., 1992; Philippidis, 1996).

5. Modeling enzymatic hydrolysis of lignocellulosic substrates

5.1 Reaction schemes based on products

To simplify model development, sugars produced in the enzymatic hydrolysis can be consolidated to two sugars: cellobiose and glucose. Grouping products in cellobiose and glucose entails the recognition of at least two enzyme activities: cellulase (EG/CBH) and β-glucosidase (BG). Although it is understood that cellulase contains many components, it is treated as a single enzyme system since the components function synergistically to solubilize cellulose. The reaction system can be visualized as consisting of three, two or one reaction. Reaction schemes based on final products are summarized in Figure 3.

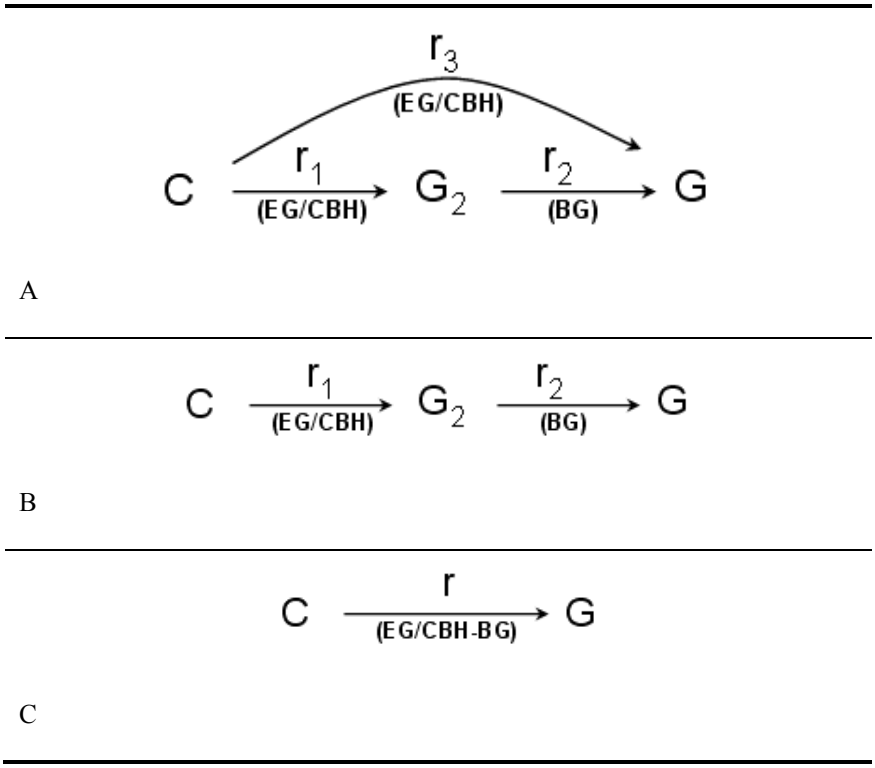

Figure 2. Reactions schemes of the enzymatic hydrolysis of lignocellulosic biomass. a) Three reactions scheme, b) two reactions scheme, c) one reaction scheme

The mass balances for cellulose, cellobiose, and glucose are as follow:

$$\frac{dC}{dt} = -r_1 - r_3 \tag{1}$$

$$\frac{dG_2}{dt} = 1.056r_1 - r_2 \tag{2}$$

$$\frac{dG}{dt} = 1.111r_2 + 1.053r_3 \tag{3}$$

Where:

C: cellulose concentration

G_2: cellobiose concentration

G: glucose concentration

r_1: cellulose to cellobiose reaction

r_2: cellobiose to glucose reaction

r_3: cellulose to glucose reaction

In Equations 1, 2 and 3, the factors 1.056, 1.111 and 1.053 account for water hydrolysis. The mass balances do not change if modifications are made in the kinetic rate expression. In the two reaction scheme, direct glucose production from cellulose is not taken into account (r_3) and for the one reaction scheme the final product considered can be reducing sugars (meanly cellobiose and glucose) or glucose, if no cellobiose accumulation is considered, which is the case when hydrolysis is performed with BG concentrations high enough.

5.1.1 The heterogeneous reactions (r_1 and r_3)

r_1 and r_3 are the rates of hydrolysis of cellulose to cellobiose and cellulose to glucose. These reactions are catalyzed by cellulase enzymes adsorbed on the cellulose fraction of the substrate. In addition to inhibition of cellulase by cellobiose, substrate reactivity and deactivation of the adsorbed enzyme has been included in reported models (see Table 3). As described in section 3.3.1, to date there is still no consensus about the inhibition pattern of cellulase by cellobiose. Different ways to incorporate substrate reactivity are discussed in the following sections.

5.1.2 The homogeneous reaction (r_2)

r_2 is the rate of hydrolysis of cellobiose to glucose. This reaction has been studied using pure cellobiose as substrate and the purified cellobiase fraction of enzyme (Gong et al., 1977; Lee and Fan, 1983; Dekker, 1986; Grous et al., 1985). According to these researches:

- Kinetic expressions for homogeneous enzymatic reactions can be directly applied to the hydrolysis of cellobiose.
- Glucose inhibits the activity of cellobiase enzymes and the competitive inhibition mode has been the most accepted.
- Cellobiase enzymes from different sources have shown different kinetic parameters.

The most recent kinetic models of the enzymatic hydrolysis of lignocellulosic substrates assume that the conversion of cellobiose is a homogeneous enzymatic reaction with competitive inhibition by glucose (Ljunggren, 2005; Zhen et al., 2009) or glucose and xylose (Kadam et al., 2004).

5.1.3 The pseudo-homogeneous reaction (r)

Glucose yield can be limited by either low EG/CBH concentration or low BG concentration. If the enzyme loading is increased maintaining a high enough BG loading to avoid cellobiose accumulation, glucose yield will reach a maximum because the substrate becomes saturated with enzyme. If there is no cellobiose accumulation, glucose yield could be predicted with a pseudo-homogeneous kinetic model of one apparent reaction rate. In an enzyme catalyzed reaction of an insoluble substrate the effective concentration of the substrate is dramatically reduced because much of the substrate is below the surface and is inaccessible to enzyme. Additionally, many surface substrate sites are covered by adsorbed enzyme, making them inaccessible to free unadsorbed enzyme (Rusell and Holtzapple, 1990). Due to the heterogeneous nature of the system, the classic Michaelis-Menten model is inadequate to explain the action of cellulase on insoluble cellulose

Holtzapple et al. (1984-a) proposed an “insoluble substrate equivalent” of the Michaelis-Menten model by the inclusion of parameters to account of the adsorption step and the fraction of total substrate available to bind with enzyme. Nakao et al. (1990) proposed the inclusion of a hypothetical soluble substrate whose initial concentration corresponds to the concentration of glucose produced ultimately, assuming a Micahelis-Menten mechanism. These models are especially useful in the absence of experimental data

on enzyme adsorption and substrate features others than concentration, but their applicability is limited because they consider only a single enzyme activity and do not predict cellobiose accumulation.

5.2 Features of reported kinetic models

Kinetic modeling of enzymatic hydrolysis is difficult by the heterogeneous nature of the substrate and the multiple enzyme activities. These facts determine that the mechanisms of the hydrolytic reaction are highly complex, rendering it difficult for mathematical modeling without complicated and sometimes unreliable input of many physical, kinetic and mass transfer parameters. A kinetic model useful for reactor design and optimization can be developed by incorporating the phenomena of enzyme adsorption (productive adsorption on cellulose and non-productive adsorption on lignin), end product inhibition (glucose and cellobiose), enzyme deactivation (thermal and mechanical effects) and substrate reactivity. A kinetic model should be sophisticated enough to describe the complexities of the enzymatic hydrolysis of lignocellulosic materials, but the parameters should be based mainly on observable phenomena to simplify the process of obtaining parameters and the portability towards different substrates (i.e., the same raw material with different pretreatment) (Kadam et al., 2004).

Although the full extent of the enzymatic hydrolysis of lignocellulosic substrates is not represented in any quantitative model proposed to date (Shao et al., 2009), there are common characteristics among the different models in the literature and consensus about the main features that a general kinetic model must contain. Table 3 shows the main factors related to enzyme adsorption on cellulose and lignin, substrate reactivity, and enzyme deactivation (thermal and/or mechanical) that have been incorporated into proposed kinetic models.

Table 3. Summary of models attributes for enzymatic hydrolysis of cellulosic and lignocellulosic substrates

Reaction scheme		Adsorp. on cellulose	Adsorp. on lignin	Substrate		Enzyme deacti-vation	Pret. substrate
				Reactivity	Amorph-crystalline		
One reaction	Holtzapple et al. 1984	+	-	-	-	-	Solka Floc
	Nakao et al. 1990	-	-	-	-	-	Wood pulp
Two reactions	Dwivedi and Ghose (1979)	+	-	-	-	-	Sugarcane bagasse
	Wald et al. (1984)	+	-	-	+	-	Rice straw
	Borchert and Buchholz (1987)	+	-	-	+	+	Wheat straw
	Gusakov et al. (1992)	+	+	-	-	+	Cellolignin
	South et al. (1995)	+	+	+	-	-	Wood
	Philippidis (1996)	+	+	-	-	+	---
Three reactions	Kadam et al. (2004)	+	-	+	-	-	Corn stover
	Ljungren (2005)	-	-	+	-	-	Sugarcane bagasse
	Drissen et al. (2007)	+	-	+	-	+	Wheat straw
	Zheng et al. (2009)	+	+	+	-	-	Rye grass

Note: +, included; -, non included

5.2.1 Modeling enzyme adsorption on cellulose and lignin

The Langmuir model has been used to describe enzyme adsorption on lignocellulosic substrates (Wald et al., 1984; South et al., 1995; Kadam et al., 2004; Ljungreen et al., 2005; Drissen et al., 2007; Zhen et al., 2009). It should be noted that the underlying assumptions for the Langmuir model, i.e., uniform binding sites and no interactions between the adsorbing molecules, may not be necessarily valid for cellulase adsorption on lignocellulosic substrates. As mentioned in section 4.1, since the enzyme system was divided into two groups, the adsorption of both cellulase (EG/CBH) and β-glucosidase (BG) on cellulose and lignin must be determined to determine the concentration of EG/CBH adsorbed on cellulose and BG free in solution.

Figure 3 depicts an overview of factors limiting efficient hydrolysis of cellulose in lignocellulosic biomass. 1) Product inhition of β-glucosidases and cellobiohydrolases by

glucose and cellobiose; 2) Unproductive binding of cellobiohydrolases on a cellulose chain; 3,4) Hemicelluloses and lignin associated with or covering the microfibril prevent the cellulases from accesing the cellulose surface; 5) Cellulase enzymes can be unspecifically adsorbed on lignin surface; 6) Denaturation or loss of enzyme activity due to mechanical shear proteolytic activity or low themostability (Jørgensen et al., 2007-b).

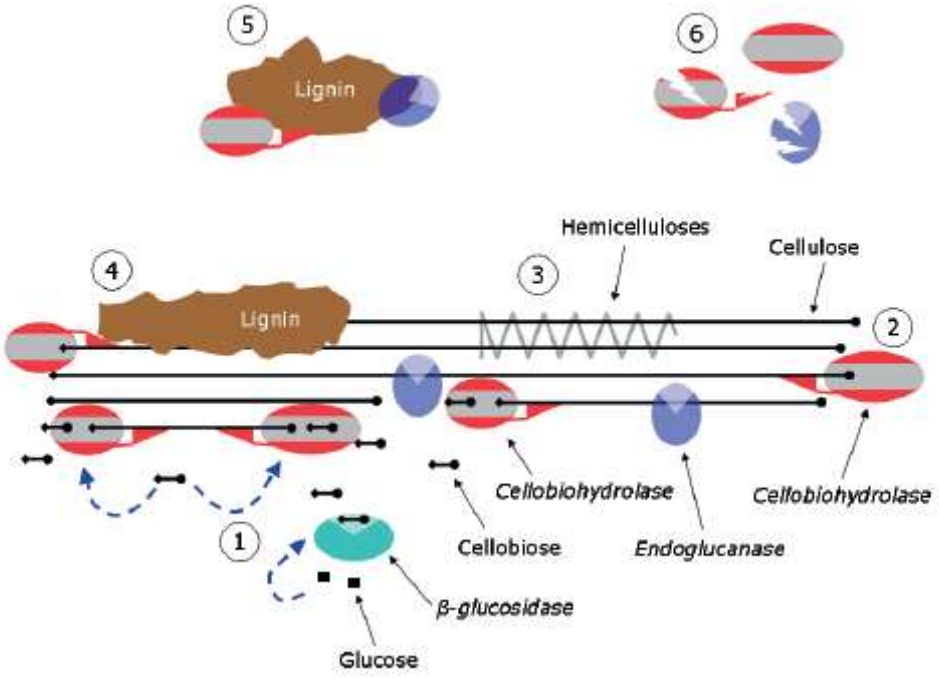

Figure 3. Simplistic overview of factors affecting the adsorption of cellulase and β-glucosidase enzyme on lignocellulosic biomass (Jørgensen et al., 2007-b)

Zhen et al. (2009) incorporated the negative role of lignin (nonproductive adsorption) using a Langmuir-type isotherm adsorption. Let *S* specify the concentration of pretreated substrate. The one component Langmuir isotherm for the adsorption of EG/CBH or β-glucosidase on *S* can be written as follow:

$$E_{1bS} = \frac{E_{1\max S} E_{1fS} S}{1 + K_{1adS} E_{1fS}} \tag{4}$$

$$E_{2bS} = \frac{E_{2\max S} E_{2fS} S}{1 + K_{2adS} E_{2fS}} \tag{5}$$

where 1=EG/CBH; 2=BG

Since EG/CBH is also adsorbed on lignin, and BG is adsorbed only on lignin, the Langmuir isotherms for EG/CBH and BG on lignin were expressed as follow:

$$E_{1bL} = \frac{E_{1\max L} E_{1fL} L}{1 + K_{1adL} E_{1fL}} \tag{6}$$

$$E_{2bL} = \frac{E_{2\max L} E_{2fL} L}{1 + K_{2adL} E_{2fL}} \tag{7}$$

where 1=EG/CBH; 2=BG

Due to the adsorption of EG/CBH on both cellulose and lignin, the amount adsorbed on the cellulose can be calculated by Equation 8 assuming a value for the ratio of lignin exposed to enzyme to the total lignin (η).

$$E_{1bC} = E_{1bS} - \eta E_{1bL} \tag{8}$$

5.2.2 Modeling substrate reactivity

5.2.2.1 Relative digestibility

All transformations of the substrate during the enzymatic hydrolysis are lumped into one parameter R_s, which is the normalized initial hydrolysis rate during the secondary hydrolysis of residual substrates. It is correlated with the normalized cellulose concentration C/C_0 as follow:

$$R_s = \alpha \frac{C}{C_0} \tag{9}$$

where R_s is a substrate reactivity parameter (dimensionless), α is a constant (dimensionless), C is the cellulose concentration at a given time (g/L) and C_0 is the initial cellulose concentration. Kadam et al. (2004) and Zhen et al. (2009) working with pretreated corn stover and rye grass respectively, reported that the best-fit value for α is closed to unit (0.97 and 1.007 respectively).

5.2.2.2 Recalcitrance

Drissen et al. 2007 pointed out that the decrease in susceptibility of the substrate towards the enzyme is because the easily hydrolysable cellulose is digested first and the more recalcitrant cellulose remains. To account for substrate recalcitrance, the following equation was used:

$$v = v_0 \exp[-K_{rec}(1 - C / C_0)] \tag{10}$$

were v is the *EG/CBH* activity, v_0 is the initial enzymatic hydrolysis rate of native Avicel (microcrystalline cellulose), K_{rec} is a recalcitrant constant calculated with data obtained by re-incubation of partially hydrolyzed substrate.

5.2.2.3 Reference substrate

Ljungren (2005) suggest the inclusion of a substrate dependent parameter C_{dp} (Crystallinity and degree of polymerization) set to 1 for a reference fast hydrolysable substrate and set relative to the reference substrate for others substrates. This was done by comparing the initial glucose production rates.

5.2.3 Modeling loss of mobility of adsorbed enzyme

Inactivation of cellulase adsorbed on the cellulose fraction of the substrate by loss of mobility (due to tight adsorption) and exposure to temperature and stirring has been

modeled as a first order kinetic (Gusakov et al., 1992; Drissen et al., 2007). It leads to a mechanism of exponential decay with respect to time.

$$\frac{dE_{1bC}}{dt} = -k_{D1bC}E_{1bC} \tag{11}$$

Thermal and mechanical inactivation of the enzyme in solution diminishes the amount of enzyme that can be reutilized by recycling or re-adsorption on fresh substrate, as well as the conversion of cellobiose. Quantification of active enzymes adsorbed or in solution, is vital for the design of operation strategies that allows diminishing enzyme consumption. However, up to now there are no major advances in this area, mainly due to analytical difficulties in activities experimental measurements.

6. Toward a generic kinetic model for the enzymatic hydrolysis of lignocellulosic substrates

The basic equation rate for the heterogeneous reactions (r_1, r_3) is the following (Kadam et al., 2004; Zheng et al., 2009):

$$r_1 = \frac{k_1 E_{1bC0} C}{1 + \frac{G_2}{k_{1IG2}} + \frac{G}{k_{1IG}}} \tag{12}$$

$$r_3 = \frac{k_3 E_{1bC0} C}{1 + \frac{G_2}{k_{3IG2}} + \frac{G}{k_{3IG}}} \tag{13}$$

were E_{1bC0} is the initial amount of EG/CBH adsorbed on cellulose calculated using Equation 7. The denominator represents the competitive inhibition by products. Equations 12 and 13 can be modified by adding terms related to substrate reactivity and enzyme deactivation, which as well as adsorbed enzyme, can be obtained by independent experiments. The modified rate equations for r_1 and r_3 (Equations 12 and 13) can be written as follow:

$$r_q^{'} = r_q \exp(-k_{D1bC} t) R_s \tag{14}$$

$$r_q^{'} = \frac{r_q v}{E_{1bC0}} \tag{15}$$

$$r_q^{'} = r \exp(-k_{D1bC} t) C_{dp} \tag{16}$$

were *q=1,3*, the exponential term represents inactivation of adsorbed enzyme concentration (Equation 11), and R_s (Equation 9), v (Equation 10), and C_{dp} (Section 5.2.2.3) are the three different forms proposed in the literature to incorporate substrate reactivity, which could be evaluated by analyzing initial reaction rates re-incubation of partially hydrolysed substrate to choose the best representation. The mechanism of exponential decay for the inactivation of adsorbed enzyme can be modeled with respect to time as in Equation 10, or with respect to cellulose conversion.

As kinetic expressions for homogeneous enzymatic reactions can be directly applied to the hydrolysis of cellobiose, there is consensus about the equation rate (Equation 17). However, cellobiase enzymes from different sources have shown different kinetic parameters (Gong et al., 1977; Lee and Fan, 1983; Dekker, 1986; Grous et al., 1985).

$$r_2 = \frac{k_2 E_{2fL} G_2}{k_{2M}\left[1 + \frac{G}{k_{2IG}}\right] + G_2} \tag{17}$$

7. Conclusions

The most recent kinetic models for the enzymatic hydrolysis of lignocellulosic biomass, useful for reactor design, were reviewed. Kinetic models were classified based on products as: three-reaction scheme, two-reaction scheme, and one-reaction scheme. Modeling of enzyme adsorption on cellulose and lignin, modeling of substrate reactivity, and modeling of enzyme deactivation were discussed. Although the enzymatic reaction is

very complex, with many enzymatic and substrate properties impacting reaction rates, it is important to highlight that there is consensus with regard to the main factors that must be incorporated and the general structure of the model. This review provides a solid foundation for future model refinements and proposes a model that takes all the factors that the works revised describe as affecting enzymatic hydrolysis rates.

8. Acknowledgements

The author acknowledges the financial support provided by FAPESP (The Scientific Research Foundation for the State of São Paulo).

References

Bansal P, Hall M, Realff MJ, Lee JH, Bommarius AS. 2009. Modeling cellulase kinetics on lignocellulosic substrates. Biotechnol Adv Doi:10.1016/j.biotechadv.2009.06.005.

Borchert A, Buchholz K. 1987. Enzymatic hydrolysis of cellulosic materials. Process Biochem 22:173-180.

Boussaid A, Saddler JN. 1999. Adsorption and activity profiles of cellulase during the hydrolysis of two Douglas fir pulps. Enzyme Microb Technol 24:138-143.

Dekker RFH. 1986. Kinetic, Inhibition, and Stability properties of a commercial β-D-Glucosidase (Cellobiase) preparation from *Aspergillus Niger* and its suitability in the hydrolysis of lignocellulose. Biotechnol Bioeng 28:1438-1442.

Drissen R, Maas R, Van-Der-Maarel M, Kabel M, Schols H, Tramper J, Beeftink H. 2007. A generic model for glucose production from various cellulose sources by a commercial cellulase complex. Biocatal Biotransform 25:419-429.

Dwivedi CP, Ghose TK. 1979. A model on hydrolysis of bagasse cellulose by enzyme from *Trichoderma Reesei* QM 9414. J Ferment Technol 57(1):15-24.

Eriksson T, Karlsson J, Tjerneld F. 2002. A model explaining declining rate in hydrolysis of lignocellulose substrates with cellobiohydrolase I (Cel7A) and endoglucanaggse I (Cel7B) of *Trichoderma reesei*. Appl Biochem Biotechnol 1001:41-60.

Fengel D, Wegner G. (1984). Wood: Chemistry, ultrastructure, reactions. De Gruyter, Berlin.

Gan Q, Allen SJ, Taylor G. 2003. Kinetic dynamics in heterogeneous enzymatic hydrolysis of cellulose: an overview, an experimental study and mathematical modeling. Process Biochem 38:1003-1018.

Ganesh K, Joshi JB, Sawant SB. 2000. Cellulase deactivation in a stirred reactor. Biochem Eng J 4:137-141.

Gong CS, Ladisch MR,Tsao GT. 1977. Cellobiase from *Trichoderma viride*: purification, properties, kinetics, and mechanism. Biotechnol Bioeng 19:959-968.

Gregg DJ, Saddler JN. 1996. Factors affecting cellulose hydrolysis and the potential of enzyme recycle to enhance the efficiency of an integrated wood to ethanol process. Biotechnol Bioeng 51:375-383.

Grous W, Converse A, Grethlein H, Lynd L. 1985. Kinetics of cellobiose hydrolysis using cellobiase composites from *Trichoderma reesei* and *Aspergillus niger*. Biotechnol Bioeng 27:463-470.

Gusakov AV, Sinitsyn AP, Manenkova JA, Protas OV. 1992. Enzymatic saccharification of industrial and agricultural lignocellulosic wastes. Appl Biochem Biotechnol 34:625-637.

Gusakov AV, Sinitsyn AP. 1985. Kinetics of the enzymatic hydrolysis of cellulose: 2. Aathematical model for the process in a plug-flow column reactor. Enzyme Microb Technol 7:383-388.

Himmel ME. 2008. Biomass recalcitrance, deconstructing the cell wall for bioenergy, 1 ed., Blacwell Publishing Ltd, United Kingdom.

Holtzapple Holtzapple MT, Caram HS, Humphrey AE. 1984-a. The HCH-1 model of enzymatic cellulose hydrolysis. Biotechnol Bioeng 26:775-780.

Holtzapple MT, Caram HS, Humphrey AE. 1984-b. Determining the inhibition constants of the HCH-1 model of cellulose hydrolysis. Biotechnol Bioeng 26:753-757.

Holtzapple M, Cognata M, Shu Y, Hendrickson C. 1990. Inhibition of Trichoderma reesei cellulase by sugars and solvents. Biotechnol Bioeng 36:275-287.

Howard RL, Abotsi E, Jansen van Rensburg EL, Howard S. 2003. Lignocellulose biotechnology: issues of bioconversion and enzyme production. Afr J Biotechnol 2:602–19.

Jackson LS, Heitmann JA, Joyce TW. 1993. Enzymatic modifications of secondary fiber. Tappi J 76:147-154.

Jørgensen H, Kristensen JB, Felby C. 2007-b. Enzymatic conversion of lignocellulose into fermentable sugars: challenges and opportunities. Biofuels Bioprod Biorefin 1:119-134.

Kadam KL, Rydholm EC, McMillan JD. 2004. Development and validation of a kinetic model for enzymatic saccharification of lignocellulosic biomass. Biotechnol prog 20:698-705.

Kelin GL, Snodgrass WR. 1993. Cellulose. In: R. Macre, R.K. Robinson, M.J. Saddler, Editors. Encyclopedia of food science, food technology and nutrition. London: Academic Press, 758-767.

Laureano-Perez L, Teymouri F, Alizadeh H, Dale BE. 2005. Understanding factors that limit enzymatic hydrolysis of biomass. Appl Biochem Biotechnol 124:1081-1099.

Lee YH, Fan LT. 1983. Kinetic studies of enzymatic hydrolysis of insoluble cellulose (II): analysis of extended hydrolysis times. Biotechnol Bioeng 25:936-966.

Lenz J, Esterbaurer H, Sattler W, Schurz J, Wrentschur E. 1990. Changes of structure and morphology of regenerated cellulose caused by acid and enzymatic hydrolysis. J Appl Polym Sci 41:1315-1326.

Ljunggren M. 2005. Kinetic analysis and modeling of enzymatic hydrolysis and SSF. MSc thesis, Department of Chemical Engineering, Lund University.

Lynd LR, Weimer PJ, van Zyl WH, Pretorius IS. 2002. Microbial cellulose utilization: Fundamentals and Biotechnology. Microbiol Mol Biol Rev 66(3):506-577.

Mansfield SD, Mooney C, Saddler JN. 1999. Substrate and enzyme characteristics that limit cellulose hydrolysis. Biotechnol Prog 15:804-816.

Medve J, Stahlberg J, Tjerneld F. 1997. Isotherms for adsorption of cellobiohydrolase I and II from *Trichoderma reesei* on microcrystalline cellulose. Appl Biochem Biotechnol 66:39-56.

Money CA, Manfield SD, Beatson RP, Saddler JN. 1999. Effect of fiber characteristics on hydrolysis and cellulase accessibility to softwood substrates. Enzyme Microb Technol 25:644-650.

Mosier N, Wyman C, Dale B, Elander R, Lee YY, Holtzapple M, Ladish M. 2005. Features of promising technologies for pretreatment of lignocellulosic biomass. Bioresour Technol 96:673-686.

Mukataka S, Tada M, Takahashi J. 1983. Effects of agitation on enzymatic hydrolysis of cellulose in a stirred-tank reactor. J ferment Technol 61:615-621.

Nakao K, Fukunaga K, Yasuda Y, Kimura M. 1990. Enzymatic hydrolysis of lignocellulosics with continuous irradiation of supersonic waves. Ann NY Acad Sci 613:802-807.

Ohmine K, Ooshima H, Harano Y. 1983. Study on enzymatic hydrolysis of cellulose by cellulase from *Trichoderma Viride*. Biotechnol Bioeng 20:637-663.

Ooshima H, Burns DS, Converse AO. 1990. Adsorption of cellulose from *Trichoderma reesei* on cellulose and lignacious residue in wood pretreated by dilute sulfuric acid with explosive decompression. Biotechnol Bioeng 36:446-452.

Peter W, Wojciechowski. 1996. Interfacial phenomena and bioproducts. Ed Bioprocess Technology, Berkeley California.

Philippides GP. 1996. Cellulose bioconversion technology, Handbook on bioethanol: production and utilization, ed by Charles Wyman, Taylor & Francis, 12, 0253-285.

Puls J, Wood TM. 1991. The degradation pattern of cellulose by extracellular cellulases of aerobic microorganisms. Biorecour Technol 36:15-19.

Ramos LP, Breuil C, Saddler JN. 1993. The use of enzymes recycling and the influence of sugar accumulation on cellulose hydrolysis by Trichoderma cellulases. Enzyme Microb Technol 15:19-25.

Rowell MR. 1992. Opportunities for lignocellulosic materials and composites. Emerging technologies for material and chemicals from biomass: Proceedings of symposium. Washington, DC: American Chemical Society; 1992. p. 26–31. Chap 2.

Rusell F, Holtzapple MT. 1990. A comparison of the Michaelis-Menten and HCH-1 models. Biotechnol Biong 36:1151-1154.

Shao X, Lynd L, Wyman C, Bakker A. 2009. Kinetic modeling of cellulosic biomass to ethanol via simultaneous saccharification and fermentation: Part I. Accomodation of intermittent feeding and analysis of staged reactors. Biotechnol Bioeng 102:59-69.

Sinitsyn AP, Mitkevich OV, Gusakov AV, Klyosov AA. 1989. Decrease in reactivity and change of physico-chemical parameters of cellulose in the course of enzymatic hydrolysis. Carbohydr Polym 10:1-14.

South CR, Hogsett DAL, Lynd LR. 1995. Modeling simultaneous saccharification and fermentation of lignocellulose to ethanol in batch and continuous reactors. Enzyme Microb Technol. 17:797-803.

Tanaka M, Nakamura H, Taniguchi M, Morita T, Matsumo R, Kamikubo T. 1986. Elucidation of adsorption processes of cellulases during hydrolysis of crystalline cellulose. Appl Microbiol Biotechnol 23:263-268.

Wald S, Wilke CR, Blanch HW. 1984. Kinetic of enzymatic hydrolysis of cellulose, Biotechnol Bioeng 26:221-230.

Zhang RH, Zhang ZQ. 1999. Biogasification of rice straw with an aerobic-phased solids digester system. Bioresour Technol 68:235-245.

Zhang YP, Lynd LR. 2004. Toward and Aggregated Understanding of Enzymatic Hydrolysis of Cellulose: Noncomplexed Cellulase systems. Biotechnol Bioeng 88(7):797-824.

Zheng Y, Zhongli P, Zhang R, Jenkins BM. 2009. Kinetic modeling for enzymatic hydrolysis of pretreated creeping wild ryegrass, Biotechnol Bioeng 102(6):1558-1569.

Zhu L, O'Dwyer JP, Chang VS, Branda CB, Holtzapple MT. 2008. Structural features affecting biomass enzymatic digestibility. Bioresour Technol 99:3817-3828.

2.3 Conclusões

Neste capítulo foram levantados os modelos cinéticos da reação de hidrólise enzimática de substratos lignocelulósicos com ênfase nos modelos apropriados para otimização, avaliação econômica e projeto de sistemas de reação. Os modelos foram classificados de acordo com os produtos considerados como: esquema de uma reação, esquema de duas reações e esquema de três reações. A modelagem da adsorção das enzimas sobre celulose e lignina, a modelagem da reatividade do substrato e a modelagem da desativação das enzimas são discutidas. Apesar da complexidade da reação de hidrólise enzimática é importante ressaltar que há consenso a respeito da estrutura geral do modelo cinético. A revisão aqui apresentada é uma boa base para futuros refinamentos na modelagem cinética da hidrólise enzimática de substratos lignocelulósicos.

O esquema mais geral da reação de hidrólise enzimática é o de três reações que incluem duas reações heterogêneas para a produção de glicose e celobiose a partir da celulose é uma reação homogênea para a produção de glicose a partir de celobiose. Ao contrario da reação homogênea onde a taxa de reação é proporcional á atividade da β-glicosidase na solução, as reações heterogêneas dependem da quantidade de enzima adsorvida na celulose. Porém, a modelagem da adsorção tem de incluir o papel negativo da lignina como adsorvedor das enzimas e como bloqueador da depolimerização da celulose. Os fatores adicionais que deveriam ser incluídos no modelo cinético são: a reatividade do substrato para levar em conta as transformações do substrato durante a reação, e a desativação das enzimas devida a efeitos térmicos, mecânicos e de perda de mobilidade. A reatividade do substrato e a desativação das enzimas podem ser estudadas através de experimentos independentes dos usados para o ajuste de parâmetros cinéticos restantes com o objetivo de tornar o modelo cinético mais robusto. A inclusão destes fatores no modelo cinético possibilita a avaliação de estratégias de alimentação de substrato e enzima, assim como fechar o balanço de enzima ativa.

Na falta de dados experimentais da adsorção e de outras propriedades do substrato além da concentração (como acontece em trabalhos exploratórios), um modelo cinético pseudo-homogêneo (de uma reação) foi utilizado neste trabalho como descrito no Capítulo 3. Se não houver acúmulo de celobiose durante a hidrólise, a produção de glicose pode ser predita satisfatoriamente. Se houver acúmulo de celobiose, o produto considerado deveriam

ser açúcares redutores totais, ao invés de glicose. Porém, a aplicabilidade deste modelo cinético no projeto de reatores é limitada já que este não permite estudar o efeito das cargas enzimáticas de celulase e β-glicosidase na produção de glicose.

No próximo capítulo será apresentado em detalhe um modelo cinético pseudo-homogêneo. O modelo será ajustado com dados cinéticos da hidrólise enzimática de bagaço de cana prétratado com peróxido de hidrogênio alcalino obtidos no Laboratório de Engenharia de Processos Fermentativos e Enzimático (LEPFE) da Faculdade de Engenharia Química da Universidade Estadual de Campinas (UNICAMP).

Capítulo 3 – Modelagem Cinética da Hidrólise Enzimática de Bagaço de Cana Pré-tratado com Peróxido de Hidrogênio Alcalino

3.1. Introdução

A conversão da fração celulósica da biomassa lignocelulósica em açúcares fermentescíveis tem ganho um interesse considerável na última década devido ao seu potencial para a produção de etanol. No Brasil, o bagaço de cana é uma matéria prima com grande potencial para a produção de etanol via hidrólise enzimática. O bagaço de cana é hidrolisado após um pré-tratamento para tornar o substrato mais susceptível à digestão causada pelas enzimas. A hidrólise enzimática é uma etapa critica do processo em termos técnicos e econômicos, de forma que, um modelo cinético se constitui numa ferramenta imprescindível na modelagem, simulação, otimização e controle dos reatores de hidrólise.

Este capítulo se dedica a apresentar um modelo cinético pseudo-homogêneo, ajustado com dados experimentais da hidrólise enzimática de bagaço de cana pré-tratado com peróxido de hidrogênio alcalino. São discutidos a estrutura do modelo, a inclusão da predição do perfil de xilose a partir do perfil de glicose, o ajuste dos parâmetros cinéticos e os alcances e limitações do modelo cinético.

3.2 Obtençao dos dados experimentais (Reis, 2008)

3.2.1 Pretratamento do bagaço

Antes que se utilizasse o bagaço para qualquer análise, este material foi seco ao tempo (por um período de quatro dias), moído em moinhos de facas Wiley Mill modelo n° 3 e de martelo General Eletronic durante 10 minutos em cada moinho, para que apresentasse maior uniformidade. Posteriormente, foi peneirado usando peneira Tyler 35 para todas as análises, exceto para a determinação de extrativos, e armazenado em freezer em sacos plásticos hermeticamente fechados e identificados. O pré-tratamento foi realizado nas condições ótimas determinadas por Reis (2008), 1 h de reação, 25ºC, 11% de peróxido, 8 g de bagaço em 100 mL de solução, pH de 11,5.

3.2.2 Hidrólise enzimática

Para avaliar a influência da variação de massa de bagaço na cinética de hidrólise, foram consideradas diferentes massas deste substrato: 1, 2, 3, 4 e 5 g, em 100 mL de solução (água destilada e azida de sódio). A azida foi adicionada para evitar a proliferação de microorganismos que pudessem interferir neste processo. O pH foi 4,8, a temperatura de 50ºC e a rotação foi mantida em 150 rpm em incubadora. A máxima concentração de bagaço possível de se trabalhar nas condições experimentais deste trabalho foi de 5%.

Alíquotas foram retiradas em intervalos de 10 min, 20 min, 30 min, 40 min, 50 min, 1 h, 3 h, 6 h, 12 h, 24 h, 36 h, 48 h, 60 h e 72 h e as leituras foram feitas em HPLC com detector de índice de refração. Foi possível quantificar celobiose, glicose, xilose e arabinose. Nesta etapa foi empregada carga enzimática de 500 FPU/L de celulase e 500 CBU/L de β-glicosidade, fixas para todas as porcentagens de sólidos. Estas concentrações de enzima correspondem a concentrações na faixa de 50 FPU/g biomassa e 50 CBU/g biomassa (para a concentração de 1% de bagaço) a 10 FPU/g de biomassa e 10 CBU/g biomassa (para a concentração de 5% de bagaço). Todos os experimentos foram realizados em triplicata.

3.3. Desenvolvimento

O desenvolvimento deste capítulo é apresentado a seguir, no manuscrito intitulado *Kinetic Modeling of the Enzymatic Hydrolysis of Sugarcane Bagasse Pretreated with Alkaline Hydrogen Peroxide.*

Kinetic Modeling of the Enzymatic Hydrolysis of Sugarcane Bagasse Pretreated with Alkaline Hydrogen Peroxide.

Abstract

A semimechanistic one-reaction kinetic model was used to describe the enzymatic hydrolysis of Sugarcane Bagasse pretreated with alkaline hydrogen peroxide. The model assumes that there is no cellobiose accumulation, employs one pseudo-homogeneous reaction of cellulose-to-glucose, and predicts xylose concentration based on the glucose concentration. Local and global parameter estimation techniques were employed to estimate kinetic parameters based on experimental data generated under 1%, 2%, 3%, 4%, and 5% (w/w, dry basis) initial substrate concentrations, corresponding to enzyme loadings of 50, 25, 16.7, 12.5, and 10 FPU-CBU/g-substrate, respectively. The kinetic model satisfactorily simulates glucose and xylose yields over the design space. The present model can serve as a tool for process simulation and reactor optimization and design in the absence of experimental data on enzyme adsorption and substrate features others than concentration.

Keywords: *enzymatic hydrolysis; kinetic model; glucose; xylose; sugarcane bagasse*

1. Introduction

The conversion of biomass, specifically lignocellulosic biomass, into fuels and chemicals via enzymatic hydrolysis has gained considerable interest in the last decade because of its potential to provide reducing sugars, which serve as a raw material for ethanol production. In Brazil, sugarcane bagasse, the major by-product of the sugarcane industry, seems to be economically viable for ethanol production via enzymatic hydrolysis (Rabelo et al., 2007). Sugarcane bagasse is hydrolyzed after a previous pretreatment to decrease the recalcitrance and make cellulose more susceptible to digestion by enzymes. The enzymatic hydrolysis step is still a critical cost step in the overall bioconversion

process (Zheng et al., 2009). In this context, a kinetic model of the enzymatic hydrolysis could be a useful forecasting tool for optimization and economic evaluation.

The full extent of the complexity of the enzymatic hydrolysis of lignocellulosic biomass is not represented in any quantitative model proposed to date (Shao et al., 2009). According to the classification of Zhang and Lynd (2004), semimechanistic models with respect to substrate or with respect to enzyme, usually intended for optimization and economic evaluation, take a minimalist approach in which only those phenomena and parameters needed to describe the observed behavior are included. A kinetic model that considers the concentration as the only substrate state variable and a single enzymatic activity fits in this category and is used here.

In this work, sugarcane bagasse pretreated with alkaline hydrogen peroxide was hydrolysed at initial substrate concentrations of 1%, 2%, 3%, 4%, and 5% w/w (dry basis), and enzyme loadings of 50, 25, 16.7, 12.5, and 10 FPU-CBU/g-substrate (FPU/CBU ratio 1), respectively. A simplified kinetic model was fitted to predict the time course of glucose and xylose production under the various operation conditions. Local and global parameter estimation techniques were employed to estimate kinetic parameters based on experimental data.

2. Kinetic model

Because lignocellulosic biomass is an insoluble substrate and enzymes are soluble catalysts, enzymatic hydrolysis is a heterogeneous catalytic process. The most recent reports in the literature describe the reaction system as consisting of three reactions (Kadam et al., 2004; Drissen et al., 2007; Zheng et al., 2009): (*i*) a heterogeneous reaction for glucose production from cellulose catalyzed by endoglucanase (EG) and cellobiohydrolase (CBH) enzymes adsorbed onto cellulose, (*ii*) a heterogeneous reaction for cellobiose production from cellulose catalyzed by EG and CBH enzymes adsorbed onto cellulose, and (*iii*) a homogeneous reaction for glucose production from cellobiose catalyzed by β-glucosidase (BG) enzymes in solution. The heterogeneous reactions under a synergistic action of EG and CBH may be considered to govern the overall rate of saccharification.

Results collected by Kristensen et al. (2009) indicate that decreasing conversion at increasing initial substrate concentrations is a general effect for enzymatic hydrolysis of

different kinds of biomass. With respect to enzymes, glucose yield can be limited by either low EG/CBH concentration or low BG concentration. Unlike a homogeneous system where the reaction rate is first order in enzyme concentration, in the enzymatic hydrolysis an adsorption process is controlling (Wald et al., 1984). If the enzyme loading is increased maintaining a high enough BG loading to avoid cellobiose accumulation, glucose yield will reach a maximum because the substrate becomes saturated with enzyme. For initial substrate concentrations for which a sufficient mobile phase remains in the reaction to ensure adequate enzyme mobility, the enzyme/substrate ratio will provide information concerning the adsorption process. In addition, if there is no cellobiose accumulation, the glucose yield can be predicted with a simplified kinetic model of one apparent reaction rate.

2.1 Reaction rate

In this work the kinetic model proposed by Nakao et al. (1990) was fitted to experimental profiles of glucose of the enzymatic hydrolysis of sugarcane bagasse pretreated with alkaline hydrogen peroxide. The reaction rate is given by the following equation**:**

$$\frac{dG}{dt} = \frac{v_{mG}(G^{\inf} - G)}{k_{mG}\left(1 + \frac{G}{k_{inh}}\right) + 0.9(G^{\inf} - G)} \tag{1}$$

where glucose (G) is produced from a hypothetical soluble substrate (S^h=G^{inf}-G) whose initial concentration corresponds to the concentration of glucose produced ultimately (G^{inf}), assuming a Michaelis-Menten mechanism with competitive inhibition by glucose. v_{mG}, k_{mG}, and k_{inh} are the apparent rate constant, the apparent Michaelis-Menten constant, and the apparent inhibition constant, respectively. The constant 0.9 is the ratio of the molecular weight of glucose unit in cellulose to that of glucose. k_{mG} and k_{inh} are assumed as intrinsic to the reaction system while v_{mG} is assumed as dependent on the enzyme/substrate ratio and fitted as a function of substrate concentration. It should be noted that v_{mG} results from grouping a rate constant and the enzyme concentration.

As the pretreatment with alkaline hydrogen peroxide does not remove all the hemicelluloses from the bagasse and commercial cellulase enzymes have xylanase activity

(Juhász et al., 2005; Chen et al., 2007), significant amounts of xylose (*Xy*) were released during the enzymatic hydrolysis of sugarcane bagasse pretreated with alkaline hydrogen peroxide. Instead of predict xylose concentration with an independent reaction rate, it was related to glucose concentration (Equation 2). It implies that xylan hydrolysis is directly proportional to cellulose hydrolysis (i.e. xylanase adsorption is directly proportional to cellulase adsorption).

$$Xy = k_{Xy} G^{v_{Xy}} \tag{2}$$

k_{Xy} is assumed intrinsic to the reaction system, while v_{Xy} is assumed as dependent on the enzyme/substrate ratio and fitted as a function of substrate concentration.

3. Materials and methods

3.1 Substrate and enzyme

Sugarcane bagasse was initially pretreated with alkaline hydrogen peroxide (11%, w/w) at 25ºC for 1 h. The pretreated sugarcane bagasse slurry was washed to remove the solubilized contents, and then the solid fraction was used in this study as a model substrate which was composed of 60% cellulose, 17% xylan, and 10% lignin (mass fraction on dry basis). The enzymes used for hydrolysis were cellulase (Sigma-Aldrich ATCC 26921) and β-glucosidase (Novo 188). Cellulase and β-glucosidase had respective activities of 64 FPU/mL and 309 CBU/mL.

3.2 Enzymatic hydrolysis

The experimental data were generated under the following conditions: total working weight of 100 g; enzyme concentration of 0.5 FPU/g-slurry supplemented with extra β-glucosidase of 0.5 CBU/g-slurry; substrate concentrations of 1%, 2%, 3%, 4%, and 5%; incubation temperature 50ºC; pH = 4.8; shaking speed of 150 rpm; total incubation time of 72 h; and sampling times of 0.17, 0.33, 0.5, 0.67, 0.83, 1, 3, 6, 12, 24, 36, 48, 60, and 72 h.

3.3 Sampling and analysis

The samples were kept in boiling water for ten minutes to inactivate enzymes and then filtered to remove the unreacted substrate. The glucose, cellobiose, xylose and arabinose in supernatant of liquid samples were analyzed on a high-performance liquid chromatograph (Waters Corporation, Massachusetts, USA) equipped with a refractive index detector. The separation was performed in a Sugar-Pak I column (Waters Corporation, Massachusetts, USA) at 70 °C with a flow rate of 0.5 mL/min, using filtered deionized water as the mobile phase.

3.4 Parameter estimation

The kinetic parameters of the glucose production rate (v_{mG}, k_{mG}, and k_{inh} of Equation 1) were estimated by minimizing an objective function. Let θ specify a kinetic parameters vector, which contains all kinetic rate constants. The optimal kinetic parameter vector was found out by minimizing the objective function $F_G(\theta)$:

$$F_G(\theta) = \sum_{k}^{np} \sum_{l}^{ns} \left(\frac{G_{l,k}^{p} - G_{l,k}^{e}}{G_k^{\inf}} \right)^2 \tag{3}$$

where np, ns, $G^p_{l,k}$, $G^e_{l,k}$, and G^{inf}_k are the number of experimental profiles, the number of experimental sampling points, the predicted glucose concentration for the profile k at the sampling point l, the experimental glucose concentration for the profile k at the sampling point l, and the ultimate glucose concentration for the profile k, respectively. $G^p_{l,k}$ was obtained by the time-integration of Equation 1. Five time-profiles of batch glucose production corresponding to initial substrate concentrations of 1%, 2%, 3%, 4%, and 5% with an enzyme/substrate ratio of 50, 25, 16.7, 12.5 and 10, respectively, were used to fit the kinetic model.

Subsequently, the kinetic parameters of the mathematical expression of xylose production (k_{Xy} and v_{Xy} of Equation 2) were estimated by minimizing an objective function similar to the aforementioned for glucose. The optimal kinetic parameter vector was found out by minimizing the objective function $F_{Xy}(\theta)$:

$$F_{Xy}(\theta) = \sum_{k}^{np} \sum_{l}^{ns} \left(\frac{Xy_{l,k}^{p} - Xy_{l,k}^{e}}{Xy_{k}^{\inf}} \right)^2 \quad (4)$$

where $Xy^{p}_{l,k}$, $Xy^{e}_{l,k}$, and Xy^{inf}_{k} are the predicted xylose concentration for the profile k at the sampling point l, the experimental xylose concentration for the profile k at the sampling point l, and the ultimate xylose concentration for the profile k, respectively.

A genetic algorithm (Charbonneau, 2002) available electronically from the anonymous .ftp archive of the High Altitude Observatory (http://www.download.hao.ucar.edu/archive/pikaia) was used to obtain an appropriate initial guess of the kinetic parameters, which was inserted in a Levenberg-Maquard algorithm (routine DRNLIN of the IMSL MATH LIBRARY FORTRAN-90) for finalizing the parameter estimation procedure.

4. Results and discussion

Figure 1 shows the order of magnitude of the sugars concentrations at different reaction times. Glucose and xylose were the major sugars released during hydrolysis, while arabinose was not released in significant quantities. The first 3 h of hydrolysis were characterized by the rapid production of sugars. Cellobiose concentration reaches its maximum value between 3 and 6 h, while glucose and xylose exhibit an upward trend that passes through a transition (12-24 h) followed by a region of slow production. Cellobiose concentrations for initial substrate concentrations up to 3% were not significant. For the experiment with the higher initial substrate concentration, (5%) corresponding to the lower enzyme/substrate ratio (10 FPU-CBU/g-substrate), cellobiose exhibits an upward trend during the first 6 h of reaction but it does not reach values higher than 1.4 g/L and later it drops to 0.6 g/L at 72 h of reaction.

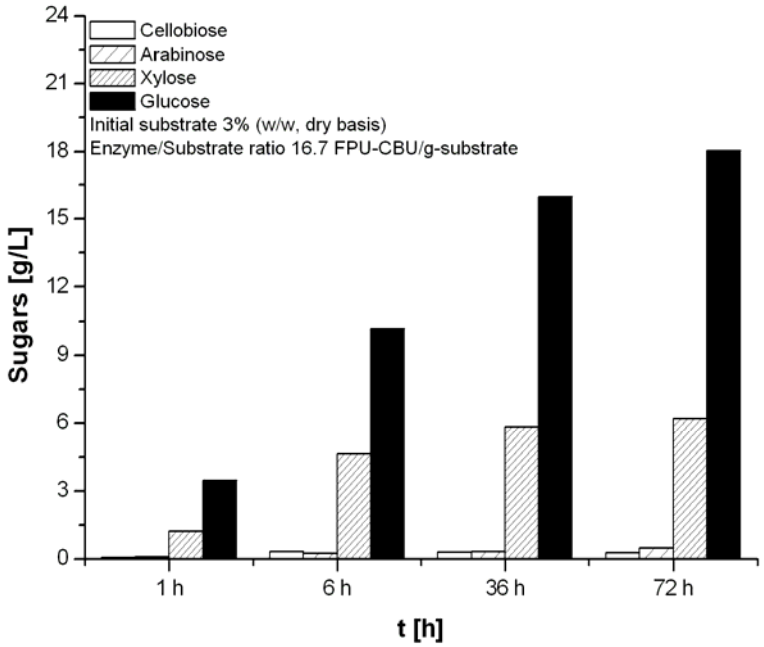

a)

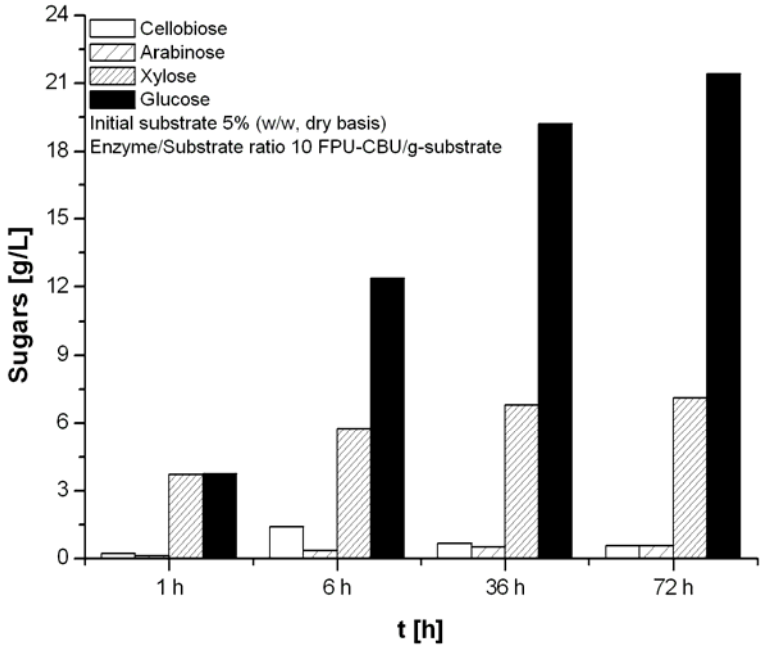

b)

Figure 1. Sugars released at different reaction times; initial substrate concentration of a) 3%, b) 5%

The dependence of cellulose conversion (X_C) (Equation 5) on enzyme/substrate ratio exhibits a similar pattern at different times of reaction. The cellulose conversion is proportional to the enzyme substrate ratio (i.e. inversely proportional to initial substrate concentration under the experimental conditions reported here). The trend observed (Figure 2) is similar to that reported by Wald et al. (1984) during the enzymatic hydrolysis of rice straw. Due to the heterogeneous nature of the system, the hydrolysis rate, mainly at the beginning of the reaction, is proportional to the enzyme adsorbed on the cellulose fraction of the substrate. It should be noted that this manner of correlating the data obscures the effect of concentration of the products and substrate. For instance, an enzyme substrate ratio of 50 FPU-CBU/g-substrate had an initial substrate concentration of 1% and the concentration of glucose (inhibitor) reach 5.130 g/L, while an enzyme substrate ratio of 10 FPU-CBU/g-substrate had a initial substrate concentration of 5% and the concentration of glucose (inhibitor) reach 21.53 g/L

$$X_C = \frac{0.9G}{C_0} \tag{5}$$

where C_0 is the initial content of cellulose in the substrate, and the constant 0.9 is the ratio of the molecular weight of glucose unit in cellulose to that of glucose.

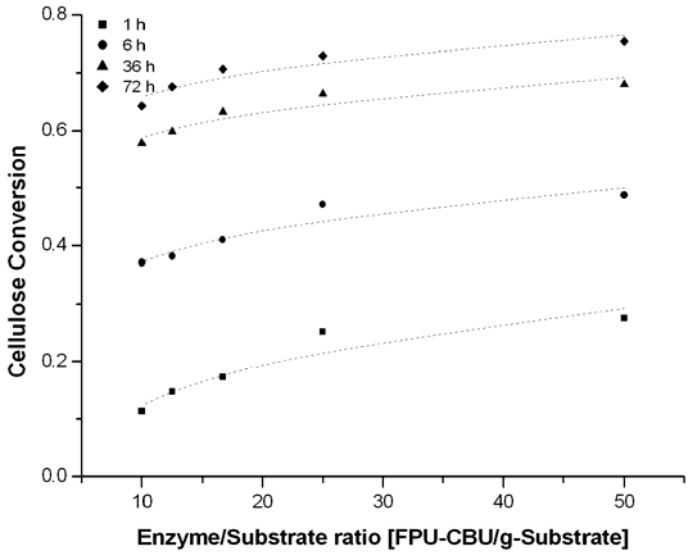

Figure 2. Dependence of cellulose conversion on enzyme/substrate ratio using initial substrate concentrations from 1% to 5%

Enzyme loading is implicit in the parameter v_{mG} which depends on the contact efficiency between insoluble substrate and enzymes in solution, and hence, on the properties of the substrate as well as the various operating conditions such as reactor type and size, mixing, substrate concentration, enzyme loading, etc. Enzyme loading is implicit in the parameter v_{mG}, thereafter it was estimated for each experimental profile, and subsequently related to the substrate concentration. An expression similar to Equation 1 was fitted to experimental profiles of enzymatic hydrolysis of various paper pulps by Li et al. (2004). For each pulp a good agreement was obtained between the simulated and experimental profiles assuming the parameters k_m and k_{inh} as intrinsic to the reaction system and the parameter v_m as dependent on the initial pulp concentration. The same assumption with respect to parameters k_m and k_{inh} were made in this work.

During enzymatic hydrolysis of sugarcane bagasse pretreated with alkaline hydrogen peroxide, significant amounts of xylose are released (Figure 1). Xylose profiles exhibit a similar pattern to the glucose profiles, for this reason an attempt was made to predict xylose production like a function of glucose concentration (Equation 2). The xylose/glucose ratio shows a value nearly constant for reaction times higher than 24 h and the mathematical form of Equation 2 reflects this fact. Despite not having a solid mechanistic basis, the prediction of xylose concentration presented here is very important in reactor design to assess the potential of ethanol production from xylose.

Table 1. Estimated kinetic parameters

Enzyme/Substrate ratio [FPU-CBU/g-substrate]	**10.0**	**12.5**	**16.7**	**25.0**	**50.0**
Initial Substrate [w/w %, dry basis]	**5**	**4**	**3**	**2**	**1**
G^{inf} [g/L]	21.53	18.04	14.24	9.734	5.130
v_{mG} [g/Lh]	249.3	235.6	204.0	169.5	82.23
v_{Xy} [g/L]	1.865	1.658	1.599	1.588	1.175
k_{mG} [g/L]	1.005				
k_{Xy} [g/L]	$4.475*10^{-1}$				
k_{inh} [g/L]	$3.161*10^{-3}$				

For modeling purposes the enzyme/substrate ratio ($R_{E/S}$), G^{inf}, and v_{mG} were correlated over the design space with the initial substrate concentration (S_0) by Equations 6, 7, and 8.

$$R_{E/S} = 50.01 S_0^{-0.9998} \qquad r^2 = 1 \tag{6}$$

$$G^{\inf} = 4.101 S_0 + 1.409 \qquad r^2 = 0.9964 \tag{7}$$

$$v_{mG} = 104.5 \ln(S_0) + 88.08 \qquad r^2 = 0.9904 \tag{8}$$

were r is the correlation coefficient.

For each experimental profile of glucose, a satisfactory agreement was obtained between the simulated and observed time courses (Figure 3), which confirms the applicability of the kinetic model and the assumption of the constant values for both k_{mG} and k_{inh} independent of the enzyme/substrate ratio. It was found that the influence of the enzyme/substrate on the parameter v_{mG} was more significant at initial substrate concentrations lower than 3% (Table 1).

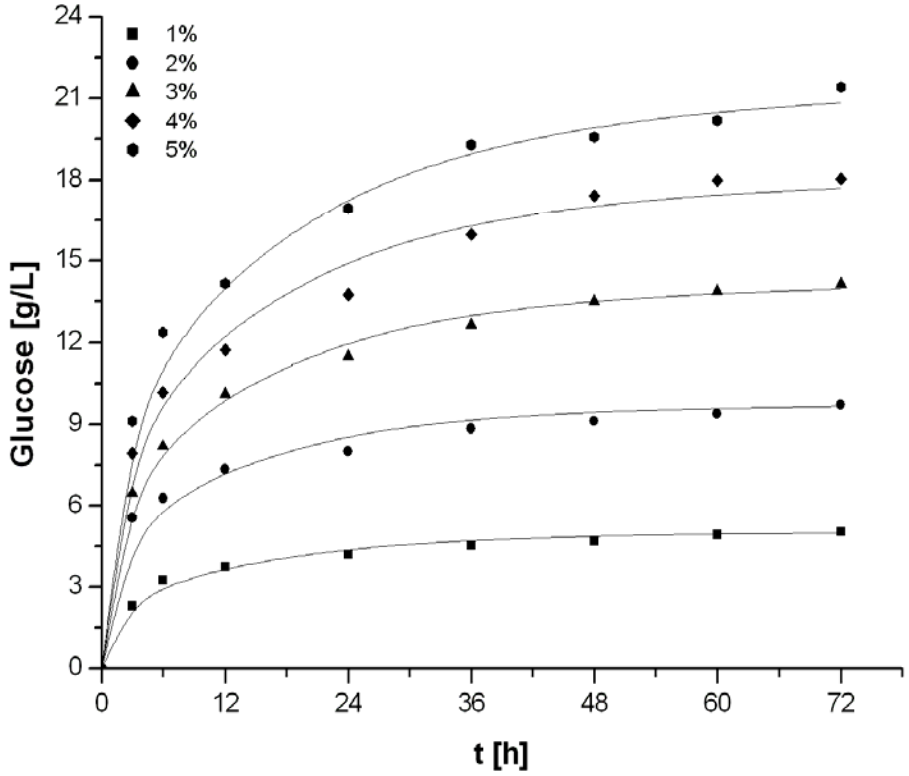

Figure 3. Model prediction (continuous line) and experimental values of glucose concentration for initial substrate concentrations of 1%, 2%, 3%, 4%, and 5% corresponding to enzyme/substrate ratios of 50, 25, 16.7, 12.5 and 10 FPU-CBU/g-substrate

In contrast to v_{mG}, v_{xy} did not show a good correlation with S_0 over all the design space, although it shows an upward trend similar to that of v_{mG}. For modeling purposes v_{xy} can be correlated with satisfactory accuracy for S_0 values ranged from 2% to 5% (Equation 9). The predicted glucose concentration was more accurate than the predicted xylose concentration. The model closely simulated the xylose concentration for reaction times higher than 24 h, but for reaction times of 6 h and 12 h and initial substrate concentration of 4% and 5%, the predicted xylose concentrations were lower than the experimental ones (Figure 4). This is understandable considering that the empirical equation used for prediction had only two adjustable parameters and depended on glucose concentration profile. Nevertheless, bearing in mind that to date there are not mechanistic kinetic models that incorporate xylan hydrolysis, the model remains useful for predictions.

$$v_{Xy} = 1.581 + (3.906E - 4)^{(1.318S_0)} \qquad r^2 = 0.9998 \tag{9}$$

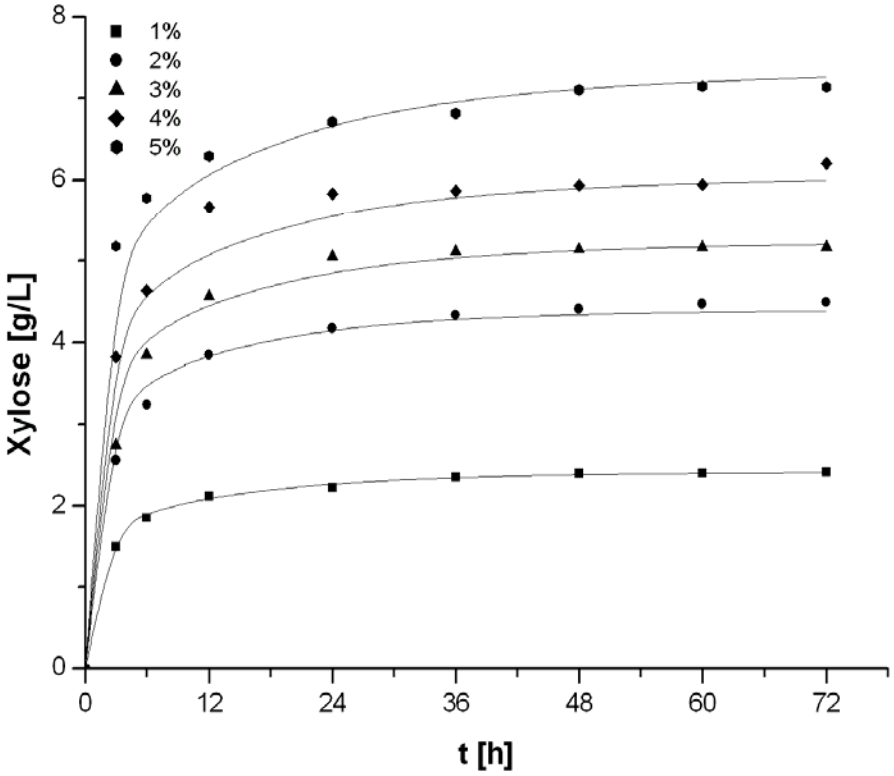

Figure 4. Model prediction (continuous line) and experimental values of xylose concentration using substrate concentrations of 1%, 2%, 3%, 4%, and 5% corresponding to enzyme/substrate ratios of 50, 25, 16.7, 12.5 and 10 FPU-CBU/g-substrate

It should be noted that the kinetic modeling reported here is intended for data correlation, reactor design, and identification of essential features of the reaction system. The kinetic model is especially useful in the absence of experimental data on enzyme adsorption and substrate features others than concentration. The initial substrate concentrations under which the experiments were carried out is beneath the upper limit at which biomass can be mixed and hydrolyzed in conventional stirred-tank reactors (10%-

12%) (Kristensen et al., 2009), thus the current kinetic model will be used in a next work to predict residence times, and glucose and xylose yields in continuous reactors.

5. Conclusions

A semimechanistic one-reaction kinetic model was fitted for a batch enzymatic hydrolysis of alkaline hydrogen peroxide pretreated sugarcane bagasse. The kinetic parameters were estimated for an initial substrate concentration of 1%, 2%, 3%, 4%, and 5% (w/w, dry basis) with enzyme/substrate ratios of 50, 25, 16.7, 12.5, and 10 FPU-CBU/g-substrate, respectively. The combination of global searching (genetic algorithm) and local optimization (Levenberg Maquardt) techniques was successful to solve the kinetic parameter optimization problem. In general, this model can simulate glucose and xylose concentration over the design space with reasonable accuracy. This model differs from previous models in that it predicts xylose concentration based on glucose concentration. This model can serve as a tool for data correlation and reactor design, especially in the absent of experimental data on enzyme adsorption and substrate features others than concentration.

6. Acknowledgements

The author acknowledges the financial support provided by PAPESP (The Scientific Research Foundation for the State of São Paulo).

References

Charbonneau P. 2002. Release notes for PIKAIA 1.2 NCAR Technical Note 451+IA (Boulder: National Center for Atmospheric Research).

Chen M, Jing Z, Liming X. 2007. Enzymatic hydrolysis of maize straw polysaccharides for the production of reducing sugars. Carbohyd Polym 71:411-415.

Drissen R, Maas R, Van-Der-Maarel M, Kabel M, Schols H, Tramper J, Beeftink H. 2007. A generic model for glucose production from various cellulose sources by a commercial cellulase complex. Biocatal Biotransform 25:419-429.

Juhász T, Szengyel Z, Réczey K, Siika-Aho M Viikari L. 2005. Characterization of cellulases and hemicellulases produced by *Trichoderma reesei* on various carbon sources. Process Biochem 40:3519-3525.

Kadam KL, Rydholm EC, McMillan JD. 2004. Development and validation of a kinetic model for enzymatic saccharification of lignocellulosic biomass. Biotechnol Progr 20:698-705.

Kristensen JB, Felby C, Jørgensen H. 2009. Yield-determining factors in high-solids enzymatic hydrolysis of lignocellulose. Biotechnol Biofuels. Doi 10.1186/1754-6834-2-11.

Li C, Yoshimoto M, Tsukuda N, Fukunaga K, Nakao K. 2004. A kinetic study on enzymatic hydrolysis of a variety of pulps for its enhancement with continuous ultrasonic irradiation. Biochem Eng J 19:155-164.

Nakao K, Fukunaga K, Yasuda Y, Kimura M. 1990. Enzymatic hydrolysis of lignocellulosics with continuous irradiation of supersonic wave. Ann NY Acad Sci 613:802-807.

Rabelo SC, Maciel Filho R, Costa AC. 2007. A comparisson between lime and alkaline hydrogen peroxide pretreatments of sugarcane bagasse for ethanol production. Appl Biochem Biotechnol 100:87-100.

Shao X, Lynd L, Wyman C, Bakker A. 2009. Kinetic modeling of cellulosic biomass to ethanol via simultaneous saccharification and fermentation: Part I. Accomodation of intermittent feeding and analysis of staged reactors. Biotechnol Bioeng 102:59-69.

Wald S, Wilke CR, Blanch HW. 1984. Kinetic of enzymatic hydrolysis of cellulose, Biotechnol Bioeng 26:221-230.

Zhang YP, Lynd LR. 2004. Toward and aggregated understanding of enzymatic hydrolysis of cellulose. Biotechnol Bioeng 26:221-230.

Zheng Y, Zhongli P, Zhang R, Jenkins BM. 2009. Kinetic modeling for enzymatic hydrolysis of pretreated creeping wild ryegrass. Biotechnol Bioeng 102(6):1558-1569.

3.3. Conclusões

Neste capítulo foi apresentado e ajustado um modelo cinético pseudo-homogêneo para a hidrólise enzimática de bagaço de cana pré-tratado com peróxido de hidrogênio alcalino. Os parâmetros cinéticos foram estimados para concentrações iniciais de substrato de 1%; 2%; 3%; 4% e 5% w/w (base seca) correspondentes a razões enzima/substrato de 50; 25; 16,7; 12,5; e 10 FPU-CBU/g-substrato. A combinação de um algoritmo de busca global (algoritmo genético) e um algoritmo de otimização local (Levenberg Maquardt) mostrou-se robusta na solução do problema de estimação de parâmetros.

O modelo difere de outros modelos publicados na literatura em que prediz a concentração de xilose a partir da concentração de glicose. Em geral o modelo serve para simular a concentração de glicose e xilose na faixa de concentrações em que foi ajustado. O modelo é uma ferramenta útil na correlação de dados experimentais e no projeto de reatores, especialmente devido a falta de dados experimentais da adsorção de enzimas e propriedades do substrato diferentes da concentração.

Tendo sido apresentados o levantamento de modelos cinéticos e a modelagem cinética da hidrólise enzimática de bagaço de cana, o capítulo seguinte apresenta o projeto de reatores contínuos de tanque agitado e do reator tubular. A modelagem faz uso do modelo cinético apresentado neste capítulo, mas os dados experimentais foram tomados da literatura. Isso se justifica, pois a modelagem e simulação foram realizadas antes dos dados experimentais referidos neste capítulo estarem disponíveis. O leitor interessado nos resultados obtidos fazendo uso do modelo ajustado neste capítulo pode passar diretamente ao capítulo 5, o qual além da modelagem apresentada no capítulo 4 apresenta a modelagem para reatores contínuos de tanque agitado com alimentação distribuída de substrato e enzima.

Capítulo 4 – Hidrólise Enzimática de Substratos Lignocelulósicos: Modelagem e Simulação para *n*-CSTR's Em Serie

4.1. Introdução

O estudo das condições e estratégias de operação de reatores contínuos para a hidrólise enzimática de substratos lignocelulósicos é um ponto de grande importância na busca de alternativas para abaixar o custo do processo. A modelagem e simulação dos reatores demandam não somente os balanços de massa, mas também que a modelagem leve em conta o caráter multifásico do sistema. A distribuição de tempos de residência pode ser usada para predizer a conversão que será alcançada nos reatores se a taxa de reação e o grau de micromistura das partículas são conhecidos. Os extremos de micromistura resultam de considerar o material alimentado como pequenos agregados que permanecem diferentes tempos no reator continuo e reagem de forma independente como se fossem pequenos reatores batch (macrofluido), ou considerar que o material alimentado se mistura completamente quando entra no reator (microfluido).

Em seguida, é apresentado um estudo que analisa a conversão de celulose atingida em reatores contínuos utilizando os modelos de macrofluido, microfluido e fluxo pistão. Os tipos de reatores considerados são: uma série de tanques agitados com alimentação contínua de substrato e enzima no primeiro reator da série, e um reator tubular. Até hoje, não há maior informação publicada acerca da hidrólise enzimática de substratos lignocelulósicos em reatores contínuos. Assim, este estudo é relevante porque ilustra gargalos técnicos na implementação da tecnologia tais como o volume de reação requerido, o consumo de água, e a baixa concentração de glicose na corrente de saída. O uso de uma série de reatores de tanque agitado permite alcançar conversões de celulose perto das alcançadas em reatores tubulares e oferece a possibilidade de incrementar as concentrações de substrato, evitando problemas de agitação devido à alta viscosidade, por meio de alimentação distribuída. Esta última alternativa surge de forma natural da análise dos resultados obtidos neste capítulo e é modelada em detalhe e simulada no capítulo seguinte (Capítulo 5).

4.2. Desenvolvimento

O desenvolvimento deste capítulo é apresentado a seguir, no manuscrito intitulado *Enzymatic Hydrolysis of Lignocellulosic Substrates: Modeling and Simulation for n-CSTR's in Series.*

Enzymatic Hydrolysis of Lignocellulosic Substrates: Modeling and Simulation for *n*-CSTR's in Series.

Abstract

A pseudo-homogeneous kinetic model was fitted to reducing sugar profiles of the enzymatic hydrolysis of delignified sugarcane bagasse, at 50 °C, constant cellulase activity of 1.36 $IUmL^{-1}$ and initial bagasse concentrations of 2.6, 5.0 and 7.5% (w/w, dry basis). The fitted kinetic model was used to predict cellulose conversion in continuous reactors by the macrofluid, the microfluid, and the plug flow models. Both the macrofluid and the microfluid models give closer results to the plug flow model in the last reactor of a series with more than three reactors and for mean residence times higher than 60 h. For series of less than three reactors and mean residence times less than 60 h, the conversion calculated by the macrofluid model is significantly greater than the calculated by the microfluid model. For well stirred *n*-CSTRs in series with continuous enzyme and substrate addition, it is possible to achieve cellulose conversions close to the cellulose conversion predicted by an ideal plug flow reactor for residence times higher than 60 h with 3 CSTR's in series.

Keywords: *Enzymatic hydrolysis; kinetic model; continuous reactors; macrofluid model; microfluid model; plug flow model*

1. Introduction

Enzymatic hydrolysis of lignocellulosic biomass has gained considerable interest in the past decades because it can provide reducing sugars, which serves as a raw material for the production of ethanol and others chemical products. The biomass is hydrolizated after a previous pretreatment to decrease the recalcitrance and make the cellulose in the feedstock more susceptible to digestion by cellulase enzymes. The study of the conditions and operating strategies of the bioreactor in which enzymatic hydrolysis of lignocellulosic biomass occurs is a logical focal point in pursuing cost reduction. To date, there is no

available information about the enzymatic hydrolysis of lignocellulosic biomass in continuous reactors at industrial scale.

Continuous reaction systems for enzymatic hydrolysis of lignocellulosic biomass have significant applied potential at industrial scale. The residence time distribution (RTD) can be used to predict the conversion that will be achieved in a real reactor provided that the reaction rate and the degree of mixing of particles are known. Flowing material is in some particular state of aggregation, depending on its nature, but in the extremes, these states can be considered as macrofluid and microfluid. The macrofluid model considers the fluid as little clumps staying for different lengths of time in the reactor, each clump reacts away as a little batch reactor and the mean composition in the exit stream will have to account for the kinetics and the RTD. The microfluid model considers that clumps of different ages are completely mixed as soon as they enter the reactor. A stream of solids always behaves as a macrofluid while a single-phase system lie somewhere between the extremes of macrofluid and microfluid (Levenspiel, 1999). South et al., (1995) modeled the simultaneous saccharification and fermentation of lignocellulose to ethanol in batch and continuous reactors, considering the reaction of particulate biomass as equivalent to macrofluid and found good agreement between experimental and predicted hydraulic residence time to achieve substrate conversions between 0.5 and 0.85 in a single continuous stirred tank reactor (CSTR).

The full extent of the complexity of enzymatic hydrolysis of lignocellulosic biomass is not represented in any quantitative model proposed to date (Shao et al., 2009). According to the classification of Zhang and Lynd (2004), semimechanistics models with respect to substrate or with respect to enzyme, usually intended for design purposes, take a minimalist approach in which only those phenomena and parameters needed to describe the observed behavior are included. The model of Nakao et al., (1990), which considers the concentration as the only substrate state variable and one solubilizing activity fits in this latter category and was used in this work.

In this work, experimental reducing sugars profiles for enzymatic hydrolysis of delignified sugarcane bagasse were used to fit a kinetic model for an initial bagasse concentration of 2.6, 5.0 and 7.5% (w/w, dry basis) and constant initial cellulase activity of 1.36 IU/mL. This model is used for a simulation study considering the macrofluid and microfluid approaches in *n*-CSTRs in series with continuous substrate and enzyme addition.

A comparison between the above modeling approaches and plug flow reactor in terms of predicted mean hydraulic residence time for various substrate conversion is made in order to show the differences between the models predictions and the different options in reaction systems to carry out the enzymatic hydrolysis of biomass.

2. Kinetic model

The kinetic model proposed by Nakao et al. (1990) was used to represent the saccharification reaction.

$$\frac{dT}{dt} = \frac{v_m (T_\infty - T)}{k_m [1 + (T / k_i)] + 0.923(T_\infty - T)} \tag{1}$$

This model considers that reducing sugars (T) are produced from a hypothetical soluble substrate (T_∞-T) whose initial concentration would correspond to the concentration of reducing sugar produced ultimately (T_∞) assuming a pseudo-homogeneous Michaelis-Menten mechanism. The constant 0.923 is the ratio of the molecular weight of product unit (assuming as [molecular weight of glucose + molecular weight of cellobiose]/2) in cellulose to that of soluble product. v_m is the apparent rate constant representing the frequency of binding between cellulose and enzymes and depends of the substrate concentration. It should be noted that v_m results from grouping a rate constant and enzyme concentration. k_m and k_i are the apparent Michaelis constants representing the affinity between cellulose and enzymes, and the apparent competitive inhibition constant between reducing sugars and enzymes. k_m and k_i are assumed intrinsic to a given system, and hence independent of the operating variables. Reducing sugars profiles during enzymatic hydrolysis of alkali delignified sugarcane bagasse (Dwivedi and Ghose, 1979) were fitted to the kinetic model. The initial bagasse (S_{T0}) and the initial cellulose (S_{C0}) concentrations on dry weight basis and ultimate reducing sugars concentrations T_∞ are shown in the Table 1. The predicted and experimental reducing sugar profiles and the sum of square error (SSE) for the fitting are shown in the Fig. 1 for different initial bagasse concentrations.

The kinetics parameters estimation problem is stated as minimizing an objetive function that measures the goodness of the fit of the model with respect to the experimental

data set using least squares. The differential equation used to predict the kinetic (Eq. 1) and the nonlinear optimization were solved numerically by a Runge-Kutta-Verner sixth-order and a modified Levenberg-Marquardt method, respectively. The FORTRAN IMSL routines IVPRK and RNLIN were used for this purpose.

3. Reactor modeling and simulation

The following assumptions were found to be necessary for modeling the *n*-CSTRs in series:

- Reactors are well mixed in the macroscopic sense; therefore, there is a uniform distribution of temperature and composition in the reactors.
- Reactors operate at steady state.
- The volumetric flow of substrate and liquid and the mean hydraulic residence time are the same for all reactors.
- Particle size distribution of the solid particles in the reactor is uniform.

3.1 Macrofluid model for *n*-CSTRs in series

The residence time of the substrate and liquid are considered to be the same. For a well mixed series of *n*-CSTRs, the RTD function *E(t)* is given below (Levenspiel, 1999):

$$E(t) = \frac{t^{n-1}}{(n-1)!\tau_i^n} e^{-t/\tau_i} \tag{2}$$

where *n* is the number of reactors and τ_i is the residence time of the liquid and substrate in each reactor.

The conversion of substrate at the outlet of the *nth* reactor is expressed in terms of the kinetic model, time and the number of reactors as follow:

$$1 - X_{sh} = \int_{t=0}^{t\to\infty} \left(\frac{S_h}{S_{h0}} \right)_{Batch} E(t)dt \tag{3}$$

where S_h is the hypothetical soluble substrate (T_∞-T).

According to Equation 3, the substrate composition was calculated as the weighted sum of particles that spent varying times in the reactor as defined by the residence time distribution *E(t)*. The weight, *W*, allocated to the conversion of a particle of substrate that resided in the reactor between t_i and (t_i + Δt) was given by evaluating the integral of the exit age distribution *E(t)* over this interval as per Equation 4. To ensure an adequate range of particle residence times, the procedure was repeated until the time integral of the exit age distribution, $\sum_i(E(t_i)\Delta t)$, reached 0.999.

$$W_i(t) = \int_{t_i}^{t_i+\Delta t} E(t)dt \tag{4}$$

3.2 Microfluid model for *n*-CSTRs in series

In the microfluid model, the substrate and liquid are assumed to be perfectly mixed. For a reactor in series, the mass balance is expressed as follows:

$$\tau_i = \frac{V_{Ri}}{\varphi} = \frac{S_{h(i-1)} - S_{hi}}{r(S_{hi})} \tag{5}$$

where τ_i is the mean hydraulic residence time of reactor *i*, V_{Ri} is the volume of reactor *i*, φ is the volumetric flow through reactor *i* and $r(S_{hi})$ is the rate of disappearance of hypothetical substrate.

$$r(s) = \frac{v_m S_h}{k_m(1 + (S_{h0} - S_h)/k_i) + 0.923S_h} \tag{6}$$

substitution in Equation 5 gives:

$$\tau_i = \frac{V_{Ri}}{\varphi} = \frac{S_{hi-1} - S_{hi}}{v_m S_{hi}} (k_m + \frac{k_m}{k_i}(S_{h0} - S_{hi}) + 0.923 S_{hi}) \tag{7}$$

In terms of dimensionless variables, Equation 7 can be written as follow:

$$\theta_i = \frac{V_{Ri} v_m}{\varphi S_{h0}} = \frac{S_{hi-1} - S_{hi}}{S_{hi}} (\frac{k_m}{S_{h0}} + \frac{k_m}{k_i}(1 - \frac{S_{hi}}{S_{h0}}) + 0.923 \frac{S_{hi}}{S_{h0}}) \tag{8}$$

where θ_i is the dimensionless residence time of reactor *i*.

$$\alpha = \frac{S_{hi}}{S_{h0}}, \quad k_m^{'} = \frac{k_m}{S_{h0}}, \quad \xi = \frac{k_m}{k_i}$$

Substitution in Equation 8 gives:

$$\theta_i = \frac{\alpha_{i-1} - \alpha}{\alpha_i} (k_m^{'} + \xi(1 - \alpha_i) + 0.923 \alpha_i) \tag{9}$$

Applying Equation 9 to reactors *i* and (*i +1*) under the condition of equal dimensionless residence time:

$$\alpha_{i-1} = \left\{ \frac{\left[\frac{\alpha_i}{\alpha_{i+1}} - 1 \right] \left[k_m^{'} + (0.923 - \xi)\alpha_{i+1} + \xi \right]}{k_m^{'} + (0.923 - \xi)\alpha_{i+1} + \xi} + 1 \right\} \alpha_i \tag{10}$$

The above equation is solved for the intermediate substrate ratios through the following algorithm:

- A value of α_n is fixed.
- α_{n-1} is fixed as a $\alpha_n + \Delta$. ($\Delta = 1.0^{-6}$)
- With α_{n-1} and α_n a value for α_{n-2} is calculated trough the Eq. 10 and the procedure is repeated until α_0.

- If abs(*1- α_0*) is greater than a previously specified tolerance, the procedure is repeated with a new value of Δ until convergence is attained.

α intermediate values are determined by the above procedure to correspond to reactors with the same dimensionless residence time. Finally, the value of τ_i is calculated with the Eq. 7.

3.3 PFR model

For a plug flow reactor, the mass balance is expressed as follow:

$$\frac{dV_R}{\varphi} = -\frac{dS_h}{r(S_h)} \tag{11}$$

In terms of the above dimensionless variables the following equation is obtained:

$$d\theta = -\frac{k_m^{'} + \xi(1-\alpha) + 0.923\alpha}{\alpha} d\alpha \tag{12}$$

Integrating the Equation 12 under the conditions $\alpha_0=1$, $\theta_0=0$ and $\alpha=\alpha_{PFR}$, $\theta=\theta_{PFR}$ results in:

$$\theta_{PFR} = (1-\xi)(1-\alpha_{PFR}) - (k_m^{'} + \xi)\ln(\alpha_{PFR}) \tag{13}$$

4. Result and discussion

Figure 1 depicts experimental data for a batch enzymatic hydrolysis of delignified sugarcane bagasse run together with the predicted time-course of reducing sugar production based on the integration of Equation 1. Despite its simplicity, the kinetic model used in this work satisfactorily fitted batch data. The model works well for reproducing experimental enzymatic hydrolysis data over the range of conditions to which it has been applied. As this range includes initial substrate concentration between 2.6 to 7.5% (w/w, dry basis), the model is particularly useful for the prediction of residence times that would be required to achieve a given conversion in continuous reactors systems at industrial scale, but its

applicability is limited as it does not include the effect of different enzyme loadings. A most detailed model that takes into account different enzyme activities, others substrates properties in addition to concentration and the heterogeneity of the system is need for futures studies, but the predictions of the present work give rise to valuable conclusions on the feasibility of enzymatic hydrolysis of biomass at industrial scale.

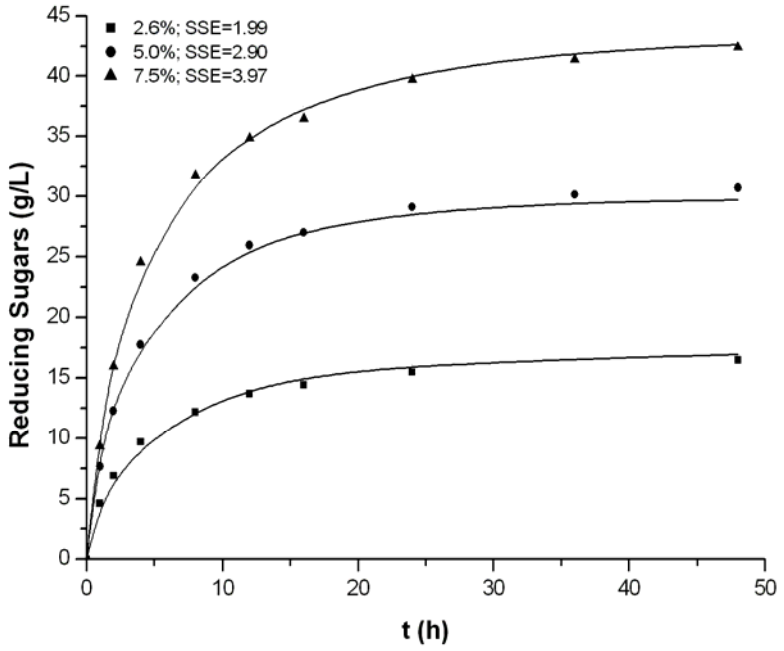

Figure 1. Observed time course of enzymatic hydrolysis of bagasse (Dwivedi and Ghose, 1979) and predicted profiles. (SSE: Sum of square error between predicted and experimental values along each profile)

Table 1. Initial bagasse (S_{T0}), cellulose (S_{C0}), ultimate reducing sugar concentration (T_∞), and kinetic model parameters

S_{T0}[g/L]	S_{C0}[g/L]	T_∞ [g/l]	v_m [$gL^{-1}h^{-1}$]	k_m [gL^{-1}]	k_i [gL^{-1}]
26.0	20.8	17.1	16.3	27.0	3.0
50.0	40.0	29.8	30.7	27.0	3.0
75.0	60.0	43.0	34.2	27.0	3.0

Enzyme activity, FP=1.36 $IUmL^{-1}$, T_∞ correspond to a reaction time of 48 h, Temperature 50ºC, $S_{C0}=0.8S_{T0}$.

Substrate loading is one of the main factors that affect the glucose yield and hydrolysis rate, especially the initial rate of enzymatic hydrolysis of lignocellulosic biomass. When the substrate level is low (<1% w/w), an increase in substrate loading normally results in increased yields and hydrolysis reaction rates (Wyman et al., 1992). Low substrate loadings increase the capital cost of equipment and operation and lead to low concentrations of glucose. However, because of the high viscosity at the beginning of enzymatic hydrolysis of most lignocellulosic substrates, it is difficult to operate at solids loadings much higher than approximately 10% w/w (Rosgaard et al., 2007). For a typical system of reaction, the initial substrate concentration should be below 10% w/w and it is expected that the solids concentration and the viscosity of the suspension decrease due to the cellulose solubilization during the enzymatic hydrolysis.

Real fluids in continuous flow reactors generally do not exhibit the macrofluid or microfluid extremes in mixing behavior and are termed partially segregated. For the enzymatic hydrolysis of biomass a mixing behavior close to macrofluid is expected for short residence times and for intermediates and long residence times there is the gradual evolution to partially segregated flow. The two extremes of micromixing give the upper and lower limits on conversion for the series of *n*-CSTR's assuming that the reactors are well mixed at macroscopic level.

Computational fluid dynamic simulations of the flow pattern of biomass in a pipe showed higher solid particles concentration under the central axis and absence of solid particles near the top (Martínez et al., 2009). As a result, the predicted residence times required to achieve a given conversion assuming ideal plug flow could display significant deviations from the real behavior of the enzymatic hydrolysis of biomass in a tubular reactor. Despite the ideality of plug flow, this is included in the simulation as a basis of comparison.

Figures 2 and 3 illustrates the results predicted for the total mean hydraulic residence times (τ_T) in the range of 10-120 h for the series of *n*-CSTRs by the macrofluid and the microfluid models. The results are compared with the mean hydraulic residence times for a plug flow reactor. The results indicate that for a given residence time, the predicted conversion of cellulose at the exit of the n^{th} CSTR by the macrofluid model is greater than that the predicted by the microfluid model but lower than the conversion achieved in a plug flow reactor with the same residence time (Figures 4 and 5). The present

result is in accordance with the results obtained by a CSTR modeling for the simultaneous saccharification and fermentation of biomass presented by South et al. (1995). It is worth to note that the results of the macromixing and micromixing models get closer to each other as the number of reactors and mean hydraulic residence times are increased.

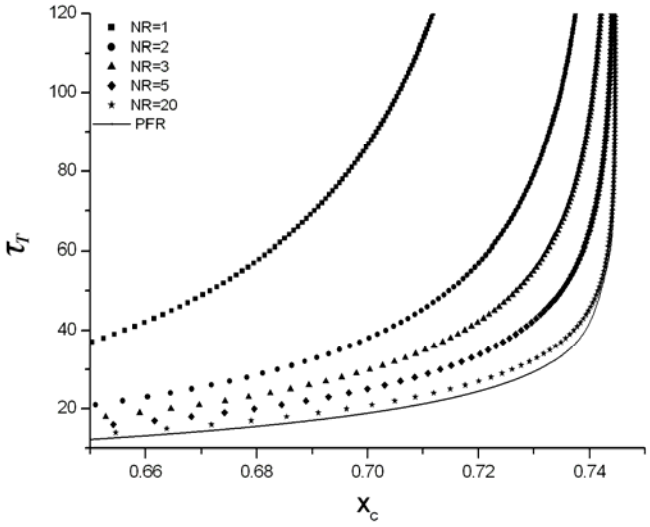

Figure 2. Total mean hydraulic residence time (τ_T) as a function of cellulose conversion (X_c) predicted by the macrofluid model. Initial bagasse concentration S_{T0}=50 g/L; initial cellulose concentration S_{C0}=40g/L.

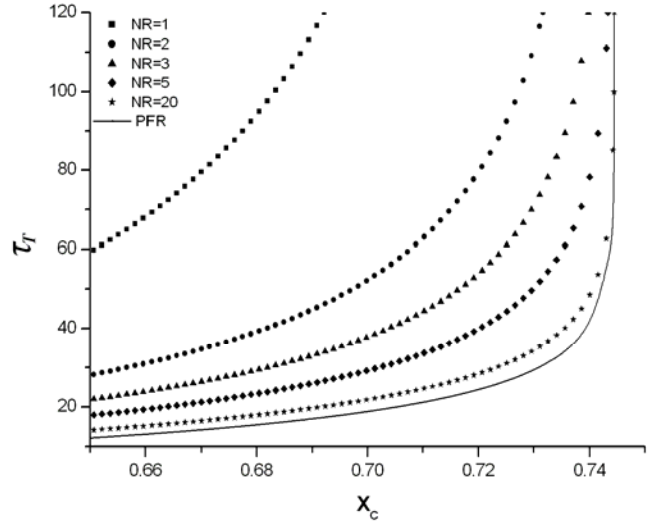

Figure 3. Total mean hydraulic residence time (τ_T) as a function of cellulose conversion (X_c) predicted by the microfluid model. Initial bagasse concentration S_{T0}=50 g/L; initial cellulose concentration S_{C0}=40g/L.

The cellulose conversion achieved in 3 CSTRs in series, predicted by the macrofluid and microfluid model by a mean hydraulic residence time of 60 h is 98.4% and 97.4 %, respectively, of the cellulose conversion achieved in an ideal PFR with the same mean hydraulic residence time. The same results for a mean hydraulic residence time of 120 h are 99.7 and 99.4 (See Table 2 and Figs. 4 and 5). The above results indicate that for well stirred *n*-CSTRs in series with continuous enzyme and substrate addition, it is possible to achieve cellulose conversions close to the cellulose conversion predicted by an ideal PFR for residence times higher than 60 h with 3 CSTRs in series. Strategies for diminishing the local concentration gradient of solids along the tube, such as the use of internal baffles, must be considered for the use of the plug flow reactors.

Table 2. Ratio between the cellulose conversion achieved in a series of *n*-CSTRs predicted by the macrofluid and microfluid model and the substrate conversion achieved in a plug flow reactor

N° CSTRs	**Model**	**$(X_{cCSTRs}/X_{cPFR})*100\%$**	
		τ=60 h	**τ=120 h**
1	Ma	91.7	95.6
	Mi	87.5	93.0
2	Ma	97.0	99.1
	Mi	95.1	98.3
3	Ma	98.4	99.7
	Mi	97.4	99.4
5	Ma	99.3	99.9
	Mi	98.8	99.8
20	Ma	99.9	100
	Mi	99.8	100

High substrate loading is more economical than low substrate loading, but the viscosity and poor mass transfer problems with high substrate loadings need to be solved. One alternative is, instead of adding substrate and enzymes continuously only at the first reactor of the series of CSTRs or at the entrance of the PFR, feed substrate and enzymes at different reactors in the series for the CSTRs or at different lengths in the case of the PFR.

The different feed points should be calculated to overcome the limitations of viscosity. In these systems, it is expected a mixing behavior closed to macrofluid.

Due to the low levels of substrate loadings and the slow kinetics, one of the most important problems for the implementation of enzymatic hydrolysis at industrial scale is the reaction volume necessary to convert the big amounts of available raw material reaching high cellulose conversion. The minimum reaction volume required to achieve a given cellulose conversion is obtained by the use of an ideal tubular reactor, but the inability to maintain the solid-liquid suspension in this kind of reactor suggests the use of a series of *n*-CSTRs or a baffled tubular reactor. For the series of *n*-CSTRs, the mean hydraulic residence time to achieve a given cellulose conversion drops off sharply with the number of stages. An economical number of stages are often 3 to 6 (Perry, 1999), since the benefits of reduced volume may be out-weighed by the increased cost of multiple agitators, pumps, and controls if a large number of reactors are used.

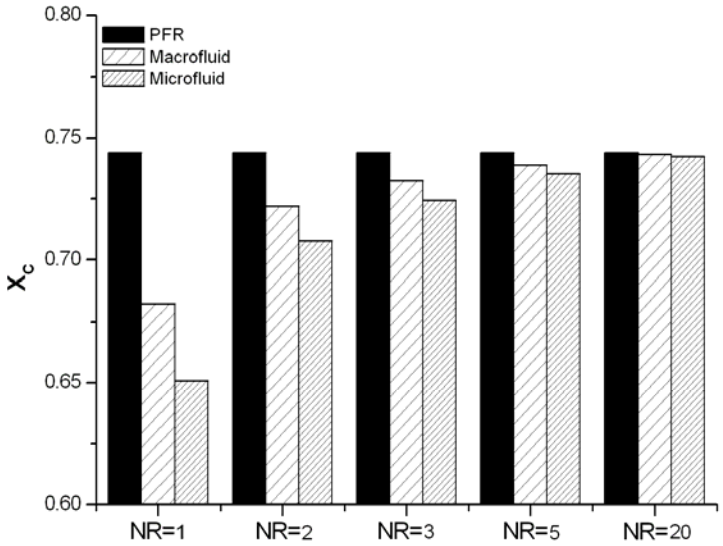

Figure 4. Final cellulose conversion for a mean hydraulic residence time of 60 h calculated by the macrofluid, the microfluid, and the plug flow models. Initial bagasse concentration S_{T0}=50 g/L; initial cellulose concentration S_{C0}=40g/L.

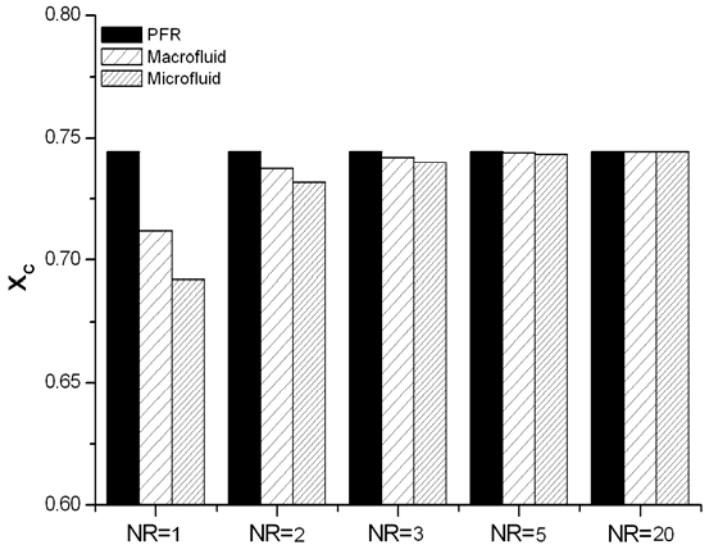

Figure 5. Final cellulose conversion for a hydraulic residence time of 120 h calculated by the macrofluid, the microfluid, and the plug flow models. Initial bagasse concentration S_{T0}=50 g/L; initial cellulose concentration S_{C0}=40g/L.

In a series of 3 well mixed CSTRs, for a substrate loading of 5% w/v, a flow of 1Ton/h of pretreated bagasse and a cellulose conversion of 0.7, the reaction volume is from 600 m^3 (200 m^3 by reactor, predicted by the macrofluid model) to 754 m^3 (251 m^3 by reactor, predicted by the microfluid model). For the same substrate loading, flow of raw material and cellulose conversion in a series of 5 well mixed CSTRs, the reaction volume is from 500 m^3 (100 m^3 by reactor, predicted by the macrofluid model) to 584 m^3 (117 m^3 by reactor, predicted by the microfluid model). The predicted reaction volume in an ideal tubular reactor for the above conditions is 377 m^3. Due to the high required reactor volume and high cost of downstream processing (glucose separation and water recirculation), the feeding of substrate and enzymes at different reactors in the series for the CSTRs or at different lengths in the case of the PFR is necessary. Fluid dynamics studies of the water-biomass suspension that takes into account the decreasing viscosity and substrate concentration for long reaction times are required to evaluate a distributed feeding strategy and the fluid dynamic behavior of a baffled tubular reactor.

5. Conclusions

In this work, experimental data for the enzymatic hydrolysis of delignified sugarcane bagasse were fitted to a pseudo-homogeneous kinetic model. The model was shown to reproduce experimental enzymatic hydrolysis data satisfactorily over the range of conditions to which it has been applied. The kinetic model was used for a simulation study of enzymatic hydrolysis in continuous reactors.

Two models were used to define the multiphase reactive system of enzymatic hydrolysis of lignocellulosic biomass, the macrofluid and microfluid models. The macrofluid and microfluid modeling approaches can be used to obtain the upper and lower limits of conversion for a well mixed series of *n*-CSTRs, which are of great value in the initial evaluation of the performance of different reactor systems at industrial scale in the absence of experimental RTD data. Experimental RTD data are necessary to predict the exact conversion obtained in real reactors, but it is not easily obtained.

Among the reactors considered, the ideal tubular reactor requires the lowest reaction volume to achieve a given cellulose conversion, but previous studies have shown that the dynamics of an ideal plug flow can display significant deviations from the real behavior (Martínez et al., 2009), mainly due to the inability to maintain the solid-liquid suspension in this kind of reactor. The use of a series of *n*-CSTRs with distributed feeding or of a baffled tubular reactor with distributed side feeding should be considered.

6. Acknowledgements

The authors acknowledge the financial support provided by FAPESP (The Scientific Research Foundation for the State of São Paulo).

References

Dwivedi CP, Ghose TK. 1979. A model on hydrolysis of bagasse cellulose by enzyme from *Trichoderma Reesei* QM 9414. J Ferment Technol 57:15-24.

Nakao K, Fukunaga K, Yasuda Y, Kimura M. 1990. Enzymatic hydrolysis of lignocellulosics with continuous irradiation of supersonic wave. Ann NY Acad Sci 613:802-807.

Levenspiel, O. 1999. Chemical Reaction Engineering, 3rd ed., John Wiley and Sons Inc, New York.

Martínez EL, González Quiroga A, Jardini AL, Maciel Filho R. 2009. Computational fluid dynamics simulation of the water-sugar cane bagasse suspension in pipe with internal static mixer, in 19th European Symposium on Comp Aided Chem Eng 26:683-688.

Perry RH, Green DW, Maloney JO. 1999. Chemical Engineering Handbook, 7th ed., McGraw Hill, New York.

Rosgaard L, Andric P, Dam-Johansen K, Pedersen S, Meyer AS. 2007. Effects of substrate loading on enzymatic hydrolysis and viscosity of pretreated barley straw. Appl Biochem Biotechnol 143:27-40.

Shao X, Lynd L, Wyman C, Bakker A. 2009. Kinetic modeling of cellulosic biomass to ethanol via simultaneous saccharification and fermentation: Par I. Accomodation of intermittent feeding and analysis of staged reactors. Biotechnol Bioeng 102:59-69.

South CR, Hogsett DAL, Lynd L. 1995. Modeling simultaneous saccharification and fermentation of lignocellulose to ethanol in batch and continuous reactors. Enzyme Microb Technol 17:797-803.

Wyman CE, Spindler DD, Grohmann K. 1992. Simultaneous saccharification and fermentation of several lignocellulosic feedstocks to fuel ethanol. Biomass Bioenergy 3:301-307.

Zhang YP, Lynd L. 2004. Toward and aggregated understanding of enzymatic hydrolysis of cellulose. Biotechnol Bioeng 88:797-824.

4.3. Conclusões

Este capítulo apresentou a modelagem de reatores contínuos de tanque agitado e do reator tubular para a hidrólise enzimática de substratos lignocelulósicos. O estudo da conversão como função do tempo de residência e do número de reatores da série mostrou que conversões similares às preditas num reator tubular ideal podem ser alcançadas no mínimo com 3 reatores de tanque agitado em série e um tempo de residência total de 60 h. O estudo mostrou que velocidade de reação lenta, as baixas concentrações de substrato que podem ser hidrolisadas e consequentemente o grande volume de reação requerido limitam fortemente a hidrólise enzimática em modo continuo em nível industrial.

O principal aporte do capítulo a seguir é a modelagem de reatores de tanque agitado em série com alimentação distribuída de substrato e enzima numa tentativa de incrementar a concentração de substrato e consequentemente a concentração de glicose na corrente de saída dos reatores. Além da alimentação distribuída de substrato e enzima, são considerados diferentes arranjos de reatores de tanque agitado e reatores tubulares com o intuito de diminuir o volume de reação e incrementar a concentração de glicose na corrente de saída.

Capítulo 5 – Hidrólise Enzimática de Substratos Lignocelulósicos: Análise da Conversão e Estratégias de Operação em Reatores Contínuos com Alimentação Distribuída

5.1. Introdução

A modelagem e simulação de reatores de tanque agitado em série com alimentação distribuída de substrato e enzima, assim como o desempenho de reatores de tanque agitado em série ou um reator tubular após os reatores com alimentação distribuída, é o foco deste capítulo. Devido aos resultados preliminares obtidos no Capítulo 4, que evidenciam a necessidade de aumentar a concentração de substrato, a alimentação distribuída de substrato e enzima é avaliada conjuntamente com diferentes arranjos de reatores de tanque agitado e reatores tubulares. A alimentação distribuída de substrato e enzima aplicada a reatores contínuos de hidrólise enzimática é apresentada pela primeira vez neste estudo e foi inspirada nos experimentos de batelada alimentada a nível de bancada. A literatura concernente à batelada alimenta é completamente revisada e discutida. O modelo cinético ajustado no capítulo 3 é utilizado conjuntamente com os modelos de micromistura correspondentes a macrofluido e microfluido, assim como o modelo de fluxo pistão para descrever os reatores contínuos. A alimentação distribuída de substrato permitiu incrementar a concentração de substrato que entra nos reatores de hidrólise acima de 10% w/w (base seca) mantendo conversões semelhantes às alcançadas quando o substrato é alimentado só no primeiro reator da série.

O mesmo procedimento de modelagem e simulação apresentado neste capítulo foi realizado usando um modelo cinético apresentado e ajustado na literatura. Os resultados são apresentados no apêndice ***A*** desta dissertação. A justificação desta extensão do trabalho é que o modelo cinético é o mais completo dos que têm sido proposto e ajustado até agora na literatura. De forma que usando este modelo se podem obter conclusões adicionais às obtidas neste capítulo, e este modelo cinético se constitui num modelo candidato para ser ajustado a dados da hidrólise enzimática de bagaço de cana em próximos trabalhos.

5.2. Desenvolvimento

O desenvolvimento deste capítulo é apresentado a seguir, no manuscrito intitulado *Enzymatic Hydrolysis of Lignocellulosic Substrates: Analysis of Conversion and Operation Strategies in Continuos Reactors with Distributed Feeding.*

Enzymatic Hydrolysis of Lignocellulosic Substrates: Analysis of Conversion and Operation Strategies in Continuos Reactors with Distributed Feeding

Abstract

Design considerations for enzymatic hydrolysis of lignocellulosic biomass in two and three continuous stirred tank reactors (CSTR) in series with distributed feeding of substrate and enzyme followed by a series of *n*-CSTR's or a tubular reactor are discussed. A previously fitted and validated kinetic model is used along with the macrofluid and microfluid models of micromixing in a series of *n*-CSTR's or the plug flow model of tubular reactors to describe the reaction system. The capability of the continuous reactors proposed is explored in a range of cumulative substrate concentrations from 3% w/w to 13.6% (w/w, dry basis). Distributed feeding enables to increasing substrate concentration avoiding mixing limitations common to reactions with initial substrate concentration higher than 10% w/w, and allows achieving conversions similar to those achieved in a series with feeding only at the first reactor.

Keywords: *enzymatic hydrolysis; continuous reactor; distributed feeding; macrofluid; microfluid*

1. Introduction

The enzymatic hydrolysis of lignocellulosic biomass has gained considerable interest in the past decades because it can provide reducing sugars which serve as a raw material for the production of ethanol and other chemical products. Lignocellulosic biomass, including agricultural and forestry residues, is particularly attractive in this context because it is widely available at low cost. Continuous reaction systems for enzymatic hydrolysis have significant applied potential at industrial scale. If ethanol produced from lignocellulosic biomass is to become a cost-effective substitute or

complement for gasoline on a larger scale, its cost of production must be reduced substantially. So, the study of the conditions and operating strategies of continuous reactors to carry out the enzymatic hydrolysis of lignocellulosic biomass is a logical focal point in pursuing cost reduction. To evaluate the performance of continuous reactors three main factors were considered here: the kinetic, the residence time distribution (RTD) of fluid in the reaction system, and whether the fluid is a micro or macorfluid.

The full extent of the complexity of the enzymatic hydrolysis of lignocellulosic biomass is not represented in any quantitative model proposed to date (Shao et al., 2009). According to the classification of kinetics models for enzymatic hydrolysis proposed by Zhang and Lynd (2004), semmimechanistic kinetic models with respect to substrate or with respect to enzyme, usually intended for desing purposes, take a minimalist approach in which only those phenomena and parameters needed to describe the observed behavior are included. A kinetic model that considers the concentration as the only substrate variable and a single enzymatic activity fits in this category ans was used here.

Due to the heterogeneous nature of the hydrolytic reaction, the overall reaction rate is determined by the rate of three events in sequence: the external enzyme mass transfer rate through the stagnant liquid film layer adjacent to the solid substrate, the rate of enzyme adsorption on the substrate surface, and the rate of cellulase catalysis (Gan et al., 2003). Van Dyke (1972) and Huang (1975) observed that the intensity of agitation had little effect on cellulose hydrolysis when the substrate particles were fully suspended. Although mixing of substrate and enzymes is crucial for an efficient liquefaction, Jørgensen et al. (2007-a) showed that it does not appear that lack of mixing is the cause of the decreasing conversion, at least up to initial substrate concentrations of 40% w/w. This is in accordance with the findings of Hodge et al. (2008) who concluded that possible mass transfer limitation caused by insoluble solids were not apparent at below 20% insoluble solids content. The above findings suggest that the reaction rate is not significantly affected by mass transfer in the film surrounding non-solubilized substrate and that mixing is required mainly to maintain solids suspension.

An important question is if the classic perfectly mixed assumption (ideal CSTR) can be used in continuous stirred tank reactors for enzymatic hydrolysis of lignocellulosic biomass. Two important issues must be addressed here: the maximal concentration of

substrate that can be mixed and hydrolysed in continuous stirred-tank reactors and the concept of blend time. Twelve to fifteen per cent total solids is often considered the upper limit of insoluble solids at which pretreated biomass can be mixed and hydrolyzed in conventional stirred tanks (Kristensen et al., 2009). It is usually feasible to achieve well-mixed conditions in turbulent stirred vessels unless the reactions are very fast such as acid-base neutralizations. If the blend time is small compared to the residence time in the reactor, the reactor can be considered well mixed (Paul et al., 2004). The initial substrate concentrations considered here are below 15% (w/w, dry basis) and the mean residence times in a stirred-tank reactor considered were ranged from 10-50 h. So, for modeling purposes was considered that the residence time distribution in stirred-tank reactors corresponds to a well mixed tank.

The fluid dynamic behavior of the reactive biomass slurry through a tubular reactor can be framed between two limiting situations depending on the aspect ratio of the particles: (*i*) flow of pulp fiber suspensions where fibers entanglement is predominant, and (*ii*) flow of settling slurries. Due to the low solid/liquid density ratio, in any case, a flow pattern closed to plug flow can be reached by adjusting the flow rate (Ventura et al, 2008, Turian et al., 1987). Consequently, in this work was considered that the tubular reactor performs as an ideal plug flow reactor (PFR).

The challenging solid-liquid flow through the series of reactors can be very complex. Zwitering (1959) has shown how obtain rigorous bounds on possible conversions directly from residence time distribution (RTD) at the exit of the reactors. These bounds correspond to two extremes states of micromixing namely microfluid and macrofluid. The state of microfluid can prevail if the incoming feed material immediately comes into intimate contact with other fluid elements of all ages at molecular level as in an ideal CSTR. In the other extreme, the incoming fluid is broken up into discrete clumps in which molecules entering the fragment together, remain together indefinitely, fluid elements of different ages do not intermix at all while in the vessel and reaction proceeds independently in each fluid element. Between these two limiting situations falls a continuum of small scale mixing namely micromixing. The flow of biomass was considered as equivalent to macrofluid for the modeling of simultaneous saccharifiaction and fermentation (South et

al., 1994). A good agreement between experimental and predicted residence times to achieve cellulose conversions between 0.50 and 0.85 in a single CSTR was found.

An important factor in the process economic and energy balance is the concentration of substrate in the stream entering the hydrolysis step (Jørgensen et al., 2007-a). The advantages of high initial substrate concentration (>15% w/w) over conventional concentration (3-8% w/w) includes lower capital costs because of a reduced reactor volume; lower operating costs that result from reduction in heating, cooling and mixing power if a proper strategy and design are used; lower downstream processing costs due to a higher product concentration; and reduced residual disposal cost because less water is used (Mohagheghi et al., 1992). It has been stated that the ethanol concentration in the broth entering distillation should be above 4% w/w in order to make an economically feasible process (Fan et al., 2003; Wingren et al., 2003). For most types of lignocellulosic materials this requires an initial substrate concentration above 15% w/w dry matter (assuming cellulose and mannan content of 60%, 90% conversion and an ethanol yield of 0.5 g/g) (Jørgensen et al., 2007-a).

Unfortunately, operating enzymatic hydrolysis at initial substrate concentrations above 10-15% w/w has been shown to be technically difficult, especially at laboratory scale where many of the studies have been carried out. The operation has been faced with the problems of enzyme inhibition by final product (Jørgensen et al., 2007-b) and high initial viscosity of the material, which makes mixing difficult, leading to a high power consumption in stirred tank reactors (Mohagheghi et al., 1992, Fan et al., 2003, Jørgensen et al., 2007-a). As biomass slurries can absorb water, this may cause the bulk to become unsaturated (i.e., absence of a “free” bulk water continuous phase) and portions of the “void” volume contain air instead of liquid leading the biomass to behave as a wet granular material difficult to shear and uniformly mix (Viamajala et al., 2009).

Wald et al. (1984) reported enzymatic hydrolysis of pretreated rice straw up to 33.3% w/v at laboratory scale, but a stepwise addition of substrate was required to exceed a 10% level because of viscosity limitations. Cara et al. (2007) studied the enzymatic hydrolysis of pretreated olive tree pruning using a solid range from 2 to 30% w/v, but at 30% w/v of initial substrate concentration, solids remained insoluble until 72 h of hydrolysis. Jørgensen et al. (2007-a) investigated a special reactor designed for operating

the liquefaction and hydrolysis of lignocellulosic material with up to 40% w/w initial dry matter. Although it is possible to perform enzymatic hydrolysis with initial substrate concentrations up to 40% w/w, it was shown that enzyme performance gradually decreased as substrate concentration increased (Kristensen et al., 2009). Fan et al. (2003) investigated the conversion of paper sludge to ethanol in a laboratory-scale semicontinuous solids-fed reactor at a substrate concentration of about 30% w/w, feeding substrate at 12 h intervals with a mean hydraulic residence time of 4 days, and pointed out that the semicontinuous operating mode was a satisfactory solution to the impractically of mixing unreacted paper sludge at high feed substrate concentrations.

Operating enzymatic hydrolysis in a fed-batch mode by adding fresh substrate and/or enzyme when the viscosity has decreased has been used to increase substrate concentrations (Table 1). During fed-batch enzymatic hydrolysis of pretreated corn stover, Lu et al. (2008) reported that when cumulative substrate concentration reached 30% w/w, glucose concentration reached 103.3 g/L, and a final ethanol concentration up to 49.5 g/L was obtained during fermentation. Supplementation of enzyme at each substrate addition to maintain the initial enzyme loading (Ballesteros et al., 2001; Ballesteros et al., 2002; Rosgaard et al., 2007) or an initial enzyme loading based on the final amount of substrate loaded (Rosgaard et al., 2007; Lu et al., 2008) have been reported.

Table 1. Fed-batch enzymatic hydrolysis at laboratory level

Pretreated Substrate	**Fed-Batch Strategy** **Substrate + Enzyme (time)**	**Reference**
Olive Pulp	15+E*(0 h); 5+E(24 h); 5+E (48 h); (%w/v)	Ballesteros et al. 2001
Olive Pulp	15+E(0 h); 7.5+E(24 h); 7.5+E (48 h); (%w/v)	
Olive Pulp + Olive Stones	15+E(0 h); 10+E(24 h); 5+E (48 h); (%w/v)	
Olive Pulp + Olive Stones	10+E(0 h); 15+E(24 h); 5+E (48 h); (%w/v)	
Recycled Paper	5+E(0 h); 3+E(24 h); 2+E (48 h); (%w/v)	Ballesteros et al. 2002
Barley Straw	5+E(0 h); 5(6 h); 5(24 h); (%w/w)	Rosgaard et al. 2007
Barley Straw	5+E(0 h); 10(24 h); (%w/w)	
Barley Straw	5+E(0 h); 5+E(6 h); 5+E (24 h); (%w/w)	
Barley Straw	5+E(0 h); 10+E(24 h); (%w/w)	
Corn Stover	15+E(0 h); 5(2 h); (%w/w)	Lu et al. 2008
Corn Stover	15+E(0 h); 10(2 h); (%w/w)	

Corn Stover	15+E(0 h); 7.5(2 h); 7.5(2 h); (%w/w)	

*Enzyme

Hodge et al. (2009) developed a model-based fed-batch for enzymatic hydrolysis at high substrate concentrations. A previously reported kinetic model (Kadam et al., 2004) was modified to consider the effects of fed-batch operation. A feeding profile was predicted to maintain the insoluble solids concentration at a constant manageable level throughout the course of the reaction. Experimental application in bench-scale stirred tank reactors using a feed stream of dilute-acid pretreated corn stover and cellulase enzymes resulted in similar cellulose conversion profiles to those achieved in batch shake-flask reactors. Final cellulose conversion reached approximately 80% of theoretical for fed-batch bench-scale stirred tank reactors fed to reach a cumulative solids level of 25% w/w.

Process designs for conversion of wood ships and corn stover to ethanol at industrial scale were presented by Wooley et al. (1999) and Aden et al. (2002) without considerations on reaction kinetic and mixing requirements. A series of 18 equal-size reactors (3596 m^3 each, residence time of 7 days) for simultaneous saccharification and fermentation was reported by Wooley et al. (1999), while a series of 10 equal-size reactors (3596 m^3 each, residence time of 3 days) for separate hydrolysis and fermentation with each step in five reactors was reported by Aden et al. (2002). South and Lynd (1995) and Shao et al. (2007) modeled and simulated simultaneous saccharification and fermentation of poplar ships and paper sludge to ethanol in continuous reactors. A series of 5 equal-size reactors (residence time of 5 days) was reported by South and Lynd (1995), while a series of 4 equal-size reactors (77.4 m^3 each, residence time of 3.2 days) was reported by Shao et al. (2007).

Operating enzymatic hydrolysis in a distributed feeding mode in a series of *n*-CSTR's by adding fresh substrate and/or enzyme at subsequent reactors can bring the same benefits already commented for fed-batch to continuous enzymatic hydrolysis. The slow reaction kinetics (>72 h) and the low substrate concentration typical of enzymatic hydrolysis of biomass imply a large reaction volume; therefore, the distributed feeding should takes place at the first reactors of the series and the number of subsequent reactors specified depending on the conversion that wants to be achieved. An alternative

configuration of reactors to reduce the required reaction volume may be the use of a tubular reactor from the outlet of the last CSTR with distributed feeding. Fresh substrate fed along the series should be free of water to avoid dilution effects, diminish water consumption, and increase product concentration. The feeding profile of fresh substrate and/or enzyme along the series can be based on "*ad hoc*" or model-based approaches. A model-based distributed feeding approach requires the measurement of all biomass components solubilized during the reaction to be related to the physical and rheological properties of the slurry (Roche et al., 2009) and it would be ideal for optimization and control. However, a more detailed understanding of the material properties of biomass slurries during the conversion must be developed to connect the progress of enzymatic hydrolysis with insoluble solids concentration and yield stress.

In this study, a previously fitted and validated kinetic model for enzymatic hydrolysis of sugarcane bagasse pretreated with alkaline hydrogen peroxide is extended to accommodate continuous distributed substrate feeding in a series of *n*-CSTRs with equal residence time by reactor. This model is used for a modeling and simulation study considering the macrofluid and microfluid limiting situations in two or three CSTR's in series with continuous distributed feeding of substrate and enzyme, followed by a series of *n*-CSTR's or a tubular reactor. The capability of the continuous reactors proposed is explored in a range of cumulative substrate concentrations from 3% to 13.6% (w/w, dry basis).

2. Kinetic model

2.1 Experimental data

Sugarcane bagasse pretreated with alkaline hydrogen peroxide was used as a model substrate which was composed of 60.1% w/w cellulose, 16.6% w/w xylan, 9.87% w/w lignin. Experimental data for kinetic parameter estimation were generated at initial substrate concentrations of 1%, 2%, 3%, 4%, and 5% (w/w, on dry basis) with enzyme loadings of 50, 25, 16.7, 12.5, and 10 FPU/g-substrate CBU/g-substrate, respectively; incubation temperature 50°C, shaking speed 150 rpm; initial pH 5.0; total incubation time 72 h. There are two important facts with respect to the experimental procedure referred

here: (*i*) at the beginning of the reaction when the fluid dynamic conditions are more severe the substrate did not absorb all the water present in the reaction system and substrate and enzymes were uniformly mixed; and (*ii*) no significant cellobiose accumulation was observed during the reaction.

2.2 Reaction rate

The reaction rate is given by the following equation (Nakao et al., 1990)**:**

$$\frac{dG}{dt} = \frac{v_{mG}(G^{\inf} - G)}{k_{mG}\left(1 + \frac{G}{k_{inh}}\right) + 0.9(G^{\inf} - G)} \tag{1}$$

where, glucose (G) is produced from a hypothetical soluble substrate (S^h=G^{inf}-G) whose initial concentration corresponds to the concentration of glucose produced ultimately (G^{inf}) assuming a Michaelis-Menten mechanism with competitive inhibition by glucose. v_{mG}, k_{mG}, and k_{inh} are the apparent rate constant, the apparent Michaelis-Menten constant, and the apparent inhibition constant, respectively. k_m and k_{inh} were assumed intrinsic to the reaction system while v_{mG} was assumed dependent of the enzyme/substrate ratio ($R_{E/S}$) and fitted as a function of initial substrate concentration (S_0). Significant amounts of xylose (Xy) were released during the reaction. Xylose concentration was related to glucose concentration by the following equation:

$$Xy = k_{Xy} G^{v_{Xy}} \tag{2}$$

k_{Xy} is assumed intrinsic to the reaction system while v_{Xy} is assumed as dependent on the enzyme/substrate ratio and fitted as a function of S_0.

Table 1. Estimated kinetic parameters

Parameter	Expression	Validity*
$R_{E/S}$ [FPU-CBU/g-substrate]	$R_{E/S} = 50.01 S_0^{-0.9998}$	
G^{inf} [g/L]	$G^{\inf} = 4.101 S_0 + 1.409$	
v_{mG} [g/Lh]	$v_{mG} = 104.5 \ln(S_0) + 88.08$	1%<S_0<5%
k_{mG} [g/L]	1.005	
k_{xy} [g/L]	4.475E-1	
k_{inh} [g/L]	3.161E-3	
v_{Xy} [g/L]	$v_{Xy} = 1.581 + (3.906E-4)^{(1.318 S_0)}$	2%<S_0<5%

* S_0 [w/w%, dry basis]

3. Distributed feeding

Four "*ad hoc*" operating strategies with continuous distributed feeding of substrate and enzyme were modeled, simulated, and compared in terms of cellulose and xylan conversion, and xylose and glucose yields with continuous feeding of substrate and enzyme only at first reactor of the series. It was considered that additional enzyme is supplemented at each substrate addition to maintain the initial enzyme loading. The cumulative substrate concentrations (w/w%, dry basis) along the series are the following: {3.0 R1, 5.8 R2}; {3.0 R1, 5.8 R2, 8.5 R3}; {5.0 R1, 9.5 R2}; {5.0 R1, 9.5 R2, 13.6 R3}. It should be noted that the mass of substrate fed at subsequent reactors is equal to the mass of substrate fed at the first reactor. The initial enzyme loading for the first two feeding strategies was 16.7 FPU/g-substrate and 16.7 CBU/g-substrate, while for the last two feeding strategies was 10.0 FPU/g-substrate and 10.0 CBU/g-substrate.

Each feeding event that takes place simultaneously at different reactors of the series gives rise to a new substrate population *j*. Considerations relevant to modifying the kinetic model to accommodate such distributed feeding are addressed below. Hypothetical substrate concentration (G_{inf}-G) in Equation 1 was replaced by S^h. Rate equations for the disappearing of hypothetical substrate and the glucose production from population *j* were rearranged into:

$$-r_j = -\frac{v_{mj} S_j^h}{k_m\left(1+\frac{G}{k_{inh}}\right)+0.9S_j^h} \tag{3}$$

$$r_j = \frac{v_{mj} S_j^h}{k_m\left(1+\frac{G}{k_{inh}}\right)+0.9S_j^h} \tag{4}$$

The total glucose production rate in the reactor *i* was rearranged into:

$$\frac{dG}{dt} = \sum r_j \tag{5}$$

The system of differential equations solved to find the conversion of hypothetical substrate is made up of *j* equations similar to Equation 3 that correspond to the disappearing of each substrate population present, and the glucose production rate given by Equation 5. The number of substrate populations in each reactor depends on the feeding strategy and the location of the reactor in the series.

4. Reactor modeling

The following assumptions were found to be necessary for modeling:

- CSTR reactors are well mixed; therefore, there is a uniform temperature distribution and composition in the reactors.
- Reactors operate at steady state.
- The residence time of the solid-liquid suspension in each reactor (τ) is the same.
- The tubular reactor performs as an ideal plug flow reactor.

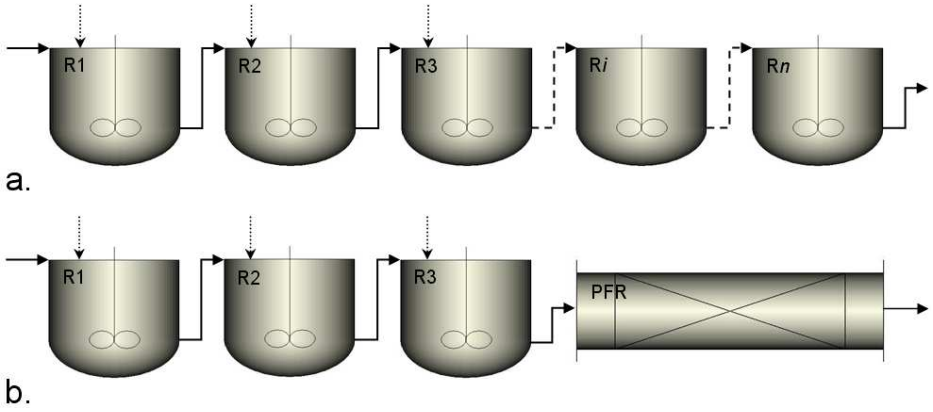

Figure 1. Schematic diagram of the configurations of reactors proposed. Dotted lines represent points of substrate and enzyme feeding; dashed lines represent the inlet and the outlet streams of an intermediate CSTR. a) Distributed feeding at the first CSTR's of the series followed by a series of *n*-CSTR's; b) distributed feeding at the first CSTR's of the series followed by a PFR.

4.1 Macrofluid model for *n*-CSTR's

For a well mixed series of *n*-CSTR's the RTD function is given below (Levenspiel, 1999):

$$E(t) = \frac{t^{nr-1}}{(nr-1)!}\exp\left(-\frac{t}{\tau}\right) \tag{6}$$

where t is the reaction time, nr is the number of reactors between the feeding point and the last reactor considered. The conversion of the population j of hypothetical substrate at the outlet of reactor i was expressed in terms of the kinetic model and the RTD function of the substrate population j as follow:

$$1 - X_{j,i}^{h} = \int_{t=0}^{t\to\infty}\left(\frac{S_j^h}{G_j^{\inf}}\right)E(t)_j\,dt \tag{7}$$

The weight allocated to the conversion of a particle of hypothetical substrate of population j that resided in the reactor between t and $t+\Delta t$ was given by evaluating the integral of its RTD function over this interval. To ensure an adequate range of residence

times, the Δt value was evaluated until the time-integral of the RTD between $t=0$ and $t\rightarrow\infty$ reached at least a value ≥ 0.999 for each substrate population.

4.2 Microfluid model

For reactor i in the series, the mass balance of the population j of hypothetical substrate and glucose were expressed respectively as follow:

$$S_{j,i-1}^{h} - S_{j,i}^{h} - \tau r_j = 0 \tag{8}$$

$$G_{i-1} - G_i + \tau \sum r_j = 0 \tag{9}$$

The conversion of the population j of hypothetical substrate at the outlet of the reactor i was calculated by:

$$X_{j,i}^{h} = \frac{G_j^{\inf} - S_{j,i}^{h}}{G_j^{\inf}} \tag{10}$$

4.3 Plug flow model

The mass balance of the population j of hypothetical substrate and glucose were expressed respectively as follow:

$$S_j^h - (S_j^h + dS_j^h) - \tau_{PFR} r_j = 0 \tag{11}$$

$$G_j - (G_j + dG_j) + \tau_{PFR} \sum r_j = 0 \tag{12}$$

The conversion of the population j of hypothetical substrate at the outlet of the PFR was calculated by:

$$X^{h}_{j,PFR} = \frac{G^{\inf}_{j} - S^{h}_{j}}{G^{\inf}_{j}} \tag{13}$$

4.4 Cellulose and xylan conversions

Cellulose conversion of the substrate population *j* at the outlet of reactor *i* was calculated from the conversion of hypothetical substrate as follow:

$$X_{C;j,i} = \frac{\underbrace{C_{0,j}}_{a} - [\underbrace{(C_{0,j} - 0.9G^{\inf}_{j})}_{b} + \underbrace{0.9G^{\inf}_{j}(1 - X^{h}_{j,i})}_{c}]}{C_{0,j}} \tag{14}$$

where *a* is the initial cellulose content of population *j*, *b* is the cellulose that remains when all hypothetical substrate is consumed, *c* is the cellulose solubilized, and the constant 0.9 is the ratio of the molecular weight of glucose unit in cellulose to that of glucose. The global cellulose conversion for all substrate populations present at the outlet of reactor *i* was calculated based on the cumulative initial cellulose concentration and the cellulose conversion of all substrate populations present.

Xylan conversion of the substrate population *j* at the outlet of reactor *i* was predicted based on the corresponding cellulase conversion (Equation 14) and Equation 2.

$$X_{Xyn;j,i} = \frac{0.88Xy_{j,i}}{Xyn_{0j}} \tag{15}$$

were Xyn_{0j} is the initial content of xylan in the substrate population *j*, and the constant 0.88 is the ratio of the molecular weight of xylose unit in xylan to that of xylose. The global xylan conversion for all substrate populations present at the outlet of reactor *i* was calculated based on the cumulative initial xylan concentration and the xylan conversion of all substrate populations present.

5. Results and discussion

An economical number of reactors in a series of *n*-CSTR's is often 3 to 6 since the benefits of reduced volume may be out-weighed by the increased cost of multiple agitators, pumps, and controls if a large number of reactors are used (Perry, 1999). In this work, a series of 10 CSTR's was considered to be an appropriate range to show the advantages of distributed feeding. For the cumulative substrate concentrations along the series of reactors considered here, it is expected that stirred tanks have not operational difficulties caused by high viscosity or not uniform distribution of substrate, enzyme, and products. Real fluids in continuous flow reactors generally do not exhibit the macrofluid or microfluid extremes in its micromixing behavior and are termed partially segregated. For the enzymatic hydrolysis of biomass, a micromixing behavior close to macrofluid is expected for short residence times and for intermediate and long residence times a gradual evolution to partially segregated flow is expected as cellulose is hydrolyzed and the solids structure of the substrate collapses. The prediction of cellulose conversion for these two limiting situations constitutes a frame for initial calculations in CSTR's performance.

A feeding profile of enzyme at the beginning of the series of CSTR's other than supplementation to maintain the initial enzyme loading was not considered due to limitations of the kinetic model that considers only one enzyme activity, and not explicitly takes into account the adsorption step. A most detailed kinetic model that takes into account the different enzyme activities (cellulase and β-glucosidase), others substrate variables in addition to concentration, and the heterogeneity of the system, is needed for futures studies. However, the modeling approach for the continuous distributed feeding presented here remains valid for any kinetic model.

Figure 2 illustrates the predicted cellulose conversion along the series when a stream with a substrate concentration of 3% w/w (Figure 2a) or 5% w/w (Figure 2b) is fed at the first reactor of the series for residence times by reactor of 10 h, 30 h, and 50 h. For each vertical line the top indicates the prediction of the macrofluid model, the bottom indicates the prediction of the microfluid model, and the horizontal line indicates the mean. Results show that for a given residence time, cellulose conversion at the exit of the n^{th} reactor predicted by the macrofluid model is greater than the predicted by the microfluid model. For the first reactor of the series the macrofluid model predict a cellulose conversion that is 21%, 16%, and 13% higher than the predicted by the microfluid model

for residence times by reactor of 10, 30, and 50 h, respectively. Cellulose conversion predicted by the macrofluid and microfluid models gets closer to each other as the numbers of reactors and/or the residence time by reactor are increased. These results are in accordance with the obtained by South et al. (1995) for the simultaneous saccharification and fermentation of lignocellulosic biomass in a single CSTR. Çakal et al. (2007) studied a solid-liquid reaction in a series of *n*-CSTR's and found out that the predictions of the macrofluid model for the first reactor was closer to the experimental value; however, microfluid provided results closer to the experimental value for the third and fourth reactors.

Cellulose conversion along the series exhibits an upward trend but tends toward a constant value at the end of the series. The cellulose conversion profiles along the series for an initial substrate concentration of 3% w/w shows two mean differences with the profiles for an initial substrate concentration of 5%: (*i*) a higher cellulose conversion is reached with a less number of reactors; (*ii*) a higher cellulose conversion is reached at the end of the series. The main reasons for this results are the differences in enzyme loading (a higher enzyme loading is added in the operation with 3% w/w) and the decrease in the performance of enzymes as substrate concentration is increased (Jørgensen et al., 2007-a; Kristensen et al., 2009). Glucose concentration at the outlet of the series of reactors does not exceed 1.4% w/w and 2.1% w/w for the initial substrate concentrations of 3% w/w and 5% w/w, respectively. So, continuous distributed substrate feeding of substrate and enzyme would be an option to be explored in order to increase glucose concentration overcoming mixing limitations.

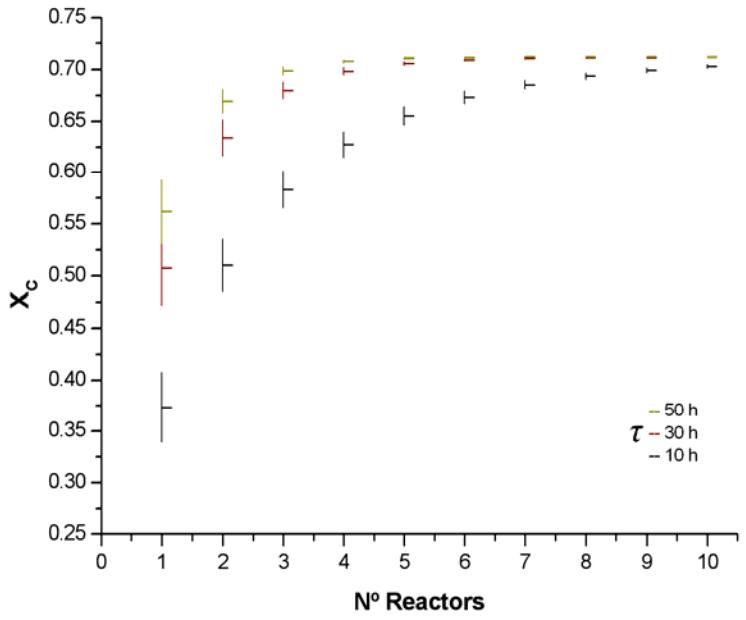

a.

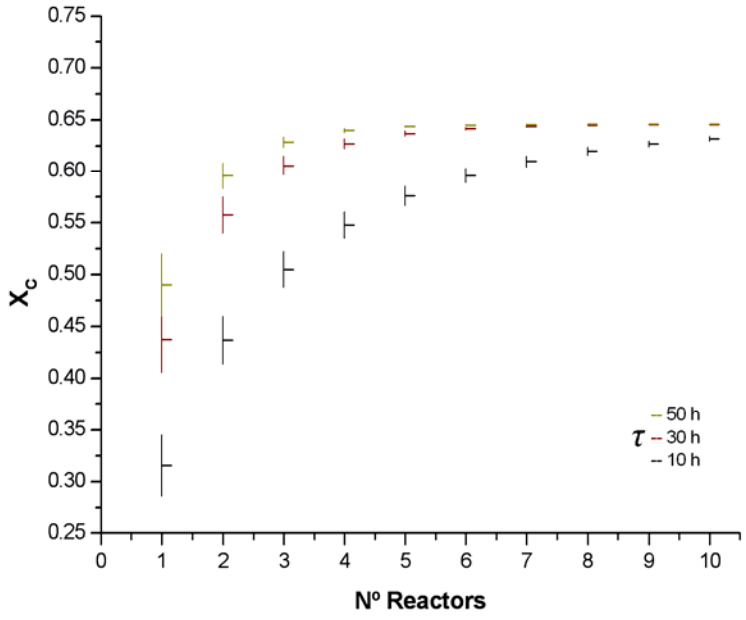

b.

Figure 2. Cellulose conversion for the operation with feeding at the first CSTR; initial substrate concentration of a) 3% w/w, b) 5% w/w

Figure 3 and Figure 4 show the intermediate cellulose and xylan conversions along the series when substrate is fed at the first two reactors in a distributed form. The growing continuous line indicates the prediction for a PFR with a residence time equivalent to the residence time of the series of CSTR's. The cumulative substrate concentrations (% w/w) along the series are: 3.0 R1 and 5.8 R2 (Figure 3a, 4a); and 5.0 R1 and 9.5 R2 (Figure 3b, 4b). As when substrate was added only at the first reactor, a less substrate concentration with a higher enzyme/substrate ratio shows higher intermediate and final cellulose and xylan conversions along the series. At the end of the series and for residence times by reactor of 30 h and 50 h, the distributed feeding allows to reach a similar cellulose conversion at the end of the series to that reached when substrate is only fed at the first reactor (Figure 2). Nevertheless, for residence time by reactor of 10 h, the cellulose conversion profile along the series is marked lower to that reached when substrate is only fed at the first reactor (Figure 2). Xylan reaches conversions higher than glucose with a less number of reactors. The use of a PFR after the distributed feeding enables to achieve higher conversions when compared to a series of CSTR's with equivalent residence time. Glucose concentration at the outlet of the series of reactors reached values up to 2.8% w/w and 4.3% w/w for the cumulative substrate concentrations of 5.8% w/w and 9.5% w/w, respectively. For the same conditions, Xylose concentration at the outlet of the series of reactors reached values up to 1.0% w/w and 1.5% w/w.

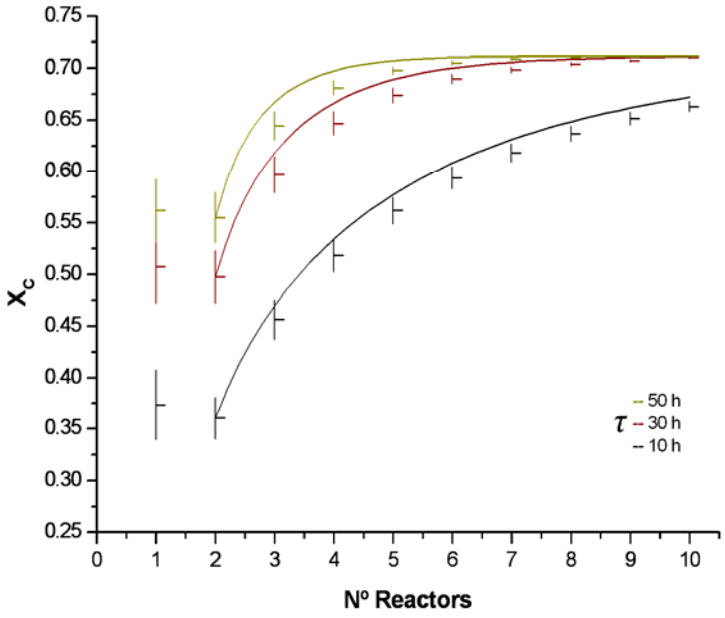

a.

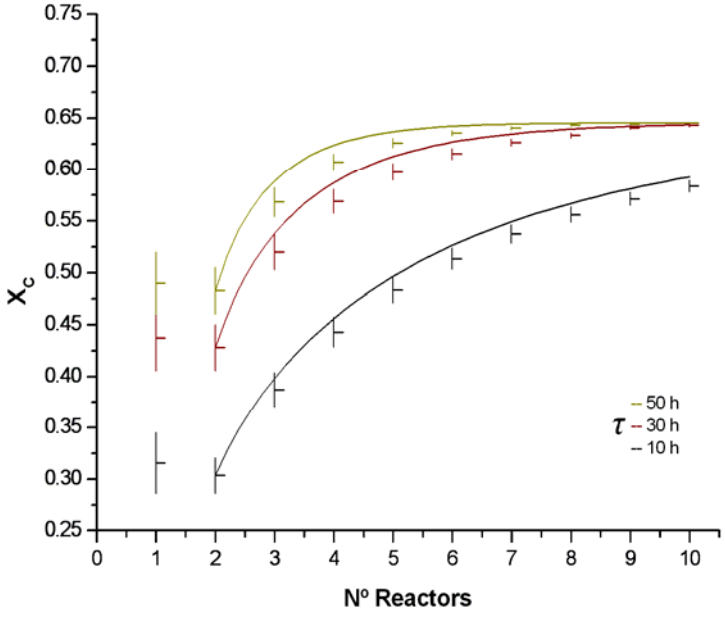

b.

Figure 3. Cellulose conversion for the operation with distributed feeding at the first two CSTR's followed by a series of *8*-CSTR's or an equivalent PFR; cumulative substrate concentration of a) 5.8% w/w, b) 9.5 % w/w

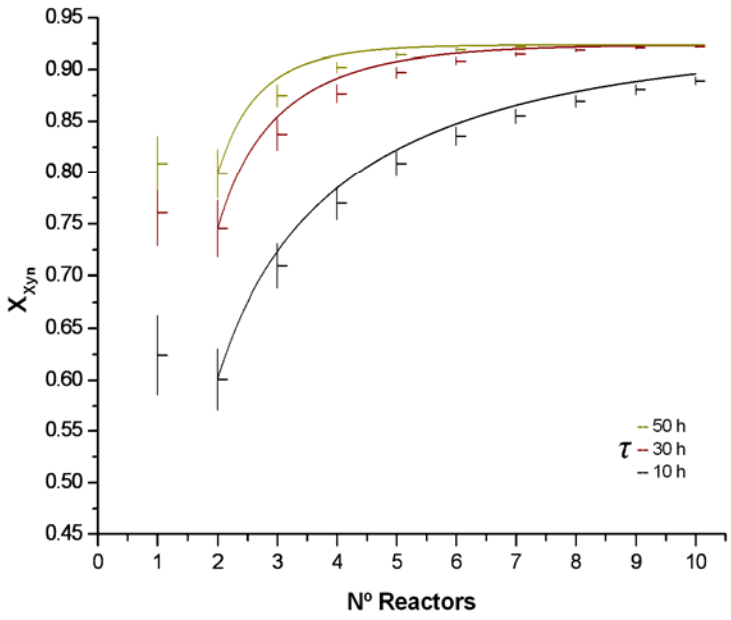

a.

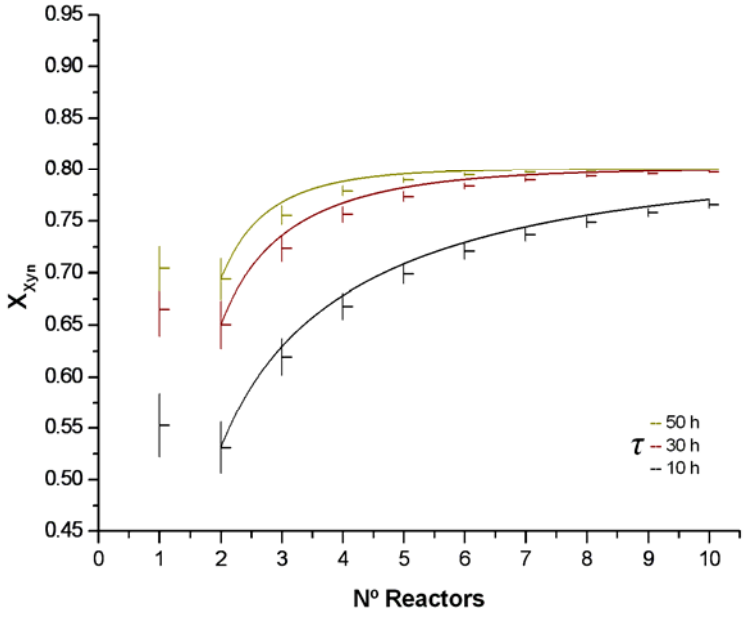

b.

Figure 4. Xylan conversion for the operation with distributed feeding at the first two CSTR's followed by a series of *δ*-CSTR's or an equivalent PFR; cumulative substrate concentration of a) 5.8% w/w, b) 9.5 % w/w

Figure 5 and Figure 6 show the intermediate cellulose conversions along the series when substrate is fed at the first three reactors in a distributed form. The cumulative substrate concentrations (% w/w) along the series are: 3.0 R1, 5.8 R2, and 8.5 R3 (Figure 5a, 6a); and 5.0 R1, 9.5 R2, and 13.6 R3 (Figure 5b, 6b). As in previous cases, a lower substrate concentration with a higher enzyme/substrate ratio shows a higher intermediate and final cellulose conversion along the series, residence times by reactor of 30 h and 50 h, and the distributed feeding allows to reach a similar cellulose conversion at the end of the series to that reached when substrate is only fed at the first reactor. Glucose concentration at the outlet of the series of reactors reached values up to 4.2% w/w and 6.3% w/w for the cumulative substrate concentrations of 8.5% w/w and 13.6% w/w, respectively. For the same conditions, Xylose concentration at the outlet of the series of reactors reached values up to 1.6% w/w and 2.3% w/w. A common characteristic of the conversion profiles along the series for the studied cases is that a higher residence time is required to achieve a given cellulose conversion when substrate is fed in a distributed form.

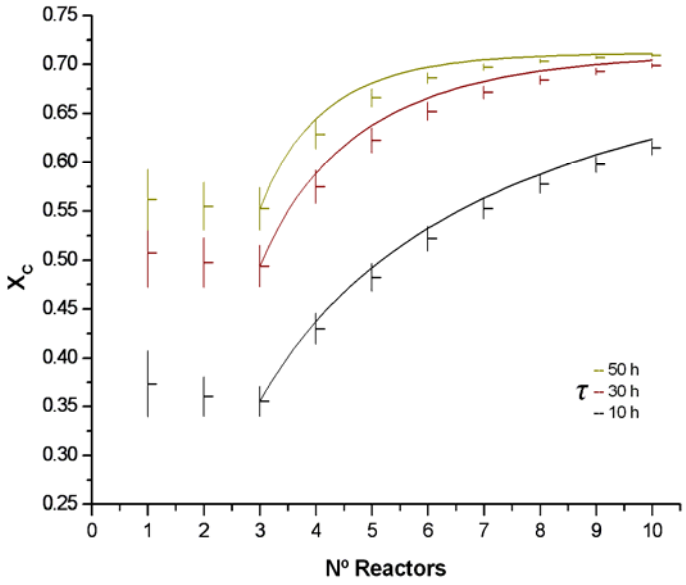

a.

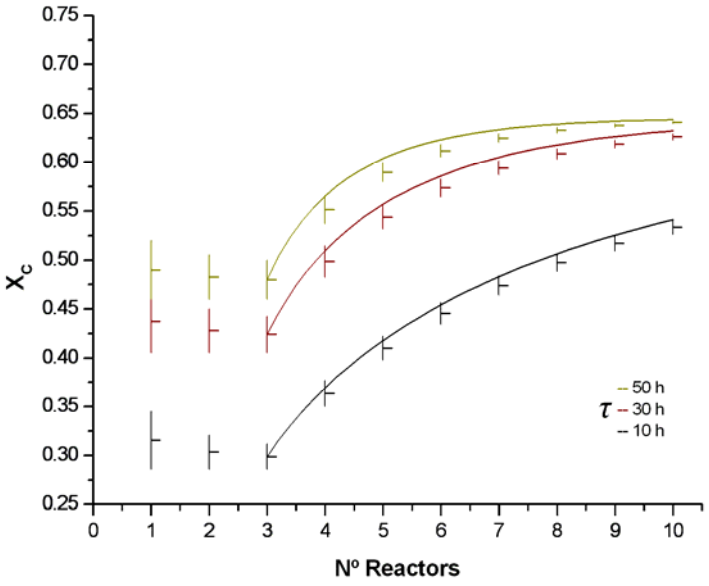

b.

Figure 5. Cellulose conversion for the operation with distributed feeding at the first three CSTR's followed by a series of *8*-CSTR's or an equivalent PFR; cumulative substrate concentration of a) 8.5% w/w, b) 13.6 % w/w

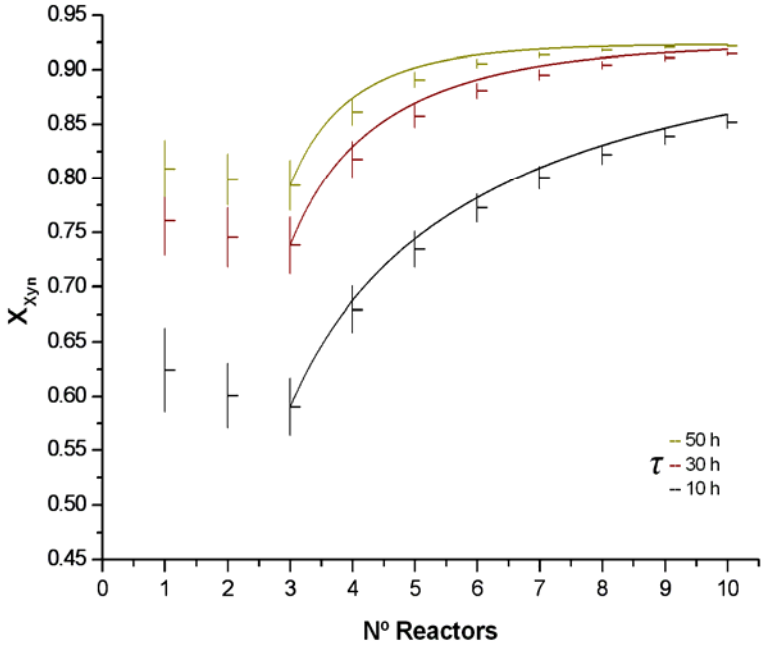

a.

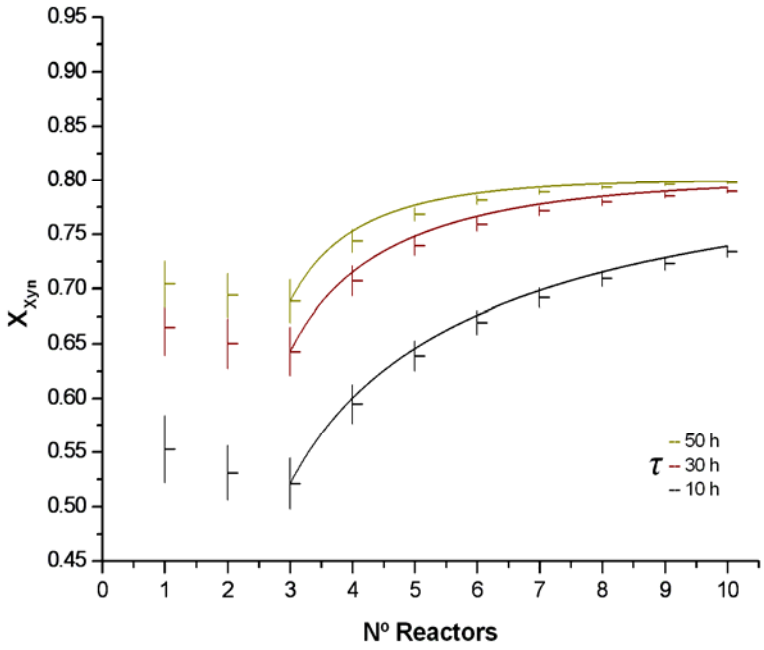

b.

Figure 6. Xylan conversion for the operation with distributed feeding at the first three CSTR's followed by a series of *8*-CSTR's or an equivalent PFR; cumulative substrate concentration of a) 8.5% w/w, b) 13.6 % w/w

The slow reaction kinetics (> 72 h) and the low substrate concentrations (< 15% w/w) render the enzymatic hydrolysis unsuitable for continuous reactor system mainly due to the high reactor volume required and the high water consumption. As assumed in this work, the substrate fed along the series should be free of water to diminish the water consumption and avoid dilution effects. Because there is a portion of substrate that remains as insoluble solids (non solubilized cellulose and xylose, lignin, and extractives), it accumulates along the series and can lead to mixing difficulties. The mass concentration of components others than cellulose and xylan does not exceed 5% w/w for the feeding strategies reported here.

Because of the kinetic model was not fitted for substrate concentrations higher than 5% w/w, concentrations higher than the depicted in the Figures 5b and 6b were not considered. However, the maximal substrate concentration that can be handled in conventional CSTR or tubular reactors may be around 10 to 12% (w/w, dry basis)

according to fed-batch studies summarized in the Table 1 and Kristensen et al. (2009).Thus, in a series with distributed feeding at the first three reactors the cumulative substrate concentration may be around 25% w/w, and the glucose concentration may reach values up to 10% w/w (assuming cellulose and mannan content of 60% and 60% conversion).

Operating hydrolysis with high substrate concentrations has been faced with the problem of enzyme inhibition by cellobiose and glucose. Removal of end products by employing membrane reactors (Gan et al., 2004) or operating the process as simultaneous saccharification and fermentation (Wingren et al., 2003) has been employed at laboratory scale in order to reduce enzyme inhibition. However the first option work well using pure cellulose substrates, but when lignocellulosic substrates are used membrane fouling is increased. As the optimum conditions for enzymes and fermenting microorganism are usually not the same, the operation of SSF is carried out under suboptimal conditions (Jørgensen et al., 2007-b). The modeling approach proposed here can be a valuable tool to analyze scenarios and choose alternatives for the above mentioned difficulties. Among the various options that can be analyzed it is important to highlight strategies of distributed feeding for enzymes, intermediate separation of final products (glucose and cellobiose), and operation with saccharification at the first reactors of the series and fermentation at the remained reactors as proposed by Aden et al. (2002).

6. Conclusions

In this work, a kinetic model of enzymatic hydrolysis fitted to experimental profiles of pretreated sugarcane bagasse was extended to accommodate continuous distributed substrate feeding in a series of *n*-CSTRs with equal residence time by reactor. This model was used for a modeling and simulation study considering the macrofluid and microfluid limiting situations in a series of two or three CSTR's with continuous distributed feeding of substrate and enzyme, followed by a series of *n*-CSTR's or by a tubular reactor. The macrofluid and microfluid models were used to obtain the upper and lower limits of cellulose conversion assuming that the CSTR's were well mixed in the macroscopic sense. Cellulose conversion predicted by the macrofluid and the microfluid model shows significant differences for the first three reactors of the series, but get closer to each other as the numbers of reactor and/or the residence time by reactor are increased. The use of a PFR

after the distributed feeding enables to achieve a higher conversion when compared to a series of CSTR's with equivalent residence time. The substrate concentration (% w/w) at the first reactor of the series was fixed at 3% and 5%, and distributed feeding in subsequent reactors to reach a cumulative substrate concentration of 5.8%, 8.5%, 9.5%, and 13.6% w/w was studied. Glucose and xylose concentrations (% w/w) at the outlet of 10 CSTR's ranged from 2.8% to 6.3%, and 1.0% to 2.3 were obtained.

The reactor configurations modeled and simulated in the present study show that cellulose conversions similar to those obtained when substrate is fed only at the first reactor may be reached in a series of 10 CSTR's with residence time by reactor higher than 30 h or a PFR with an equivalent residence time. As distributed substrate feeding allows to maintain the insoluble solids concentration at a manageable level and to reach high cellulose conversions, it is an attractive strategy of operation for continuous enzymatic hydrolysis. While these results are encouraging, experiments for enzymatic hydrolysis in continuous mode are essentials to elucidate relevant aspects such as reutilization of enzymes by readsorption on fresh substrate, feeding strategies for enzymes in a series of reactors, the effect of substrate particle size and composition on the rheological properties of biomass slurries, and operation strategies to diminish enzyme inhibition by final product. To further exploit the modeling approach proposed here, a more detailed kinetic model validated up to the maximal substrate concentration that can be handled in a conventional CSTR or a tubular reactor, that takes into account the different enzyme activities (cellulase and b-glucosidase), others substrate variables in addition to concentration, the heterogeneity of the system has to be used.

7. Acknowledgements

The author acknowledges the financial support provided by PAPESP (The Scientific Research Foundation for the State of São Paulo).

References

Aden A, Rith M, Ibsen K, et al. 2002. Lignocellulosic biomass to ethanol process design and economic utilizing co-current dilute acid prehydrolysis and enzymatic hydrolysis for corn stover: NREL, Golden, Co, USA.

Ballesteros I, Oliva JM, Saez F, Ballesteros M. 2001. Ethanol production from lignocellulosic byproducts of olive oil extraction. Appl Biochem and Biotechnol. 91-93:237-252.

Ballesteros M, Oliva JM, Manzanares P, Negro MJ, Ballesteros I. 2002. Ethanol production from paper material using a simultaneous saccharification and fermentation in a fed-batch basis. World J Microbiol Biotechnol. 18:559-561.

Cara C, Moya M, Ballesteros I, Negro MJ, González A, Ruiz E. 2007. Influence of solid loading on enzymatic hydrolysis of steam exploded or liquid hot water pretreated olive tree biomass, Process Biochem. 42:1003-1009.

Çakal GO, Eroğlu I, Özkar S. 2007. Simulation of continuous boric acid slurry reactors in series by microfluid and macrofluid models. J Crystal Growth. 306:240-247.

Fan ZL, South C, Lyford K, Munsie J, van Walsum P, Lynd LR. 2003. Conversion of paper sludge to ethanol in a semicontinuous solid-fed reactor. Bioprocess Biosyst Eng. 26:93-101.

Gan Q, Allen SJ, Taylor G. 2003. Kinetic dynamics in heterogeneous enzymatic hydrolysis of cellulose: an overview, an experimental study and mathematical modeling. Process Biochem 38:1003-1018.

Gan Q, Allen SJ, Taylor G. 2004. Design and operation of an integrated membrane reactor for enzymatic cellulose hydrolysis. Biochem Eng J. 12:223-229.

Hodge DB, Karim MN, Schell DJ, McMillan JD. 2008. Soluble and insoluble solids contributions to high-solids enzymatic hydrolysis of lignocellulose. Bioresour Technol 99:8940-8948.

Hodge DB, Karim MN, Schell DJ, McMillan JD. 2009. Model-based fed-batch for high-solids enzymatic cellulose hydrolysis. Appl Biochem Biotechnol. 152:88-107.

Huang AA. 1975. Kinetic studies on insoluble cellulose-cellulase system. Biotechnol Bioeng, 17:1421-1433.

Jørgensen H, Vibe-Pedersen J, Larsen J, Felby C. 2007-a. Liquefaction of lignocellulose at high-solids concentrations. Biotechnol Bioeng. 96:862-870.

Jørgensen H, Kristensen JB, Felby C. 2007-b. Enzymatic conversion of lignocellulose into fermentable sugars: challenges and opportunities. Biofuels Bioprod Biorefin 1:119-134.

Kadam KL, Rydholm EC, McMillan JD. 2004. Development and validation of a kinetic model for enzymatic saccharification of lignocellulosic biomass. Biotechnol prog. 20:698-705.

Kristensen JB, Felby C, Jørgensen H. 2009. Yield-determining factors in high-solids hydrolysis of lignocellulose. Biotechnol Biofuels. Doi 10.1186/1754-6834-2-11.

Levenspiel O. 1999. Chemical Reaction Engineering. New York: John Wiley & Sons Inc.

Lu Y, Wang Y, Xu G, Chu J, Zhuang Y, Zhang S. 2008. Influence of high solid concentration on enzymatic hydrolysis and fermentation of steam-exploded corn stover biomass. Appl Biochem Biotechnol. DOI: 10.1007/s12010-008-8306-0.

Mohagheghi A, Tucker M, Grohmann K, Wyman C. 1992. High solids simultaneous saccharification and fermentation of pretreated wheat straw to ethanol. Appl Biochem Biotechnol. 33:67-81.

Nakao K, Fukunaga K, Yasuda Y, Kimura M. 1990. Enzymatic hydrolysis of lignocellulosics with continuous irradiation of supersonic waves. Ann NY Sci, 613:802-807.

Perry RH, Green DW, Maloney JO. 1999. Chemical Engineering Handbook. New York. McGraw Hill. 7-17p.

Paul LE, Atiemo-Obeng VA, Kresta SM. 2004. Handbook of industrial mixing Science and Practice. John Wiley & Sons Inc, New Jersey.

Roche CM, Dibble CJ, Knutsen JS, Stickel JJ. 2009. Particle concentration and yields stress of biomass slurries during enzymatic hydrolysis at high-solids loadings. Biotechnol Bioeng. DOI 10.1002/bit.22381.

Rosgaard L, Andric P, Dam-Johansen K, Pedersen S, Meyer AS. 2007. Effects of substrate loading on enzymatic hydrolysis and viscosity of pretreated barley straw. Appl Biochem Biotechnol. 143:27-40.

Shao X, Lynd L, Wyman C, Bakker A. 2009. Kinetic modeling of cellulosic biomass to ethanol via simultaneous saccharification and fermentation: Part I. Accomodation of intermittent feeding and analysis of staged reactors. Biotechnol Bioeng. 102:59-69.

South CR, Lynd LR. 1994. Analysis of conversion of particulate biomass to ethanol in continuous solid retaining and cascade bioreactors, Appl Biochem and Biotechnol. 45-46: 467-481.

South CR, Hogsett DAL, Lynd LR. 1995. Modeling simultaneous saccharification and fermentation of lignocellulose to ethanol in batch and continuous reactors. Enzyme Microb Technol. 17:797-803.

Turian RM, Hsu FL, Ma TW. 1987. Estimation of the critical velocity in pipeline flow of slurries. Powder Technol 51:35-47.

Ventura C, Garcia F, Ferreira P, Rasteiro M. 2008. Flow dynamics of pulp fiber suspensions. Tappi J 20-25.

Wald S, Wilke CR, Blanch HW. 1984. Kinetic of enzymatic hydrolysis of cellulose, Biotechnol Bioeng. 26:221-230.

Wooley R, Ruth M, Sheehan J, Ibsen K, Majdeski H, Galvez A. 1999. Lignocellulosic biomass to ethanol process design and economic utilizing co-current dilute acid prehydrolysis and enzymatic hydrolysis current and futuristic scenarios: NREL, Golden, Co, USA.

Wingren A, Galbe M, Zacchi G. 2003. Techno-economic evaluation of producing ethanol from softwood: Comparison of SSF and SHF and identification of bottlenecks. Biotechnol Prog. 19:1109-1117.

Van Dike J. 1972. Enzymatic hydrolysis of cellulose: a kinetic study, PhD Thesis, Masscahuset Institute of Technology.

Viamajala S, McMillan JD, Schell DJ, Elander RT. 2009. Rheology of corn stover slurries at high solids concentrations – Effects of saccharifications and particle size. Bioresour Technol. 100:925-934.

Zwietering, T. 1959. The degree of mixing in continuous flow systems. Chem Eng Sci 11:1-15.

5.3. Conclusões

A conversão de celulose predita pelos modelos de macrofluido e microfluido mostram diferenças significativas nos primeiros três reatores de tanque agitado da série, mas convergem ao mesmo valor à medida em que se aumenta o número de reatores. O uso de um reator tubular após os reatores de tanque agitado com alimentação distribuída de substrato e enzima permite dimimuir o volume de reação requerido para alcançar uma conversão especificada quando comparado com uma série de reatores de tanque agitado. Como a alimentação distribuída de substrato e enzima nos primeiros três reatores da série permite incrementar as concentrações de substrato mantendo níveis de sólidos insolúveis manejáveis em reatores contínuos, esta é uma opção que deve ser estudada com mais detalhe a fim de incorporar as predições das propriedades reológicas do material ao longo da série de reatores. Embora os resultados obtidos neste capítulo sejam encorajadores, é necessário avaliar experimentalmente aspectos relevantes tais como a reutilização das enzimas por readsorção em substrato fresco, estratégias de alimentação distribuída de enzima, o efeito do tamanho de partícula nas propriedades reológicas do material e estratégias de operação para atenuar o efeito negativo da inibição de enzimas pelos produtos da reação. Para explorar a modelagem proposta neste estudo é necessário ajustar um modelo cinético mais detalhado da reação (ver capítulo 2) validado numa faixa de concentrações até a máxima concentração de substrato que pode ser atingida em reatores de tanque agitado.

Os seguintes capítulos dão enfoque a fluidodinâmica da mistura bagaço-água em tubulações horizontais com e sem defletores angulares internos. Ao invés de serem uma ruptura na linha de argumentação desta dissertação, tais estudos estão justificados na necessidade de mostrar alternativas de reatores contínuos que viabilizem a implementação da hidrólise enzimática de substratos lignocelulósicos em nível industrial. Esta é uma área de pesquisa de grande interesse na atualidade e na qual a modelagem e simulação são ferramentas obrigatórias para serem exploradas, principalmente pela dificuldade na realização de experimentos e utilidade para sugerir alternativas.

Capítulo 6 – Comportamento Fluidodinâmico de Suspensões de Polpas Fibrosas e sólidos suspensos com tendência à sedimentação

6.1. Introdução

Os processos de conversão da biomassa lignocelulósica envolvem o transporte e transformação de lamas (*slurries*) através de várias unidades de operação. Assim, o comportamento fluidodinâmico dessas lamas deve ser entendido a fim de projetar unidades de transporte, mistura, e reação. Devido à ampla distribuição de tamanhos de partícula e às formas incomuns das partículas, as partículas fibrosas interagem formando flocos e emaranhados ainda a baixas concentrações, enquanto partículas menores tendem a depositar-se. Além disso, nos sistemas com reação, a concentração, o tamanho e a forma das partículas, assim como a densidade e a viscosidade da fase líquida mudam significativamente. Como uma primeira aproximação, o comportamento fluidodinâmico das lamas de biomassa em tubulações pode ser enquadrado entre duas situações limite: (*i*) suspensões de polpas fibrosas onde o emaranhamento entre as fibras é predominante e (*ii*) sólidos suspensos com tendência à sedimentação.

A revisão aqui abordada engloba os padrões de fluxo, a queda de pressão, e as velocidades de transição entre os padrões de fluxo para suspensões de polpas fibrosas e para sólidos suspensos com tendência à sedimentação, em tubulações horizontais. A revisão visa o uso da Fluidodinâmica Computacional (CFD) com o intuito de avaliar o desempenho de um reator tubular para a hidrólise enzimática de substratos lignocelulósicos.

6.2. Desenvolvimento

O desenvolvimento deste capítulo é apresentado a seguir, no manuscrito intitulado *Fluid Dynamic Behavior of Fiber Suspensions and Settling Slurries in Pipes: A review*.

Fluid Dynamic Behavior of Pulp Fiber Suspensions and Settling Slurries in Pipe: A Review

Abstract

This work reviews the fluid dynamic behavior of fiber pulp suspensions and settling slurries in pipe with emphasis on flow patterns and transition velocities. These fluid dynamic behaviors are expected to be limiting situations for the flow of water-biomass slurries depending on aspect ratio and density of the swollen particles. Depending on the application, transportation or reaction, the bulk velocity of pulp fiber suspensions or settling slurries in pipe, and consequently the flow pattern and the pressure drop, are significantly different. The extreme properties and the heterogeneous nature of biomass particles make difficult the investigation in this area but are potentially rewarding in terms of aiding the ability of these materials to be used effectively. Further work is needed on multiphase flow of biomass materials to understand and optimize industrial biomass transportation and conversion processes.

Keywords: *pulp fiber suspensions; settling slurries; pipe; flow patterns; transition velocities*

Review Outline

1. Introduction

Conversion of biomass to sugar-derived fuels and chemicals involves the transportation and transformation of biomass slurries through the various unit operations during the process. Thus, the fluid dynamic behavior of biomass slurries needs to be understood to design appropriated transport, mixing, and reaction units. However, biomass particles are atypical. Unusual characteristics commonly include a combination of relatively large mean particle sizes, wide size distribution, extreme shapes (including flakes, chips, fibers, slivers, splinters, stalks), flexibility, compressibility, and general heterogeneity (Cui and Grace, 2007). Dependence of fluid dynamic behavior on biomass concentration is influenced by particle size, shape, size distribution and aspect ratio, because all of these parameters influence the formation of network structures within the slurry, the strength of these structures, and the types of packing within them (Viamajala et al., 2009). Fibrous particles may further interact by entanglement that can lead to formation of fiber networks or flocs that can result in complex slurry rheology (Arola et al., 1998; Switzer and Klingenberg, 2004).

Due to the wide size distribution and the extremes shapes of the biomass particles, larger fibers will become more entangled than smaller ones, whereas the smaller particles behave more like particles in slurries with smoother surfaces where increases surface area, friction, and settling tendency are the controlling phenomena (Dasari and Bergson, 2007; Rezania et al., 2009). Besides, with the progress of hydrolysis reactions, solids concentration, particles size, and particle shape undergo significant changes. Hence, the fluid dynamic behavior of biomass through pipelines can be framed between two limiting situations depending on aspect ratio and density of the swollen particles: (*i*) flow of pulp fiber suspensions where fibers entanglement is predominant, and (*ii*) flow of settling

slurries. The flow patterns, and the relationship between pressure drop and flow rates for pulp fiber suspensions and settling slurries are reviewed below.

2. Flow of pulp fiber suspensions

Basically, there are three main flow patterns in pulp fiber slurries namely plug, mixed, and turbulent flow as shown in Figure 1 (Ventura et al., 2008).

2.1 Plug flow

In this regime, the flow of fibers consists of a plug of fibers moving through the pipe as shown in Figure 1a (A-B). Plug flow is a direct result of the tendency of fibers suspensions to form networks/entanglements. Such networks have well defined mechanical strength properties and the shear stress applied as a result of flow is proportional to the pressure drop per unit length of pipe and the distance from pipe axis. Most of the pressure drop in this regime comes from mechanical friction between fibers and wall (Mmbaga, 1999). As the flow rate increases, there is a rolling regime in which fibers move away from the plug surface and roll along between the plug flow and pipe wall (Figure 1a B-C). A further increase in flow rate causes fibers to migrate away from the wall and form a sub-layer. This leads to a clear water annulus between the fiber plug and wall as shown in Figure 1a (C-D). The shear stress in this regime is laminar and velocity distribution is linear. The size of this annulus increases as velocity is increased and the shear takes place in this zone (Mmbaga, 1999).

2.2 Mixed Flow

As the flow rate increases, the clear water annulus eventually turns turbulent (Figure 1a D-E). Once turbulence occurs in the annulus, fibers peel away from the plug surface and are mixed in a random mode in the annulus. The transition from plug to mixed flow occurs at a point where the shear stress imposed on the plug is equal to the strength of the fiber network. As the flow velocity increases, the size of the turbulent annulus grows, which decreases the size of the plug Figure 1a (E-F).

2.3 Turbulent Flow

Further increases in flow rate cause the turbulent annulus to cover the entire pipe section as shown in Figure 1a (F-G). While there are some doubts if the plug can be eliminated completely while shear at the pipe axis is zero, it is fair to assume that the plug has disappeared at sufficiently high flow velocities. In the turbulent regime, fibers move relative to each other and the suspension may be considered as a conventional fluid. While flocs may form in this regime, they are continuously formed and disrupted, contrary to the plug flow regime where flocs may exist as coherent entities (Kerekes, 1993).

2.4 Pressure Drop

Considering the flow in a pipe, Figure 1c shows how the pressure drop changes in a pulp suspension as the different regimes are encountered. At low velocities (A to B) the pressure drop increases with velocity. This continues until the clear annulus of water forms (C). This annulus then grows and increases in size with increasing velocity, resulting in decrease in pressure drop. This occurs because the velocity imposed by the pulp plug creates a gradient over a large distance, and thus wall shear stress decreases. Finally, transition to turbulent flow in the annulus occurs (D), giving the mixed regime described earlier. If the velocity is increased beyond this point, the pressure drop increases. The curve eventually crosses the water line (E). Beyond this point, the suspension exhibits a phenomenon termed as drag reduction, whereby the pressure drop of the suspension is less than that of water. At very high velocities, drag reduction is diminished, and the pressure drop loss curve approaches that of water.

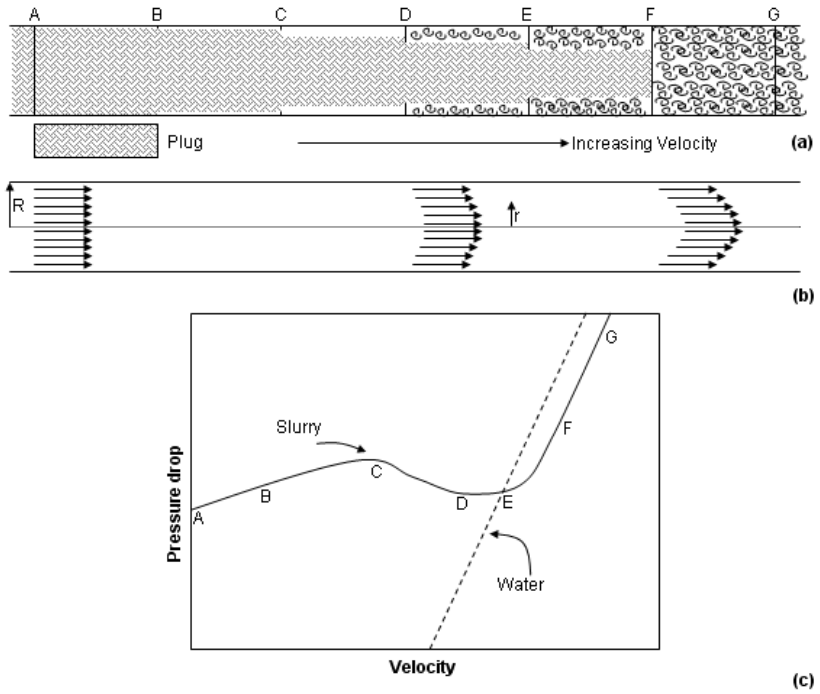

Figure 1 a) Schematic representation of the three basic flow mechanism of pulp suspensions in pipes (adapted from Mmbaga, 1999), b) velocity profiles, c) Pressure drop vs. velocity

2.5 Transition velocity from plug to mixed flow

The mass concentration of the suspension specifies the mass of fibers in the suspending medium, which is usually water. Thus,

$$C_m = \frac{m_f}{m_f + m_w} \tag{1}$$

where m_f and m_w are the mass of fiber and water, respectively. This parameter is commonly used industrially (where it is referred to as the *consistency* of the suspension and often expressed as a percentage) to calculate production and chemical applications (Paul et al., 2004).

Figure 2 illustrates the correlations obtained by Ventura et al. (2008) for the transition velocity (v_T) of three wood pulp fiber suspensions in a pipe of 0.1 m internal diameter. The mean fiber lengths for the pulps were: eucalypt 0.71 mm, pine + eucalypt 0.61 mm, and pine 2.56 mm. In general, the v_T values increase with consistency, the longest

fiber suspension shows a higher dependence of the transition velocities on consistency and for consistency values ranged from 2.0% to 3.2% the dependency is nearly linear.

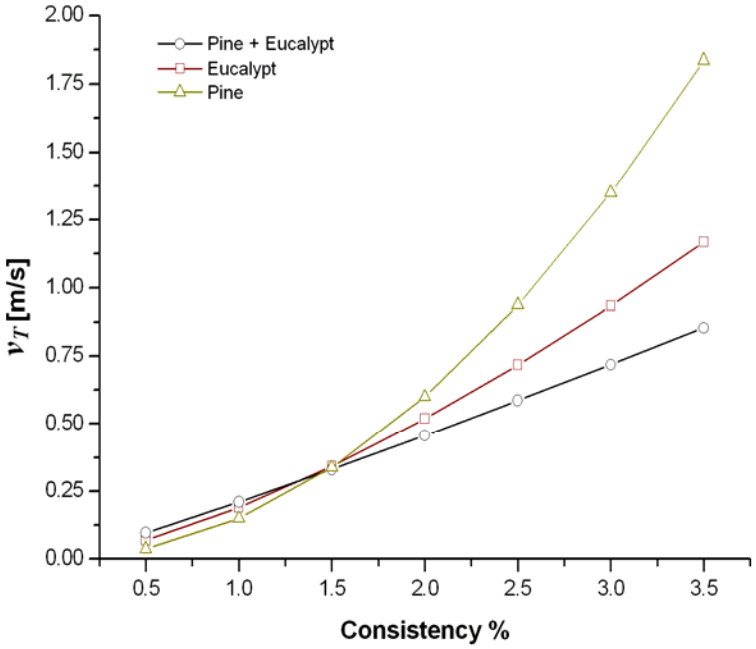

Figure 2. Transition velocities v_T the flow of wood pulp fiber suspensions (Ventura et al., 2008)

Figure 3 shows the pressure drop at the transition velocity v_T for three wood pulp fiber suspensions. The pressure drop increases with consistency, the longest fiber suspension exhibits the lower pressure drop at the transition velocity v_T.

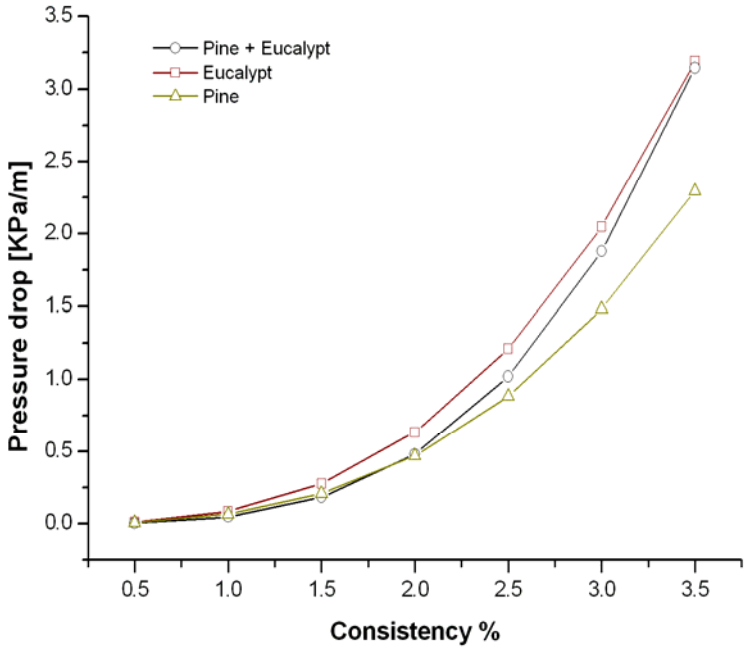

Figure 3. Pressure drop at the transition velocities v_M the flow of wood pulp fiber suspensions (Ventura et al., 2008)

These experimental results suggest that pulp flow is influenced by the type of pulp fiber because pressure drop and transition velocity differ from one pulp suspension to another. Nevertheless, for the plug flow the impact of each factor in the pressure drop is similar for all the pulps and consistency is the most important factor in all the cases, followed by pulp velocity and pipe diameter (Ventura et al., 2008).

3. Flow of settling slurries

According to Doron and Barnea, (1995) the solid-liquid flow of settling slurries in pipelines can be classified like flow with stationary bed, flow with a moving bed, and fully suspended flow.

3.1 Stationary bed

When the bulk velocity is too low to enable motion of all immersed particles, a stationary deposit is observed at the bottom of the pipe (Figure 4a A-B). On top of this deposit, particles are transported as a separate moving layer. In many cases, dune-like forms are observed on the upper part of the bed, a phenomenon known as "saltation" (Figure 4a B-C). The rest of the pipe is still occupied by a heterogeneous mixture, though its concentration profile is much steeper than in other flow patterns.

3.2 Moving bed

At lower mixture flow rates, solid particles accumulate at the bottom of the pipe. Thus they form a packed bed layer, which moves along the pipe bottom (Figure 4a C-D). The concentration of this layer corresponds to maximal packing or nearly so. The upper part of the pipe cross-section is occupied by a heterogeneous mixture.

3.3 Fully suspended flow

At high mixture flow rates all solid particles are suspended. The fully suspended flow pattern may be subdivided into two sub-patterns: (*i*) pseudo-homogeneous suspension, when the solids are distributed nearly uniformly across the pipe cross-section (Figure 4a E-F). The mixture velocities required for such flow are usually very high and cannot be considered practical; (*ii*) heterogeneous suspension flow, when there is a concentration gradient in the direction perpendicular to the pipe axis, with more particles transported at lower part of the pipe cross-section (Figure 4a D-E). This is the case in most practical applications. Further increases in flow rate cause a homogeneous distribution of solids to cover the entire pipe section as shown in Figure 4a (F-G).

3.4 Pressure Drop

The flow pattern designations depicted in Figure 4a are qualitative and may indeed constitute an incomplete description of the variations in flow behavior that takes place. Figure 4c shows how the pressure drop changes in slurry as the different regimes are encountered. At low velocities (A to B) the pressure drop is nearly constant with velocity. This continues until the moving bed forms at the bottom of the pipe (B to C). The thickness

of the moving bed then decreases, resulting in decrease in pressure drop. This occurs because the wall shear stress decreases. Finally, transition to fully suspended flow occurs (D). It is also referred to as the minimum carrying or the limiting velocity or velocity corresponds to lowest pressure drop. If the velocity is increased beyond this point, the pressure drop increases. In contrast to the flow of pulp fiber suspension where the pressure drop *vs.* flow velocity curve crosses the corresponding curve of water, pressure drop for the flow of slurries is always higher than pressure drop for water. Beyond this point, the suspension exhibits a heterogeneous flow (E to F) o homogeneous flow (F to G) where the pressure drop increases linearly with velocity.

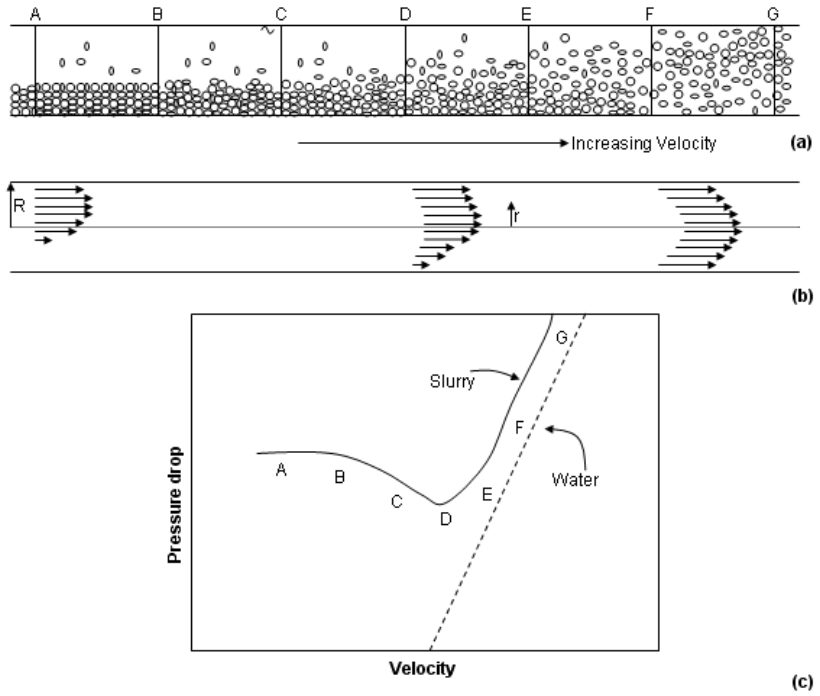

Figure 4. a) Schematic representation of the three basic flow mechanism of slurries in pipes, b) velocity profiles, c) Pressure drop vs. velocity

3.5 Tansition velocity from moving bed to fully suspended flow

The critical velocity of settling is defined as the minimum velocity demarcating flows in which solids form a bed at the bottom of the pipe from fully suspended flows. It is very difficult to determine experimentally, because the critical condition is difficult to discern, and because the flow becomes unstable near the critical condition (Turian et al.,

1987). There are some correlations for critical velocity in open literature (Wasp et al., 1977; Turian et al., 1987; Gillies and Shook, 1991). In this work, the correlation reported by Turian et al. (1987) (Equation 2) is used to depict the effect of solid/liquid density ratio and pipe diameter on the critical velocity.

$$\frac{v_C}{\left[2gD\left(\frac{\rho_s}{\rho}-1\right)\right]^{0.5}} = 1.7951 C_V{}^{0.1087}\left(1-C_V\right)^{0.2501}\left\{\frac{D\rho\left[gD\left(\frac{\rho_s}{\rho}-1\right)\right]^{0.5}}{\mu}\right\}^{0.00179}\left(\frac{d}{D}\right)^{0.06623} \qquad (2)$$

Where:

C_V: Concentration, solids volume fraction

D: pipe diameter [m]

d: particle diameter [m]

g: gravitational acceleration [m/s^2]

v_C: Critical velocity [m/s]

ρ_s: solids density [Kg/m^3]

ρ: liquid density [Kg/m^3]

μ: liquid viscosity [Kg/ms]

Turian et al. (1987) stated out that: (*i*) the dependence of the critical velocity on pipe diameter is very nearly equal to D$^{0.5}$; (*ii*) for slurries comprised of large non-colloidal particles, the critical velocity is virtually independent of particle size, and (*iii*) a substantial body of experimental data suggests that the critical velocity-volume fraction of solids relation possesses a maximum that occurs between 0.25 and 0.30 volume fraction of solids. Figure 5 illustrates the effect of pipe diameter and the particle diameter on maximal critical

velocity. The carrying fluid is water at 50°C and the solid/liquid density ratio is assumed from 1.1 to 1.20.

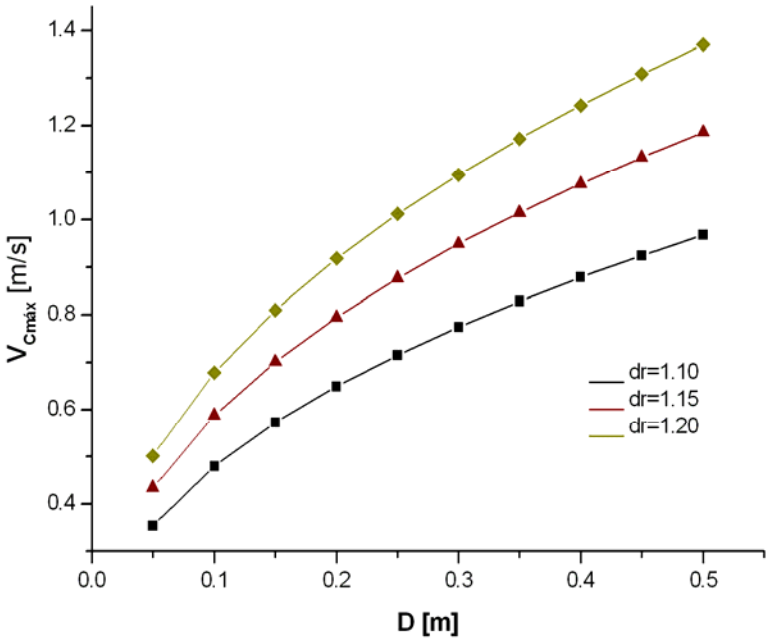

Figure 5. Effects of pipe diameter (*D*) and solid/liquid density ratio (*dr*) on maximal critical velocity. Carrying fluid: Water; Temperature 50 °C, particle diameter 1.0 mm

Various investigations have tried to show and propose correlation relating pressure drop with other parameters of solid-liquid flow namely solids density, liquid density, particle size, concentration, pipe diameter, viscosity of flowing media, velocity of suspension, etc., (Turian and Yuan, 1977; Doron et al., 1987; Gillies et al., 1991-b; Kaushal and Tomita, 2002). Some difficulties in applying published correlations to predict the pressure drop of settling slurries at the critical velocity for particles with density close to the density of water are: average error of different published empirical correlations is found around 25% when exposed to a large databank consisting different systems (Lahiri, 2009); most of experiments has been conducted at velocities higher than the critical velocity and with particle density higher than 1.2, for slurries with wide size side distribution it is no

possible to evaluate accurately the value of parameters like the drag coefficient, and hindering settling effects at high solids concentrations.

4. Discussion

Depending on the application, transportation or reaction, bulk velocity of pulp fiber suspensions or settling slurries in pipe, and consequently flow pattern and pressure drop, are significantly different. Typical velocity for pipeline transport of biomass has been set as 1.5 m/s by Kumar et al. (2004) for cost estimation. For pipeline transportation of settling slurries, a pumping velocity ranged from 1.4 to 1.8 m/s has been suggested (Woods, 2007). While in transportation flow velocity and pressure drop are variables that must be optimized, in reaction systems additional considerations about kinetics and mass transfer are needed. For instance in the presence of slow reactions were large reaction volume is obligatory, the system should be operated at the minimum velocity that assures fully suspended flow. However, if a spread in residence time distribution is harmful, the use of static mixers should be considered (Woods, 2007).

As was already discussed, depending on the fiber aspect ratio the material in the pipe will flow as pulp fiber suspension or settling slurry. For bulk velocities lower than the transition velocity v_T the pulp fiber suspension in a pipe flow like a plug, whereas for bulk velocities greater than the transition velocity V_{cmax} a settling slurry is fully suspended. The necessary and sufficient condition for plug flow is the residence time in the pipe to be the same for all elements of fluid (Levenspiel, 1999). If the flowing material behaves like a pulp fiber suspension this condition is nearly satisfied for any bulk velocities. On the other hand, if the flowing material behaves as settling slurry, significant deviations are expected for bulk velocities lower than V_{cmax}.

In the absence of more experimental data, Figures 2 and 5 provides an initial approximation of the range of velocities comprised between transition velocities from moving bed to fully suspended flow of pulp fiber suspensions, and transition velocity from plug to mixed flow of settling slurries assuming a pipe with 0.1 m internal diameter (Table 1).

Table 1. Transition velocities for pulp fiber suspension and settling slurry in pipe with 0.1 m internal diameter

Flowing Material		V_{cmax} **[m/s]**	V_T **[m/s]**	**Pressure drop [KPa/m]**	
				Slurry or Suspension	**water**
Settling Slurry. d=1.0 mm	ρ_s/ρ = 1.10	0.48	---	*nc	0.024
	ρ_s/ρ = 1.15	0.59	---	nc	0.035
	ρ_s/ρ = 1.20	0.68	---	nc	0.046
Pulp fiber suspension. Consistency 3.5%	Eucalypt	---	1.2	3.2	0.129
	Eucalypt + Pine	---	0.85	3.1	0.069
	Pine	---	1.8	2.3	0.271

* Non calculated

5. Conclusions

This work reviews the fluid dynamic behavior of fiber pulp suspensions and settling slurries in pipe. These fluid dynamic behaviors are expected to be limiting situations for the flow of water-biomass slurries depending on aspect ratio and density of the swollen particles. Depending on the application, transportation or reaction, bulk velocity of pulp fiber suspensions or settling slurries in pipe, and consequently flow pattern and pressure drop, are significantly different. While in transportation flow velocity and pressure drop are variables that must be optimized, in reaction systems additional considerations about kinetics and mass transfer are needed. The flow velocity of transition from plug to mixed flow of pulp fiber suspensions is influenced by: type of pulp, fiber consistency, fiber length, and fiber aspect ratio. The flow velocity that demarcates flows in which settling slurries display a bed at the bottom of the pipe from fully suspended flow depends mainly on particles density and pipe diameter. Some published correlations were used to predict these transition velocities for three pulp fibers and a settling slurry with physical properties similar to that expected for water-biomass suspensions

Further work is needed on multiphase flow of biomass materials to understand and optimize industrial biomass transportation and conversion processes. The extreme properties and the heterogeneous nature of biomass particles make difficult the investigation in this area but are potentially rewarding in terms of aiding the ability of these materials to be used effectively. Computational Fluid Dynamic (CFD) should be pursued

for these systems, although such flows are so complex, especially due to the nonlinear interactions among the particles (entanglement) and between the particles and the fluid.

6. Acknowledgements

The author acknowledges the financial support provided by PAPESP (The Scientific Research Foundation for the State of São Paulo).

6. References

Arola DF, Powell RL, McCarthy MJ, Li T-Q, Ödberg L. 1998. NMR imaging of pulp suspension flowing through an abrupt pipe expansion. AIChE J 44: 2597-2606.

Cui H, Grace JR. 2007. Flow of pulp suspension and slurries: a review. Int J Multiphase F 33: 921-934.

Dasari RK, Berson RE. 2007. The effect of particle size on hydrolysis reaction rates and rheological properties in cellulosic slurries. Appl Biochem Biotechnol 136-140:289-299.

Doron P, Granica D, Barnea D. 1987. Slurry flow in horizontal pipes – experimental and modeling. Int J Multiphase Flow. 13: 535-547.

Doron P, Barnea D. 1995. Flow pattern maps for solid-liquid flow in pipes. Int J Multiphase Flow. 22: 273-283.

Gillies RG, Shook CA. 1991-a. A deposit velocity correlation for water slurries. Can J Chem Eng. 69:1225-1227.

Gillies RG, Hill KB, Mckibben MJ, Shook CA. 1999. Solids transport by laminar Newtonian flows. Powder Technol 104: 269-277.

Kaushal DR, Tomita Y. 2002. Solids concentration profiles and pressure drop in pipeline flow of multisized particulate slurries. Int J Multiphase Flow. 28: 1697-1717.

Kerekes RJ. 1993. Pulp flocculation in decaying turbulence: A literature review. J Pulp Pap Sci. 9: 86-91.

Kumar A, Cameron JB, Flynn PC. 2004. Pipeline transport of biomasa. Appl Biochem Biotechnol 113-116:27-39.

Lahiri SK. 2009. Study on slurry flow modeling in pipeline. Doctoral Thesis, National Institue of Technology, Durgapur India.

Levenspiel O. 1999. Chemical Reaction Engineering. New York: John Wiley & Sons Inc.

Mmbaga JP. 1999. The use of mixing-sensitive chemical reaction to characterize mixing in the liquid phase of fiber suspensions. Doctoral Thesis. University of British Columbia.

Pande H, Rao NJ, Kapoor SK, Roy DN. 1999. Hydrodynamic behavior of nonwood fiber suspensions. Tappi J. 82: 140-145.

Paul LE, Atiemo-Obeng VA, Kresta SM. 2004. Handbook of industrial mixing Science and Practice. John Wiley & Sons Inc, New Jersey.

Rezania S, Ye Zhuoliang, Berson RE. 2009. Enzymatic saccharification and viscosity of sawdust slurries following ultrasonic particle size reduction. Appl Biochem Biotechnol 153:103-115.

Switzer LH, Klingenberg DJ. 2004. Flocculation in simulation of sheared fiber suspensions. Int J Multiphase Flow. 30:67-87.

Turian RM, Yuan T. 1977. Flow of slurries in pipelines. AIChE J. 23: 232-242

Turian RM, Hsu FL, Ma TW. 1987. Estimation of the critical velocity in pipeline flow of slurries. Powder Technol 51:35-47.

Ventura C, Garcia F, Ferreira P, Rasteiro M. 2008. Flow dynamics of pulp fiber suspensions. Tappi J 20-25.

Viamajala S, McMillan JD, Schell DJ, Elander RT. 2009. Rheology of corn stover slurries at high solids concentrations – Effects of saccharification and particle size. Bioresour Tecchnol 100:925-934.

Wasp EJ, Kenny JP, Gandhi RL. 1977. Solid-liquid flow – Slurry pipeline transportation, Trans Tech Publ., Rockport, MA.

Wood DR. 2007. Rules of thumb in engineering practice. Ed WILEY-VCH Verlag GmbH & Co. KGaA, Weinheim.

6.3 Conclusões

A revisão apresentada é bastante relevante para um entendimento qualitativo do comportamento fluidodinâmico de lamas de biomassa. Dependendo da aplicação, transporte ou reação, a velocidade de fluxo de suspensões de polpas fibrosas ou de sólidos suspensos com tendência à sedimentação e consequentemente os padrões de fluxo e a queda de pressão podem ser significativamente diferentes. Para aplicações de transporte, a velocidade de fluxo e a queda de pressão são variáveis que devem ser otimizadas, mas para sistemas com reação são necessárias considerações adicionais acerca da cinética e da transferência de massa. A velocidade de transição na qual o fluxo pistão exibido pelas suspensões de polpas fibrosas muda para fluxo misturado (fluxo pistão no centro da tubulação, fluxo turbulento perto da parede do tubo) depende do tipo da polpa, a consistência (concentração) e do comprimento das fibras. A velocidade que demarca o fluxo no qual sólidos suspensos com tendência à sedimentação apresentam um leito móvel no fundo da tubulação, do fluxo onde todas as partículas estão suspendidas depende principalmente da razão entre as densidades das partículas e do fluido assim como do diâmetro da tubulação.

Trabalhos adicionais a respeito do fluxo multifásico nos processos que envolvem a biomassa são necessários a fim de otimizar os processos de transporte e conversão. Com o conhecimento adquirido neste capítulo, o próximo capítulo apresenta a aplicação da fluidodinâmica computacional (CFD) para o estudo do comportamento fluidodinâmico de lamas biomassa-água em tubulações com e sem defletores angulares internos. Os estudos fluidodinâmicos vão permitir avaliar o desempenho de reatores tubulares com e sem defletores internos para a hidrólise enzimática de substratos lignocelulósicos.

Capítulo 7 – Estudo Fluidodinâmico de suspensões água-bagaço de cana em tubulações com e sem defletores angulares internos

7.1. Introdução

Neste capítulo é apresentado um estudo fluidodinâmico do escoamento da suspensão água-bagaço de cana em tubulações com e sem defletores angulares internos. A modelagem assume que as partículas de biomassa estão saturadas com água e não formam flocos e que a fração volumétrica de partículas saturadas é de 0.5. O estudo explora a possibilidade de usar reatores tubulares com e sem defletores para a hidrólise enzimática. O sistema multifásico é modelado em marcos de referencia Euleriano-Euleriano e Euleriano-Lagrangiano junto com o modelo padrão de turbulência k-ε. Os modelos matemáticos são solucionados no simulador comercial ANSYS CFX (de Ansys Inc., EUROPE).

O capítulo está composto por dois manuscritos em inglês. No primeiro, a configuração interna dos defletores é fixa, e são estudadas a distribuição local das partículas e a qualidade da suspensão para três velocidades médias na entrada do sistema de 0,10; 0,20 e 0,30 m/s. No outro manuscrito a velocidade de entrada da suspensão é fixa em 0.20 m/s e são estudadas a distribuição local das partículas, a qualidade da suspensão, a presença de zonas com recirculação e a queda de pressão para duas configurações de defletores. Nos dois casos, os resultados para as tubulações com defletores são comparados com os resultados para tubulação sem defletores.

7.2 Modelo CFD

As equações do modelo foram resolvidas no software comercial ANSYS CFX (de Ansys Inc., EUROPE) baseados na opção Modelo multifásico não homogêneo turbulento com dupla precisão.

Tabela 7.1 Equações do modelo

Equações de continuidade	$\frac{\partial}{\partial t}\left(r_l\rho_l\right)+\nabla\cdot\left(r_l\rho_l\boldsymbol{U}_l\right)=0$
	$\frac{\partial}{\partial t}\left(r_{si}\rho_s\right)+\nabla\cdot\left(r_{si}\rho_s\boldsymbol{U}_{si}\right)=0$
	$r_l+\sum_{i=1}^{N_{ps}} r_{si}=1$
Equações de momento	$\frac{\partial}{\partial t}\left(r_{si}\rho_s\boldsymbol{U}_{si}\right)+\nabla\cdot\left(r_{si}\left(\rho_s\boldsymbol{U}_{si}\boldsymbol{U}_{si}\right)\right)=-r_{si}\nabla p+r_{si}\nabla\cdot\bar{\bar{\tau}}_{si}+r_{si}\rho_s g+F_{l,si}^{L}+K_{l,si}(\boldsymbol{U}_l-\boldsymbol{U}_{si})$
	$\bar{\bar{\tau}}_l=\mu_l\left[\nabla\boldsymbol{U}_l+\left(\nabla\boldsymbol{U}_l\right)^T\right]-\frac{2}{3}\mu_l\left(\nabla\cdot\boldsymbol{U}_l\right)\bar{\bar{\boldsymbol{I}}}$
	$\frac{\partial}{\partial t}\left(r_{si}\rho_s\boldsymbol{U}_{si}\right)+\nabla\cdot\left(r_{si}\left(\rho_s\boldsymbol{U}_{si}\boldsymbol{U}_{si}\right)\right)=-r_{si}\nabla p+r_{si}\nabla\cdot\bar{\bar{\tau}}_{si}+r_{si}\rho_s g+F_{l,si}^{L}+K_{l,si}(\boldsymbol{U}_l-\boldsymbol{U}_{si})$
	$\bar{\bar{\tau}}_{si}=\mu_{si}\left[\nabla\boldsymbol{U}_{si}+\left(\nabla\boldsymbol{U}_{si}\right)^T\right]+(\lambda_{si}-\frac{2}{3}\mu_{si})\left(\nabla\cdot\boldsymbol{U}_{si}\right)\bar{\bar{\boldsymbol{I}}}$
Força lift	$F_{si,l}^{L}=-F_{l,si}^{L}=r_l\rho_s C_L(\boldsymbol{U}_l-\boldsymbol{U}_{si})\otimes curl(\boldsymbol{U}_{si})$
Coeficiente de intercâmbio interfacial	$K_{si,l}=\frac{3}{4}C_D\frac{r_{si}r_l\rho_l(\boldsymbol{U}_{si}-\boldsymbol{U}_l)}{d_{si}}r_l^{-2.65}$
	Wen and Yu, 1966
	$K_{si,l}=\frac{3}{4}C_{Dsi}\frac{r_{si}r_l\rho_l(\boldsymbol{U}_{si}-\boldsymbol{U}_l)}{d_{si}}r_l^{-2.65}\qquad r_l>0.8$
	$K_{si,l}=150\frac{r_{si}(1-r_l)\mu_l}{d_s}+1.75\frac{\rho_l r_s(\boldsymbol{U}_{si}-\boldsymbol{U}_l)}{d_s}\qquad r_l\le 0.8$
	Gidaspow et al., 1992
	$C_{Dsi}=\frac{24}{r_l\,\mathrm{Re}_{si}}(1+0.15(r_l\,\mathrm{Re}_{si})^{0.687})$
	$\mathrm{Re}_{si}=\frac{\rho_l d_{si}(\boldsymbol{U}_{si}-\boldsymbol{U}_l)}{\mu_l}$

7.3. Desenvolvimento

O desenvolvimento deste capítulo é apresentado a seguir, nos manuscritos intitulados *Computational Fluid Dynamic Simulations of the Water-Sugar Cane Bagsse Suspension in Pipe with Internal Static Mixer* e *CFD Simulation of Sugarcane Bagasse Ssuspension in Pipe and Baffled Pipe.*

Computational Fluid Dynamics Simulation of the Water-Sugarcane Bagasse Suspension in Pipe with Internal Static Mixer

Abstract

A comprehensive CFD model was developed to gain insight into flow characteristics of water-sugar cane bagasse suspension in pipe with and without internal static mixers. Two different modeling approaches were used: Eulerian-Eulerian and Lagragian Particle Tracking, both with the k-ε turbulence model. Local solid volume fraction distribution was studied for three mean velocity suspension; 0.10, 0.15 and 0.20 m/s. The mass volume fraction studied were 49.6 and 10 W/V of water-swollen particles. The predicted flow indicates the presence of loop flow pattern in the pipe with internal static mixers as a function of mean velocity suspension.

Keywords: *Biomass Suspension; Particle Volume Distribution; Static Mixer; Lagrangian Particle Tracking Model; Eulerian-Eulerian Model*

1. Introduction

Enzymatic hydrolysis of lignocellulosic materials to produce reducing sugars has long been pursued for its potential to provide an alternative renewable energy source. For the practical realization of technology, the biomass must be pretreated to decrease the recalcitrance and make the cellulose in the feedstock more susceptible to digestion by cellulose enzymes and finally hydrolyzed in suspension form. While many publications have dealt with development and improvement of biomass conversion processes, relatively few authors have studied biomass suspension flow characteristics (Cui and Grace, 2007). The process of enzymatic hydrolysis can be carried out in reactor of various types: batch stirred reactors (Gusakov et al., 1985; South et al., 1995), continuous stirred tank reactors (CSTR) (Gusakov et al., 1985; South et al., 1995), tubular reactors (Borchert and Buchholz, 1987; Yang et al., 2006), CSTRs in series (Shao et al., 2009) and tubular column reactors

(Gusakov et al., 1985). The tubular reactors offer advantages such as reducing required reaction volume, energy agitation requirements and enzyme inhibition by final product. In the present work, a CFD based model was used to assess the complex interactions between the suspension quality and the fluid mixing process of water-pretreated sugar cane bagasse suspension in a pipe with or without internal static mixer. Two modeling approaches are used: The Lagrangian Particle Tracking Multiphase Model and Eulerian-Eulerian Multiphase Model, along with the standard k-e turbulence model. The main advantage of using a Lagrangian framework for dispersed phase particles is that particle-level phenomena can be modeled rigorously. The Eulerian-Eulerian approach is more suitable for modeling the dispersed multiphase system with a significant volume fraction of dispersed phase (>10%) (Ranade, 2002).

2. Computational model

2.1 Eulerian-Eulerian model

The different phases are treated mathematically as interpreting continua, since the volume of a phase cannot be occupied by the other phases. These volume fractions are assumed to be continuous function of space and time and their sum is equal to one. Conservation equations for each phase are derived to obtain a set of equations, which have similar structure for all phases. Coupling is achieved through the pressure and inter-phase exchange co-effects. Any interaction between the interoperating phases is accounted for using closure laws (Van Wachem and Almstedt, 2003).

Eulerian-Eulerian approach is more suitable for modeling dispersed multiphase systems with a significant volume fraction of dispersed phase (>10%) and thus allows the computation of three-phase flow fields even with high solid hold-up. The accuracy of the Eulerian-Eulerian approach heavily relies on the empirical constitutive equations used, but it does not provide information about the hydrodynamics of individual particles and thus has limitations in predicting certain discrete flow characteristics such as particle size effect, particle agglomeration (Ranade, 2002).

2.2 Lagrangian particle tracking model

The fluid phase is treated as a continuum by solving the time averaged Navier-Stokes equations in the same manner as for a single-phase system, while the dispersed phase is solved by tracking a large number of particles through the calculated flow field using Newtonian equation of motion. The dispersed phase can exchange momentum, mass, and energy with the fluid phase. The particle models are combined with an Eulerian model for the continuous phase to simulate the disperse phase. The motion of fluid phase is calculated from the averaged fluid-phase governing equations, which are similar to Eulerian-Eulerian. The motion of the discrete phase particle is given by integrating the force balance on the particle, which is written in Lagrangian reference frame.

The advantage of Eulerian-Lagrangian approach is that the dynamics of the individual particles can be assessed, however, in the case of turbulent flows, it is necessary to simulate a very large number of particle trajectories to obtain meaningful averages. While, with the high concentrations of particles and for the large size reactors, the tracking process becomes highly memory-intensive and this approach is, therefore, suitable for simulating multiphase flows containing a low (<10%) volume fraction of the dispersed phases (Ranade, 2002).

ANSYS CFX employs a finite volume method to solve the general partial differential equations that describes fluid flow and mass momentum transport. The standard k-ε turbulence model is used for calculating the turbulent kinetic energy and the power rate dissipation. It is the most widely tested and the results are generally considered as reliable with a short calculation time [8]. For interface transfer multiple particle effects on the drag forces have included according to Wen Yu, (1966) drag model. Non-drag forces for virtual mass, lift, buoyancy, wall lubrication and turbulent dispersion have been included in the simulation.

3. Boundary conditions and solution domain

The system of study consists in a pipe with eight internal baffles (Fig. 1). The water retention volume (WRV), defined as the ratio of the weight of water retained per unit weight of pretreated sugar cane bagasse after centrifugation at 2000 rpm for 10 min, was measured (Lee and Fan, 1983). The water-swollen particles have a WRV of 9.912 and ρ=1112.2 kg/m^3. The particle size distribution is modeled through normal distribution of

Sauter diameter. Minimum, mean and maximum Sauter diameters are 5.00*10-6, $385*10^{-6}$ and $770*10^{-6}$ m respectively. Standard deviation in Sauter diameter is $128*10^{-6}$ m. The temperature was fixed at 50 ºC. The concentration of water-swollen particles used in the lagrangian-particle tracking approach was 10.0 w/v equivalents to 0.981 w/v of dry particles. The concentration of water-swollen particles used in the Eulerian-Eulerian approach was 49.6 w/v equivalents to 5.00 w/v of dry particles. The initial condition for each simulation was a parabolic solid particles and water profile with equal mean velocities (mv) of 0.10, 0.15 and 0.20 m/s inside the computational domain.

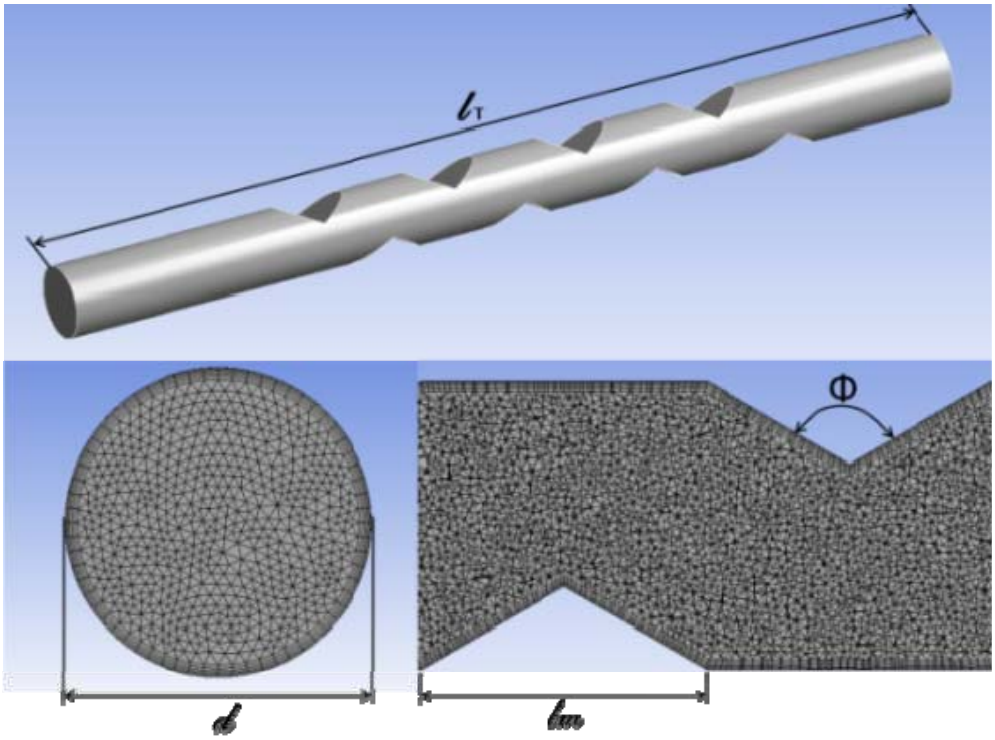

Figure 1. Pipe geometry and 3D grid details; Total length l_T=2.032 m, pipe diameter d=0.152 m, mixer length l_m=0.152 m, mixer angle Φ=120°.

4. Results and discussion

4.1 Solids volume fraction distribution

For the Eulerian-Eulerian approach, the size distribution of dispersed particles was discretized into ten size groups. The same Sauter mean diameter used in the Lagrangian Particle Tracking approach was used. Each of these size groups is considered as an

individual dispersed phase. The predicted solids volume fraction distribution shows higher solid particles concentration under the central axis and absence of solid particles near the top (Fig 2). The advantage of the static mixers is that they allow to avoid sedimentation of solids through modifications in geometry and/or increases in the mean velocity suspension.

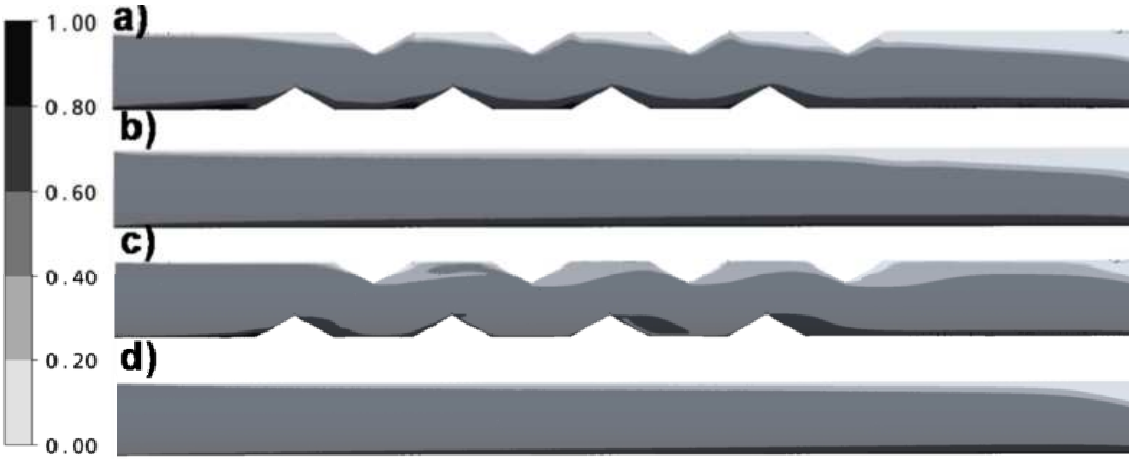

Figure 2. Predicted solids volume fraction distribution. a) Pipe with static mixers, mv'=0.1m/s; b) Pipe without static mixers, mv=0.1m/s; c) Pipe with static mixers, mv'=0.2m/s; d) Pipe without static mixers, mv=0.2m/s.

4.2 Suspension quality

The criteria based on the variation of the standard deviation (*sd*) of the radial solid volume fraction was used to predict the quality of suspension prevailing along the pipe (Fig 3). It can be see that the sd values along the pipes with internal static mixer are lower and more uniforms than the sd values for pipes without static mixers, that is to say, the quality of suspension is higher. However, increasing the mean velocity of the suspension diminishes the differences between the qualities of suspension for the two internal pipe configurations.

It is well known that the enzymatic hydrolysis requires residence times over 24 hours to reach high conversion of substrate. The main advantage of using static mixers for the reaction system is the ability to operate at lower velocities of suspension without losing the quality of the suspension. However, one must keep in mind that the simulation corresponds to the physical situation at the entrance to the reactor and it is expected that the

concentration of solid decline for long residence times (reactor length) due to the solubilization of cellulose.

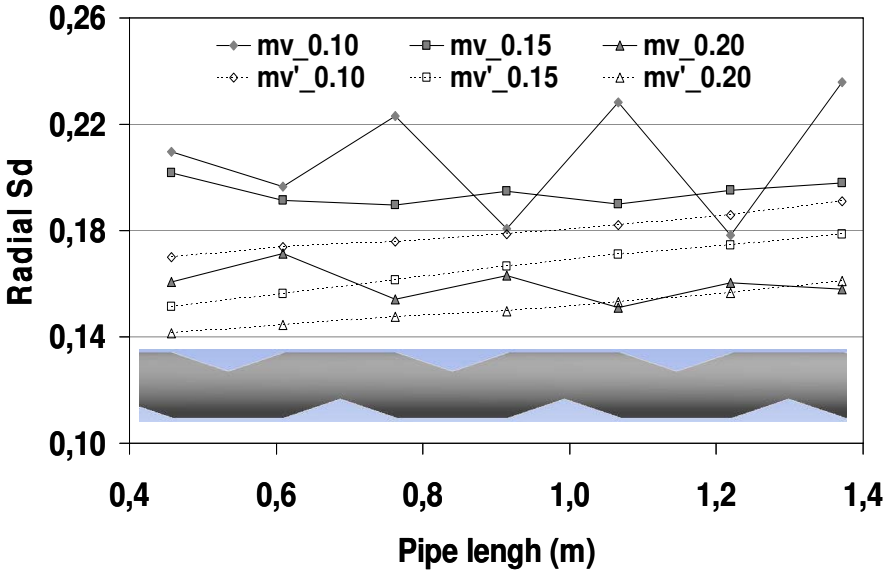

Figure 3. Predicted influence of mean solid velocity (mv) [m/s] on suspension quality: Pipe with (mv') and without (mv) static mixers.

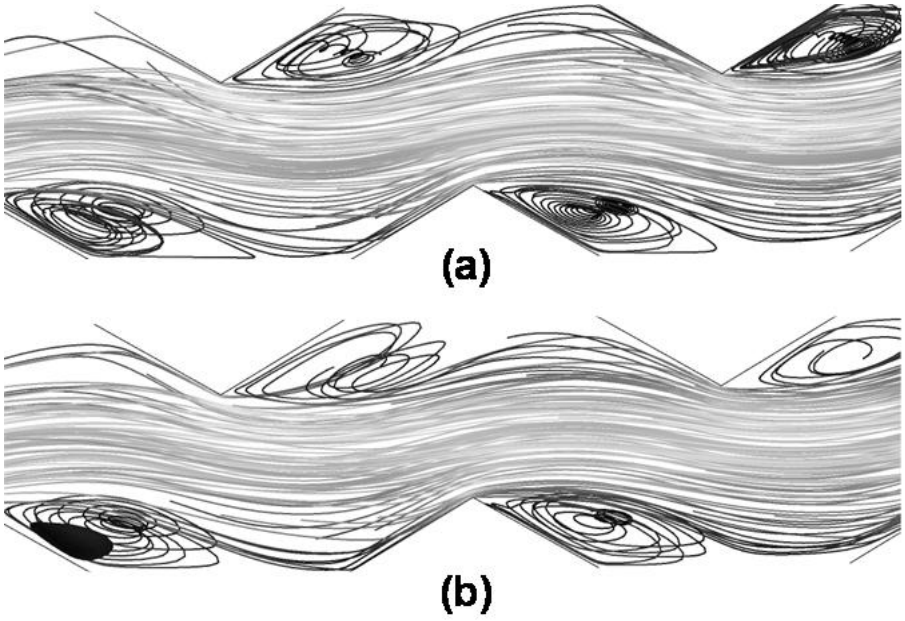

Figure 4. Particle flow pattern for mean velocity (mv) of: (a) 10 cm/s and (b) 20 cm/s.

5. Conclusions

The predicted liquid flow indicates the presence of loop flow pattern in the pipe with internal static mixers unlike the pipe without mixers. The internal static mixers are capable for generation liquid circulation which consequently leads to faster mixing. The liquid-phase flow pattern allows two limiting situations with increases in liquid-phase mean velocity: piston flow, transition between piston and loop flow and finally will predominate the loop flow. The other possibility to alter the flow pattern is changing the geometry of static mixer.

The Lagrangian Particle tracking was used for simulate the behavior of discrete particle in turbulent flow in the pipe with static mixers. The simulate result show that static mixer created confined mixing zones that affect the solid distribution inside of pipe. However, this approach appear gives an accurate insight to the particle behavior in the flow for the later optimization of the angle mixer with the aim of generated smaller turbulent length scales for to enhance suspension quality.

The model and results presented in this work are useful for extending the application of CFD model for simulating the flow of biomass suspensions in tubular reactors. The study suggests the use of other internal static mixer configurations. In addition, the advantages of configurations presented offer insides on the novel tubular reactor for the enzymatic hydrolysis of biomass.

6. Acknowledgements

The author wish to acknowledge the financial support provide by FAPESP (The Scientific Research Foundation for the State of São Paulo).

References

Borchert A, Buchholz K. 1987. Enzymatic hydrolysis of cellulosic materials, Process Biochem 22(6):173-180.

Cui H, Grace JR. 2007. Flow of pulp fibre suspension and slurries: A review, Int J Multiphase Flow 33(9):921-934.

Gusakov AV, Sinitsyn AP, Klyosov AA. 1985. Kinetics of the enzymatic hydrolysis of cellulose: 1. A mathematical model for a batch reactor process. Enzyme Microb Technol, 7(7):346-352.

Lee YH, Fan LT. 1983. Kinetic studies of enzymatic hydrolysis of insoluble cellulose: (II). Analysis of extended hydrolysis times. Biotechnol Bioeng 25(4):939-966.

Ranade VV. 2002. Computational flow modeling for chemical reactor engineering, London, U.K.

Shao X, Lynd L, Wyman C, Bakker A. 2009. Kinetic modeling of cellulosic biomass to ethanol via simultaneous saccharification and fermentation: Part I. Accommodation of intermittent feeding and analysis of staged reactors, Biotechnol Bioeng 102(1):59-65.

South CR, Hogsett DAL, Lynd LR. 1995. Modeling simultaneous saccharification and fermentation of lignocellulose to ethanol in batch and continuous reactors. Enzyme Microb Technol 17(9):797-803.

Yang S, Ding W, Chen H. 2006. Enzymatic hydrolysis of rice straw in a tubular reactor coupled with UF membrane, Process Biochem 41(3):721-725.

Van Wachem BGM, Almstedt AE. 2003. Methods for multiphase computational fluid dynamics. Chem Eng J 96(1-3):81-98.

Wen CY, Yu YH. 1966. Mechanics of fludization, Chemical Engineering Progress Symposium Series, 62, 62, 100-111.

CFD Simulation of Sugarcane Bagasse Suspension in Pipe and Baffled Pipe

Abstract

A computational fluid dynamic (CFD) model was developed to gain an insight into the fluid dynamic behavior of the sugarcane bagasse suspension in tubular and baffled tubular systems. The motivation for this study is that tubular reactor for biomass conversion, in this case sugar cane bagasse, gives the opportunity to conduct simultaneous transport and reaction with minimal agitation requirements. Solids volume fraction distribution, suspension quality (standard deviation of the radial solids volume fraction), zones of solids recirculation, and pressure drop were studied for empty and baffled tube with two configurations of internal baffles. The sugarcane bagasse concentration was 5.0% w/v on dry basis (equivalent to 49.6 % w/v of water-swollen particles) and the mean velocity of the suspension was 0.20 m/s. The modeling approach was Eulerian-Eulerian with the standard k-ε turbulence model, and the computational model with its sub-models was mapped using the commercial solver ANSYS CFX (of Ansys Inc., EUROPE). Results show that internal baffles allow operating the baffled tubular reactor of 0.152 m diameter at mean velocities below the critical ones without solids accumulation at the bottom of the pipe. However, localization and geometry of the baffles must be optimized because zones with solids recirculation that coincides with zones of high and low solids concentration are formed among the baffles.

Keywords: *Sugarcane bagasse suspension, baffled pipe, baffled tubular reactor, fluid dynamic*

1. Introduction

Conversion of biomass to sugar-derived fuels and chemicals involves the transportation and transformation of biomass suspensions through the various unit

operations during the process. Thus, the fluid dynamic behavior of biomass suspensions needs to be understood to design appropriated transport, mixing, and reaction units. Tubular in shape reactors for biomass conversion give rise to simultaneous transport and reaction. Besides, this operation offers advantages such as the lower required reaction volume and energy agitation for achieving a given conversion when compared with stirred tanks. Biomass conversion process is intensive in water consumption and reaction volume, therefore, be able to operate the tubular reactor at higher solid concentration and at lower mean suspension velocity as possible is crucial in the process economy. Biomass absorbs water and this may cause the bulk to become unsaturated at solids concentration above 10-15% w/w (Jørgensen et al., 2007) leading the biomass to behave as a wet granular material difficult to shear and uniformly mix. On the other hand, due to the settling tendency of solids particles, solids accumulation at the bottom of the pipe at lower suspension velocities may occur (Doron and Barnea, 1996). In the present simulation work, is assessed the suitability of a horizontal baffled pipe of 0.152 m internal diameter for keeping uniform distribution of solids volume fraction of a 5.0% w/v sugarcane bagasse suspension at a mean suspension velocity of 0.20 m/s.

Computational fluid dynamics (CFD) is a powerful and suitable tool for predicting flow and related phenomena. CFD-based models has been used to predict the solids-liquid flow of multisized particulate zinc (Lahiri and Ghanta, 2007) and the flow of pulp fiber suspensions (Rasteiro et al., 2008) at mean velocities from 1.66 to 4.17 m/s and 4.80 m/s, respectively. In contrast to the above applications that are focused on pressure drop, the present work focuses on the solids volume fraction distribution, the suspension quality, and the presence of zones with solids recirculation. This flow details are important for assessing the suitability of a tubular reactor (empty tube) or a baffled tubular reactor to biomass conversion.

2. Computational model

The full-scale problem of flow consists in a dispersed liquid-solid flow containing a high volume fraction of dispersed phase. It should be noted that the objective of the present work was not to capture the motion of the dispersed phase particles but to predict the overall liquid-solid phase mixing to understand the influence of internal baffles on the

flow pattern. For computational purposes, ten solid phases associated with specific narrow bands of particle size modeled through the normal distribution of Sauter mean diameter, were defined. The more suitable modeling approach for this multiphase system is the Eulerian framework for all phases with full coupling, where the different phases are treated mathematically as continuous medium. The volume fractions of each phase are assumed to be continuous functions of space and their sum equal to one. Conservation equations for each phase are derived to obtain a set of equations with similar structure for all phases. Coupling is achieved through the pressure and inter-phase exchange effects. The inter-phase drag coefficient that accounts by the multiple particle effects on the drag force was included according to the Ishii Zuber drag model (Ishii and Zuber, 1979). The difference in density between the solid and liquid phases was included through the density difference buoyancy model. The lift force exerted by the velocity gradient has been included in the simulation setting a non-dimensional lift coefficient of 0.1. The standard k-ε turbulence model was used for calculating the kinetic energy and the power rate dissipation. It is the most widely turbulence model tested and the results are generally considered as reliable with a short calculation time (Ranade, 2002).The continuity equations with the aforementioned sub-models were discretized through the finite volume method and solved using the commercial flow simulation software ANSYS CFX 11.0 (of Ansys Inc., EUROPE).

3. Boundary conditions and colution domain

For computational purposes, solids particles were assumed as entirely water-swollen. The ratio of the mass of water retained per unit of mass of biomass (WR) was obtained by centrifugation of water-swollen alkali-pretreated sugarcane bagasse at 2000 rpm for 10 min. Particles had a mean WR of 9.91 and a density of 1112 kg/m^3. The particle size distribution of water-swollen biomass was modeled through the normal distribution of Sauter mean diameter with minimum, mean, and maximum diameter of $5.0*10^{-6}$, $3.9*10^{-4}$ and $7.7*10^{-4}$ m, respectively. The temperature was fixed at 323 K. The concentration of water-swollen particles was fixed at 49.6% w/v that corresponds to 5.0% w/v of dry particles. The initial condition for each simulation was a parabolic solid particles and water profile with the same mean velocity of 0.20 m/s. A schematic layout of the studied system is illustrated in Fig. 1.

a. 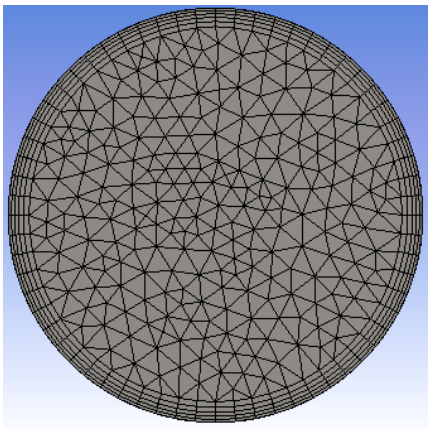

b. 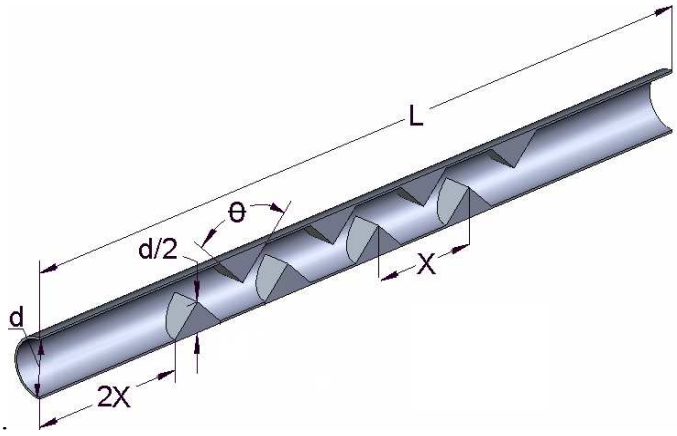

Fig. 1 a) Mesh details; b) Pipe geometry: Pipe diameter (d) 0.152 m; mixer angle (θ) 120°; separation length among baffles (x); Pipe Length (L) 8x; case 1: x_1 = 0.79 m, case 2: x_2 = 0.52 m.

4. Results and discussion

The incentive for tubular and baffled tubular reactors is that it enables the decrease of the required reaction volume and energy agitation for achieving a given conversion. Tubular reactors for enzymatic hydrolysis of biomass has been tested at laboratory scale (Yang and Ding, 2006) and modeled as plug flow (González Quiroga, 2007). Martínez et al. (2009) pointed out that internal baffles may avoid the formation of a moving or stationary bed during the transport of biomass suspension at low mean velocities (lower than 0.2 m/s).

The first two and the last two baffles located at the beginning and at the end of the pipe (Fig. 1) were not taken into account in the following analysis to avoid the effects produced by the abrupt changes in the velocity profile.

4.1 Critical velocity

The critical velocity (v_c) (defined as the minimum velocity demarcating flows in which the solids form a bed at the bottom of the pipe from fully suspended flows) for the suspension under the simulated conditions was calculated by the correlation of Turian et al. (1987) (Eq. 1).

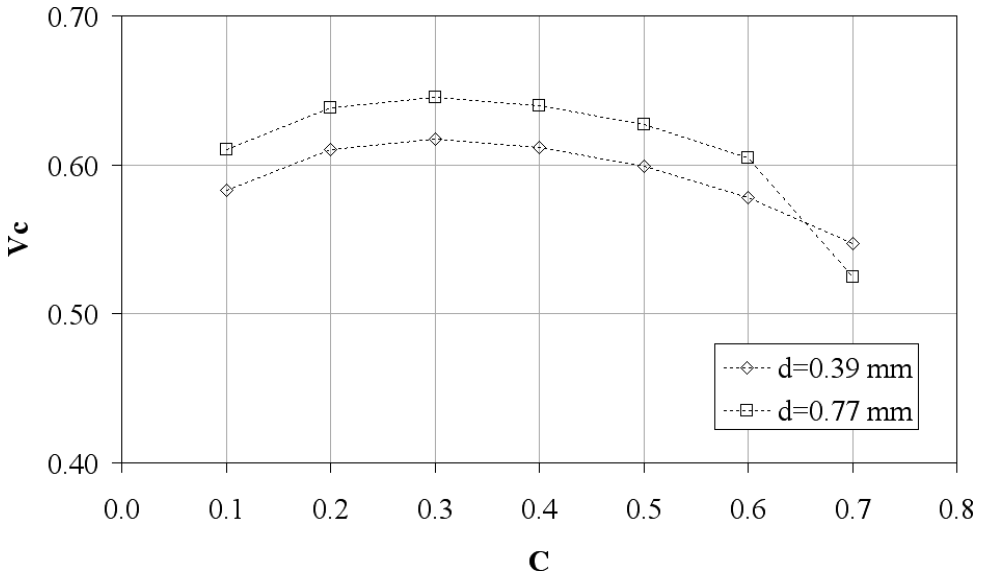

Fig. 2 Critical velocities in pipeline flow as a function of solid volume fraction for the flow conditions simulated in this work.

$$\frac{v_c}{2gD(s-1)^{0.5}} = 1.7951C^{0.1078}(1-C)^{0.2501}\left\{\frac{D\rho[gD(s-1)]^{0.5}}{\mu}\right\}^{0.00179}\left(\frac{d}{D}\right)^{0.06623} \quad (1)$$

Where:

C: solids volume fraction

D: inside diameter of pipe, [m]

d: diameter of solid particle, [m]

g: gravitational acceleration, [m/s^2]

ρ: density of liquid, [kg/m^3]

s: solid to liquid density ratio

μ: viscosity of liquid

The occurrence of a maximum in the v_c *vs.* C relationship (Fig. 2) may be explained on the basis of hindered settling which becomes more pronounced as concentration increases. The maximum in the v_c *vs* C curve occurs at the solid volume fraction of 0.3 and correspond to v_{cmax} of 0.62 and 0.65 m/s for particle diameter of $3.9*10^{-4}$ and $7.7*10^{-4}$ m, respectively (mean and maximum Sauter diameter of the current simulation). The mean velocity of the suspension was set 3.2 times lower than the v_{cmax} to

assure the presence of a bed at the bottom of the pipe without baffles and thus evaluate the effects of the baffles.

4.2 Solids volume fraction distribution (svfd)

The predicted *svfd* for a pipe without baffles shows higher solids concentration under the central pipe axis and absence of solids near the top. Efficient chemical and biochemical conversion of biomass requires uniform distribution of heat, eventually chemical catalyst and enzymes as well as mass transport of products into the bulk phase to prevent localized accumulation that could lead to product degradation or enzyme inhibition. Therefore, for the simulated velocity, a tubular reactor without baffles is not the best option and increases in velocity are needed to diminish the solids concentration gradient. Nevertheless, increases in the suspension velocity lead to increases in reaction volume to keep the same residence time of solids. In order to diminish solids concentration gradient without increases in suspension velocity, baffled pipe was proposed in this work. When the separation length among baffles was decreased, the results of the current simulation showed that the solids concentration gradient vanishes progressively.

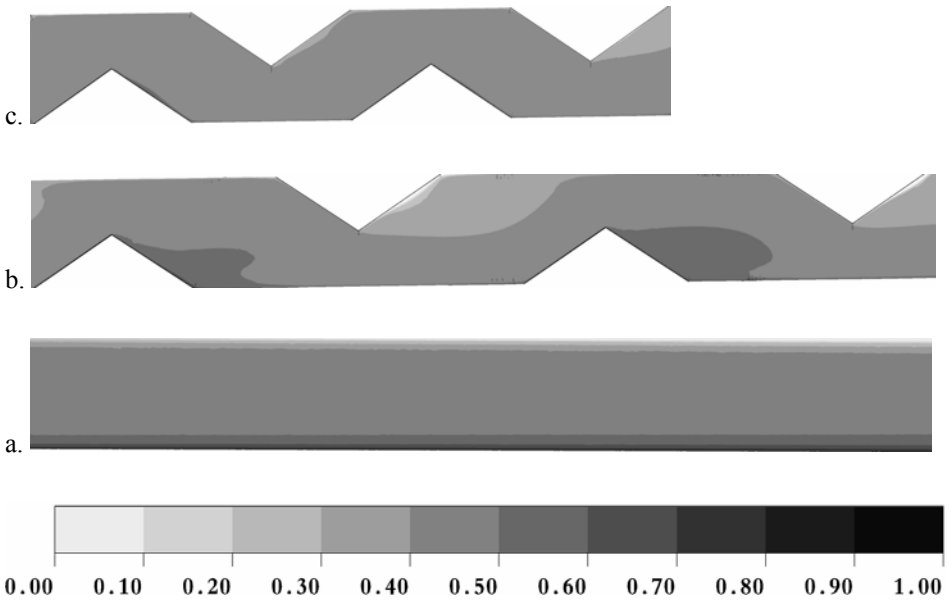

Fig. 3 Predicted solids volume fraction distribution. a) Empty pipe; b) Case 1; c) Case 2 (Pipes geometry for all cases is shown in Fig.1)

4.3 Solids velocity pattern

Solids velocity pattern was altered by the localization of the baffles. Zones of solids recirculation that coincides with zones of high or low solids concentration were formed among baffles. When the separation length among baffles was decreased, zones of solids recirculation diminished progressively but it did not disappear. The disadvantages of solids recirculation is because these zones of solids recirculation may accumulate reactants and products that could lead to inhibitions. Modifications in localization and geometry of the baffles would allow finding operational conditions that may alleviate the negative effects of solid recirculation, although, it is not possible avoid these effects completely.

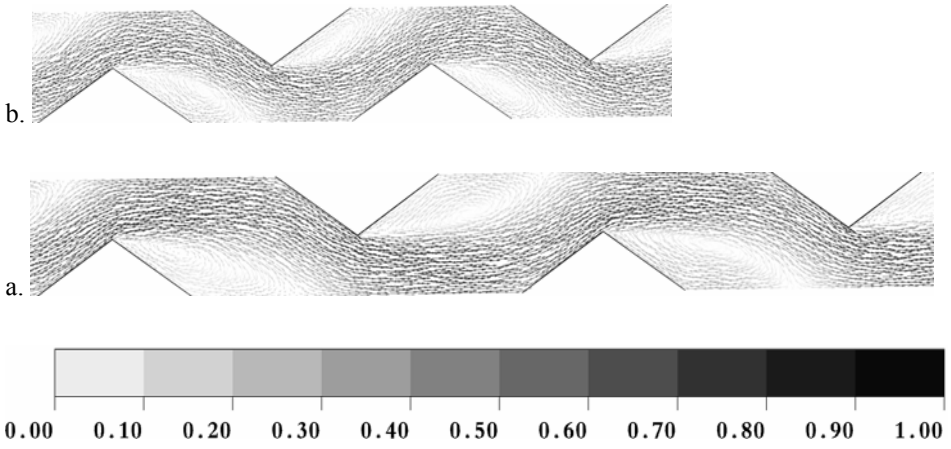

Fig. 4 Solids velocity pattern for the baffled pipes; a) Case 1; b) Case 2 (Pipes geometry is shown in Fig.1).

4.4 Suspension quality

The criteria based on the variation of the standard deviation (*sd*) of the radial solids volume fraction was used to predict the quality of the suspension prevailing along the pipe. It can be see that the quality of suspension improves significantly with the presence of baffles and by decreasing the length of separation among baffles. The quality of the suspension is an indicative of the homogeneity of the suspension in the radial direction and it can be used as a criterion for deciding among different baffles configurations.

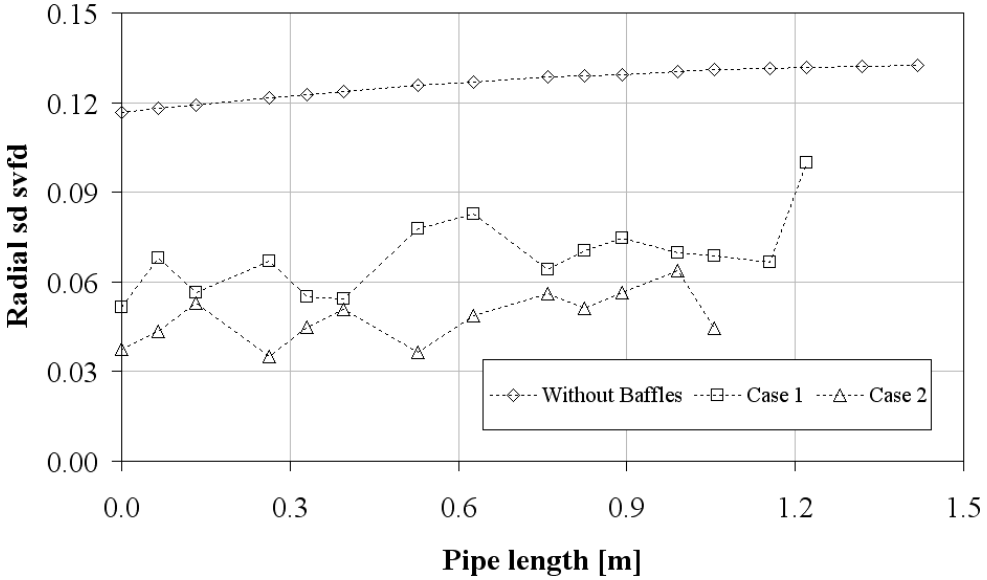

Fig. 5 Suspension quality in the empty pipe and in the baffled pipes

4.5 Pressure drop

Changes in the velocity field due to baffles causes significant changes in the pressure drop. The pressure drop per unit of length for the pipe without baffles and for the cases 1 and 2 were 3.75, 208, and 271 Pa/m, respectively. As expected, the pressure drop for the pipe without baffles is higher than the pressure drop for the flow of pure water under the same conditions, which is 2.33 Pa/m. Because rheological properties of biomass suspensions undergo dynamic changes as the conversion proceeds, pressure drop varies along the pipe. Baffles are not required when solids structure is solubilized into the liquid phase.

5. Conclusions

Tubular reactors for biomass conversion present a radial solids concentration that can lead to a solids accumulation at the bottom of the pipe, at mean velocities lower than the critical velocity. This solid accumulation can be avoided by using internal baffles. The current simulation study shows that internal baffles allow operating baffled tubular reactor of 0.152 m of diameter at mean velocities 3.2 times lower than the critical velocity for a biomass concentration of 5% w/v.

Internal baffles diminish the radial solids concentration gradient, but its localization and geometry must be optimized because zones with solids recirculation that coincides with zones of high or low solids concentration are formed among the baffles.

This study shows that CFD is a useful tool for the study of the fluid dynamic behavior of biomass suspension. This matter is the great importance for design and optimization of biomass conversion process. It is suggested experimental determination of the drag coefficient as a function of the size of water-swollen particles to improve the accuracy of the predict results.

6. Acknowledgements

The authors thank to FAPESP (The Scientific Foundation for the State of São Paulo) by financial support.

References

Doron P, Barnea D. 1996. Flow pattern maps for solid-liquid flow in pipes. Int. J. Multiphase Flow, 22:273-283.

González Quiroga A. Hidrólisis enzimática de bagazo de caña: Cinética y diseño de reactores, Undergraduate Thesis. Universidad Industrial de Santander, Colombia.

Ishii M, Zuber N. 1979. Drag Coefficient and Relative Velocity in Bubbly, Droplet, or Particulate flows, AIChE J 25:843-855.

Jørgensen H, Kristensen JB, Felby C. 2007. Enzymatic conversion of lignocellulose into fermentable sugars: challenges and opportunities. Biofuels Bioprod Bioref, 1:119-134.

Lahiri SK, Ghanta KC. 2007. Computational technique to predict the velocity and concentration profile for solid-liquid slurry flow in pipelines, in: 17th international conference on hydrotransport. Capetown, South Africa, 149-175.

Martínez EL, González Quiroga A, Jardín AL, Maciel Filho R. 2009. Computacional fluid dynamics simulation of the water-sugarcane bagasse suspensión in pipe with internal static mixer, in 19th European Symposium on Comp Aided Chem Eng. 26:683-688.

Rasteiro MG, Ventura CAF, García FAP, Ferreira PJ. 2008. CFD simulation of the turbulent flow of pulp fibre suspension, in: Particle Technology Forum, the 2008 Annual Meeting Philadelphia.

Ranade VV. 2002. Computational Flow Modeling for Chemical Reactor Engineering, First ed., Academic Press, London UK.

Yang S, Ding W, Chen H. 2006. Enzymatic hydrolysis of rice straw in atubular reactor coupled with UF membrane, Process. Biochem. 41 (2006) 721-725.

Turian RM, Hsu LF, Ma TW. 1987. Estimation of the critical velocity in pipeline flow of slurries. Powder Technol, 51:35-47.

7.4 Resultados simulação em estado transiente

7.4.1 Fração de volume dos sólidos

A Figua 1 mostra a fração de volume de sólidos em estado transiente. A geometria e o domínio da solução são as do tubo liso e o "caso 2" do segundo paper apresentado neste capítulo. Os sólidos e a água entran no sistema com um perfil de velocidade dado pela Equação 1.

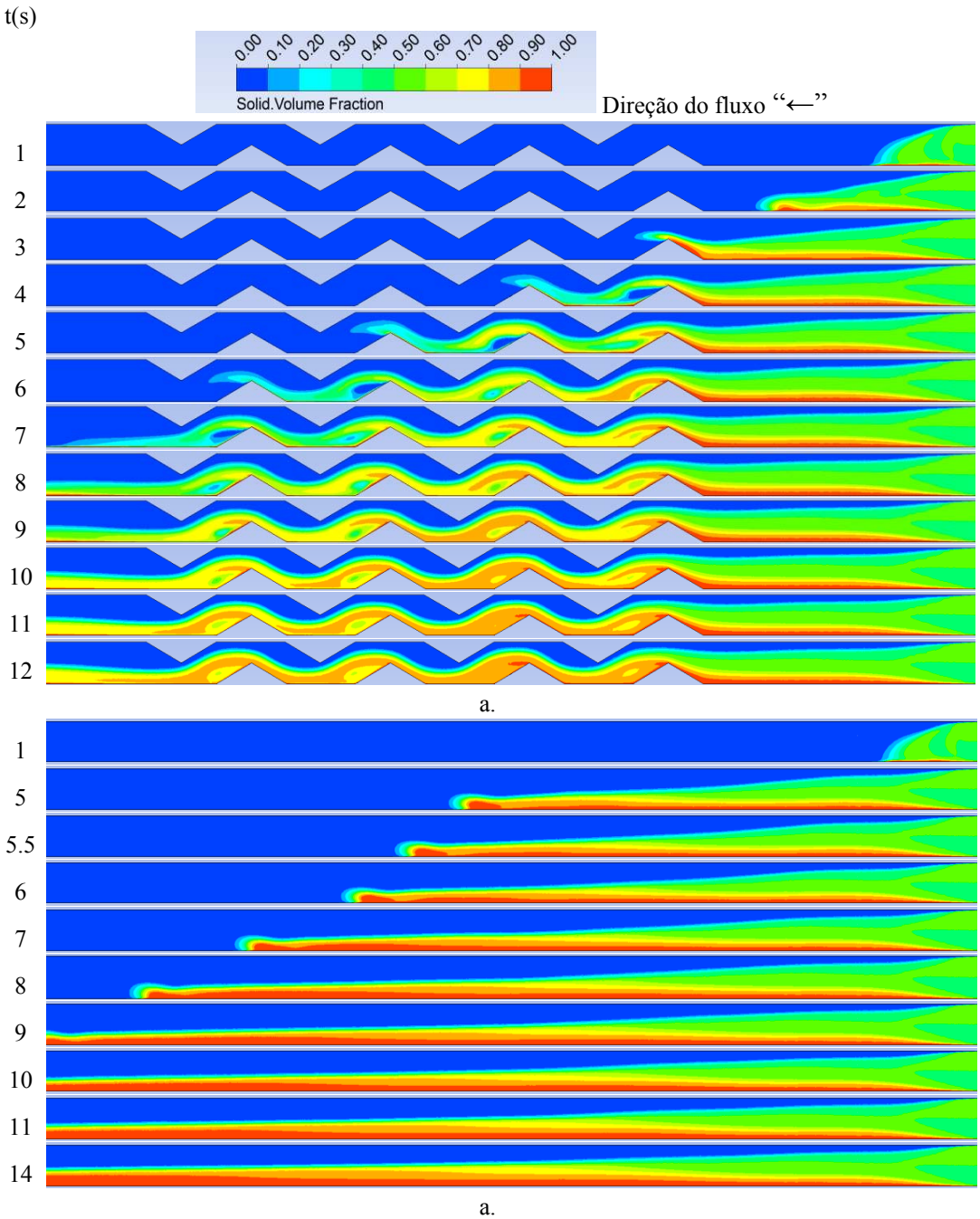

Figua 1. Fração de sólidos em estado transiente. Comparação entre (a) tubo sem defletores e (b) tubo com defletores.

$$v_{in} = 0.375\left(1-\frac{r}{R}\right)^{1/7} \quad (1)$$

A velocidade media na entrada do dominio é de 0.30 m/s.

A Figua 2 mostra a fração de volume ocupada pelos sólidos na saída do último bafle considerado. O resultado é comparado com o tubo liso e com o esprado para fluxo pistão ideal. Por inspecção qualitativa da Figura 1, e da distribuição de volume de sólidos em estado transiente da Figura 2, é evidente que os defletores permitem manter os sólidos em suspensão e a distribuição de sólidos é mais estreita quando comparada com o tubo liso. Uma velocidade média de fluxo de 0.30 m/s não é suficiente para homogeneizar a distribuição radial de sólidos pelo que se devem avaliar velocidades maiores e modificações da geometria de defletores proposta.

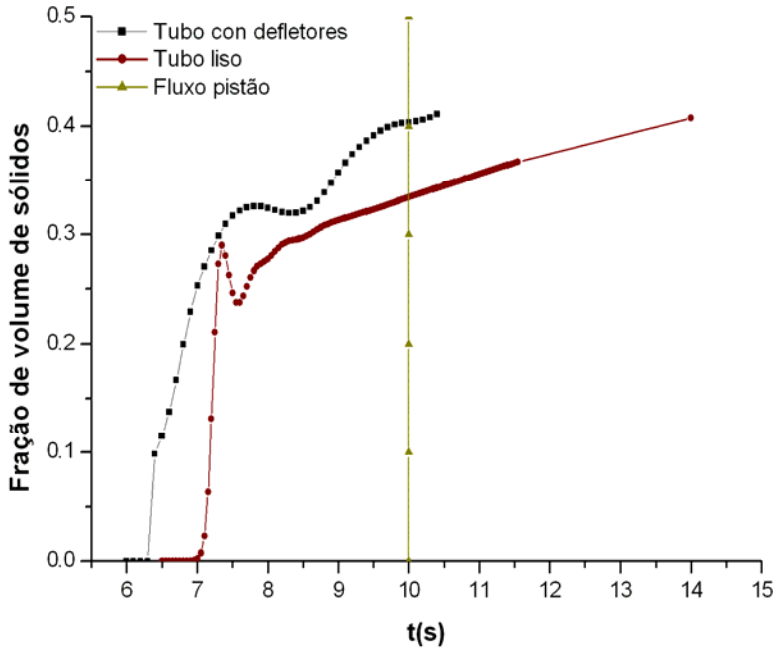

Figura 2. Distribuição da fração de volume de sólidos na saída de uma tubulação de 3.12 m para uma velocidade meia na entrada de 0.30 m/s.

7.5 Conclusões

Neste capítulo foi apresentada a modelagem fluidodinâmica de suspensões água-bagaço de cana em tubulações com e sem defletores internos. O estudo enfatiza os efeitos

da velocidade de fluxo e a configuração interna dos defletores. As condições da simulação correspondem às condições na entrada de um reator tubular onde as condições fluidodinâmicas são mais severas. Os resultados obtidos mostraram que os defletores induzem recirculação de sólidos e consequentemente diminuem os tempos de misturado. O padrão de fluxo em tubulações com defletores angulares internos muda de fluxo pistão para fluxo com recirculações de fluidos e sólidos entre defletores consecutivos. Os defletores angulares internos diminuem significativamente o gradiente de concentração de sólidos, mas a localização destes deve ser otimizada, já que zonas de alta concentração de sólidos que coincidem com zonas de recirculação de sólidos aparecem entre defletores consecutivos.

O estudo confirma que a fluidodinâmica computacional é uma ferramenta útil para o estudo do comportamento fluidodinâmico de suspensões de biomassa, e consequentemente na otimização de processos de transporte e conversão de biomassa. Contudo, as simulações apresentadas não consideram os efeitos de emaranhamento entre partículas fibrosas e os presentes resultados podem apresentar diferenças significativas com suspensões onde este efeito seja predominante. Sugere-se determinar experimentalmente o coeficiente de arraste em função do tamanho das partículas saturadas de água para aumentar a confiabilidade dos resultados.

Capítulo 8 - Análise Comparativa de Sistema de Reação Contínuos Para a Hidrólise Enzimática de Bagaço de Cana

8.1 Introdução

O aumento na demanda por etanol tem incentivado numerosos investigadores no Brasil e no resto do mundo a estudar o desenvolvimento da tecnologia de hidrólise enzimática de substratos lignocelulósicos. Com vantagens tais como a disponibilidade em grandes quantidades, a acumulação nas usinas, o alto conteúdo de celulose, o baixo conteúdo de cinzas quando comparado com outros substratos, etc., o bagaço de cana é um substrato atrativo para a hidrólise enzimática em escala industrial. Ainda hoje não há trabalhos disponíveis sobre projeto de reatores contínuos para hidrólise enzimática a nível industrial. Este fato se deve principalmente a que os estudos têm sido focados na compreensão do efeito de diversos tipos de pré-tratamento sobre a cinética da reação de hidrólise ao nível de bancada.

Neste capítulo se faz uso da maioria das informações obtidas ao longo desta dissertação para realizar balanços de massa de glicose, xilose e o substrato que solubilizado em reatores contínuos. Os sistemas de reação considerados são os referidos no capítulo 5. Tomando como base de cálculo um fluxo mássico no primeiro reator de uma série de reatores de tanque agitado ou de um reator tubular e com os perfis de conversão obtidos no capítulo 5, é possível obter uma primeira aproximação dos volumes de reação necessários. O projeto dos reatores exige considerações detalhadas acerca da agitação e mistura nos reatores. Nos capítulos 6 e 7 foram feitos o levantamento e algumas simulações do comportamento fluidodinâmico esperado num reator tubular, mas se requer mais informação experimental para um estudo mais aprofundado da agitação e mistura dos reatores. No capítulo 9 são apresentadas considerações sobre trabalhos futuros na parte experimental e de modelagem a fim de especificar os reatores de hidrólise com mais detalhe.

8.2 Considerações sobre o volume de reatores contínuos

A partir dos perfis de conversão obtidos no capítulo 5 (Capítulo 5, figuras 2b, 3b e 4b), foram calculadas as concentrações de glicose, xilose e substrato pré-tratado que não foram solubizados, o que inclui principalmente lignina, extrativos, celulose e xilana (outros) ao longo de uma série de 6 reatores CSTR com igual tempo de residência por reator (τ). Os resultados obtidos são mostrados na Tabela 1. A estratégia 1 corresponde à alimentação de 5% w/w de substrato pré-tratado (base seca) no reator 1, na estratégia 2 considerou-se que substrato pré-tratado adicional é alimentado no reator 2 para alcançar uma concentração acumulativa de 9.5% w/w (base seca) e na estratégia 3 considerou-se que substrato pré-tratado adicional é alimentado no reator 3 para alcançar uma concentração acumulativa de 13.6% w/w (base seca). As conversões de celulosa correspondem às meias entre as conversões obtidas considerando o material dentro dos reatores como macrofluido e microfluido.

Embora a alimentação de substrato de forma distribuída provoque uma queda nas conversões de celulose quando comparada com a operação convencional, os benefícios em termos da produção volumétrica do reator são muito importantes. As estratégias de alimentação 2 e 3 aumentam a concentração de glicose no sexto reator da serie por um fator de 2 e 3 respectivamente, com respeito ao valor obtido na serie convencional. Observa-se que o tempo de residência por reator (τ) tem impacto significativo na conversão final de celulose e por tanto na concentração final de glicose. Devido à proporcionalidade entre τ e o volume dos reatores, o volume da serie de 6 reatores foi calculado para três vazões e os três valores de τ da Tabela 6. Os resultados são mostrados na Tabela 2 e na Figura 1.

Tabela 1. Conversão e concentrações dos componentes ao longo da serie de reatores.

τ (h)	Estratégia	Parâmetro	R_1	R_2	R_3	R_4	R_5	R_6
10	1	Conversão	0,316	0,437	0,505	0,548	0,576	0,596
		Glicose (g/L)	10,6	14,6	16,7	18,3	19,2	19,9
		Xilose (g/L)	5,27	6,27	6,74	7,02	7,18	7,29
		Outros (g/L)	35,9	31,3	28,9	27,4	26,4	25,7
	2	Conversão	0,316	0,304	0,299	0,364	0,410	0,446
		Glicose (g/L)	10,6	20,3	25,8	29,6	32,3	34,3

		Xilose (g/L)	5,27	10,0	11,7	12,6	13,2	13,6
		Outros (g/L)	35,9	72,9	66,4	62,3	59,4	57,1
	3	Conversão	0,316	0,304	0,299	0,364	0,410	0,446
		Glicose (g/L)	10,6	20,3	30,0	36,5	41,1	44,7
		Xilose (g/L)	5,27	10,0	14,7	16,8	18,1	19,0
		Outros (g/L)	35,9	72,9	110	102	97.1	93.1

30	1	Conversão	0.438	0.558	0.606	0.627	0.637	0.642
		Glicose (g/L)	14,6	18,6	20,2	20,9	21,3	21,4
		Xilose (g/L)	6,27	7,07	7,34	7,45	7,51	7.53
		Outros (g/L)	31,3	27.0	25,3	24,6	24,2	24,1
	2	Conversão	0,438	0,428	0,520	0,569	0,598	0,615
		Glicose (g/L)	14,6	28.6	34,7	38,0	40,0	41,1
		Xilose (g/L)	6,27	12,3	13,7	14,3	14,6	14,8
		Outros (g/L)	31,3	63,5	56,7	53,2	51,2	50,0
	3	Conversão	0,438	0,428	0,424	0,499	0,544	0,574
		Glicose (g/L)	14,6	28.6	42.5	50,0	54,5	57,5
		Xilose (g/L)	6,27	12,3	18,2	20,0	20,9	21,5
		Outros (g/L)	31,3	63,5	95,8	87,4	82,5	79,3

50	1	Conversão	0,490	0,596	0,629	0,640	0,644	0,645
		Glicose	16,4	19,9	21,0	21,4	21,5	21,5
		Xilose	6,65	7,29	7,46	7,52	7,54	7,55
		Outros	29,4	25,7	24,5	24,2	24,0	24,0
	2	Conversão	0,490	0,483	0,568	0,607	0,626	0,636
		Glicose	16,4	32,3	37,9	40,5	41,8	42,5
		Xilose	6,65	13,1	14,3	14,7	14,9	15,0
		Outros	29,4	59,5	53,3	50,6	49,3	48,6
	3	Conversão	0,490	0,483	0,480	0,552	0,590	0,612
		Glicose	16,4	32,3	48,1	55,3	59,1	61,3
		Xilose	6,65	13,1	19,5	21,1	21,8	22,1
		Outros	29,4	59,5	89,6	81,7	77,7	75,4

Consideraram-se três vazões diferentes tomando a base de calculo na saída do primeiro reator da serie. O substrato alimentado em reatores subseqüentes é considerado como livre de água. A densidade meia do material dentro dos reatores é assumida como

constante ao longo da serie e igual a 1. Essa suposição é comum para lamas de biomassa a concentrações de biomassa seca menores de 12% w/w (Shao et al., 2007; Zhen et al., 2009). O volume do reator 1 (VR_1) é o mesmo nas três estratégias de operação e nos reatores 2 até 6 da estratégia 1. O volume do reator 2 (VR_2) aumenta levemente quando substrato adicional é alimentado neste reator e é o mesmo nos reatores 3 até 6 da estratégia de operação 2 e no reator 2 da estratégia de operação 3. Ao igual que VR_2, VR_3 aumenta quando substrato adicional é alimentado neste reator e é o mesmo nos reatores 4 até 6 da estratégia de operação 3 (Tabela 2). Esses resultados se devem à suposição de igual valor para τ ao longo da serie. Se o resultado desejado é o de igual volume dos reatores ao longo da serie para todas as estratégias de operação, a suposição de τ constante ao longo da serie deve ser removida em favor da suposição de VR constante ao longo da serie. Por tanto as distribuições de tempos residência usadas para simular o sistema como sendo macrofluido (Capítulo 5, Equação 6) deve ser removida em favor de uma expressão geral como à apresentada por Wen and Fan (1975).

Tabela 2. Volume dos primeiros três reatores da serie para três vazões de material à saída do primeiro reator da serie.

τ (h)	**Vazão R1 (Kg/h)**	**VR1 (m^3)**	**VR2 (m^3)**	**VR3 (m^3)**
10	1000	10,0	10,5	11,0
	5000	50,0	52,5	55,0
	10000	100	105	110
30	1000	30,0	31,5	33,0
	5000	150	158	165
	10000	300	315	330
50	1000	50,0	52,5	55,0
	5000	250	263	275
	1000	500	525	550

A Figura 1 apresenta os volumes totais para uma serie de 6 reatores com igual valor de τ para as três vazões da Tabela 2. Neste ponto é importante examinar a concentração de substrato que pode ser alimentada na serie de reatores. Este item é de grande importância devido à grande disponibilidade de matéria prima e às dificuldades para

operar os reatores com altas concentrações de substrato (>15% w/w, base seca). É evidente que a serie com alimentação distribuída nos primeiros 2 reatores incrementa o fluxo mássico de substrato que pode ser tratado por um fator de 2, em tanto a serie com alimentação distribuída nos primeiros 3 reatores incrementa o fluxo mássico de substrato que pode ser tratado por um fator de 3. Para um valor de τ de 30 h e um fluxo de material na saída do primeiro reator de 5000 kg/h, o fluxo de substrato (seco) que pode ser tratado na estratégia de operação 1 é de 250 kg/h é o volume da serie de 6 reatores é de 937 m^3. O exemplo do cálculo anterior pretende mostrar a facilidade para a obtenção de volumes de reação a partir dos perfis de conversão para as estratégias de operação propostas, modeladas e simuladas nesta dissertação. Considerações acerca do volume da serie de reatores a ser usado numa usina envolve considerações iniciais acerca das restrições impostas devido à máxima potencia de agitação que pode ser fornecida e considerações econômicas que estão além dos alcances deste trabalho.

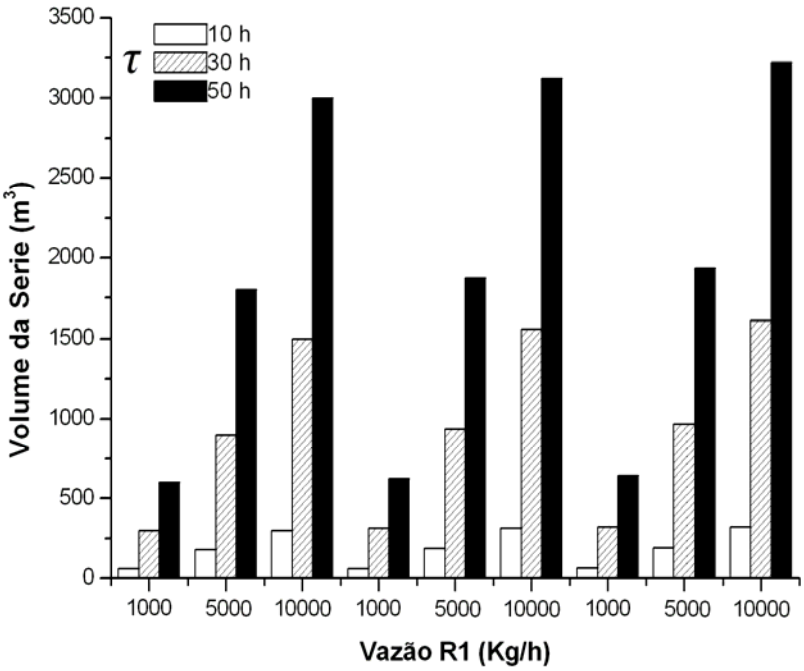

Figura 1. Volume da serie de 6 CSTR com igual tempo de residência por reator.

É claro que os grandes volumes de reação, assim como a baixa concentração de glicose no efluente do sistema de reação têm grandes implicações no consumo de água, nos

processos subseqüentes de fermentação e separação, e consequentemente na economia do processo em geral. Esses tópicos foram discorridos em detalhe no capítulo 5, e aqui só se citam alguns trabalhos da literatura que reportam volumes de reação. Na conversão de estilhaços de madeira e palha de milho em etanol via hidrólise enzimática e fermentação simultâneas Wooley et al. (1999) reportam uma serie de 18 reatores CSTR's de 3596 m^3 cada, e Aden et al. (2002) reporta uma serie de 10 CSTR's de 3596 m^3 cada, respectivamente. Uma serie 4 reatores CSTR's de 77.4 m3 cada foi reportado por Shao et al. 2007 para a hidrólise e fermentação simultânea de polpas de papel. Devido às vantagens em termos da diminuição do volume de reação requerido para atingir uma conversão determinada, uma serie de CSTR's tem sido o sistema de reação mais considerado para a hidrólise enzimática. Além da consideração da serie de reatores CSTR's, o desempenho de um reator tubular assim como considerações acerca das restrições de operação que poderia apresentar são discutidos em seguida.

A razão entre o volume de reação de uma serie convencional de 6 reatores CSTR's para os valores de τ mostrados na Tabela 1 (referido na Tabela 1 como estratégia 1) e o volume de reação de um reator PFR que atinge uma conversão de celulose equivalente são mostradas na tabela 3 (referido como estratégia 1). Na medida em que se aumentam os tempos de residência e, por conseguinte o volume de reação, o beneficio é mais notório. Para os reatores com alimentação distribuída assume-se que a corrente que ingressa no PFR é a corrente que sai do último reator com alimentação distribuída, ou seja, para estratégia de operação 2 o PFR recebe o efluente do tanque agitado 2 e para a estratégia de operação 3 o PFR recebe o efluente do tanque agitado 3. Ao igual que na estratégia de operação 1, a inclusão de um reator PFR no sistema oferece a possibilidade de diminuir o volume de reação. Apesar do beneficio em termos de diminuição do volume requerido é menor quando as estratégias de operação 2 e 3 são comparadas com a estratégia 1, considerando que o volume de reação total esperado para os reatores de hidrólise está na ordem dos 1000 m^3, as configurações propostas podem trazer importantes benefícios econômicos para o processo de forma que devem ser avaliadas com maior detalhe.

Tabela 3. Razão entre volumes de reação requeridos para atingir determinada conversão para as estratégias de operação propostas.

τ (h)	**Estratégia**	**$V_{PFR'} / V_{CSTR's}$**
10	1	0.749
	2	0.922
	3	0.957
30	1	0.668
	2	0.855
	3	0.921
50	1	0.521
	2	0.815
	3	0.890

Dentre as dificuldades para a operação do reator tubular destacam-se os grandes volumes de reação que fazem com que o reator tubular seja extremamente longo e a dificuldade para manter em suspensão o material não solubilizado. O primeiro item traz complicações na localização em planta e no controle de temperatura, enquanto o segundo item obriga a pensar alternativas de agitação como os agitadores estáticos propostos neste trabalho e que foram detalhados nos capítulos 6 e 7. Devido a que a concentração de material que não tem sido solubilizado e a que a densidade e a viscosidade da fase líquida variarem ao longo da serie de reatores CSTR's ou ao longo do reator tubular, é de grande importância caracterizar o comportamento reológico do material durante a hidrólise a fim de estudar os requerimentos de agitação (agitadores dinâmicos ou estáticos) e a possibilidade de operar com alimentação distribuída de substrato e/ou enzimas.

Com o intuito de mostrar o impacto positivo do aumento da produtividade volumétrica do reator, foi estudado o consumo de vapor é a área de troca térmica requerida para concentrar soluções de glicose até 15% w/w para uma faixa de concentrações de glicose entre 1% e 8% w/w. O estudo visa fermentar os açúcares produzidos durante a hidrólise do bagaço de cana nas dornas já existentes na indústria para fermentar o caldo de cana.

8.3 Concentração do licor hidrolisado

Foi feito um estudo das condições de operação num evaporador múltiplo efeito adequado para realizar a concentração do licor por meio de simulação utilizando-se o software SuperPro Designer.

As seguintes especificações são necessárias para simulação deste equipamento:

- Temperatura do vapor no primeiro efeito;
- Temperatura da solução no último efeito;
- Escolha da utilidade (vapor, vapor alta pressão);
- Opção de evaporação, dentre as seguintes opções:
  - Concentração final do componente chave,
  - Fração mássica do componente chave,
  - Fração evaporada dos componentes voláteis;
- Número de efeitos;
- Coeficiente de transferência de calor efetivo para cada efeito.

Foram considerados 5 efeitos, o que corresponde ao valor normalmente empregado nas usinas sucroalcooleiras. O coeficiente de transferência de calor para cada efeito foi obtido em Hugot, (1986): 2000, 1400, 1300, 800 e 500 kcal/m²h°C, do primeiro ao quinto efeito, respectivamente. Estes valores, que correspondem aos valores médios mais comuns, levam em consideração a formação de incrustações e são baseados na queda de temperatura aparente. Os valores considerados são semelhantes àqueles obtidos por Higa, (2003).

Um esquema da simulação do evaporador múltiplo efeito é apresentado na Figura 2.

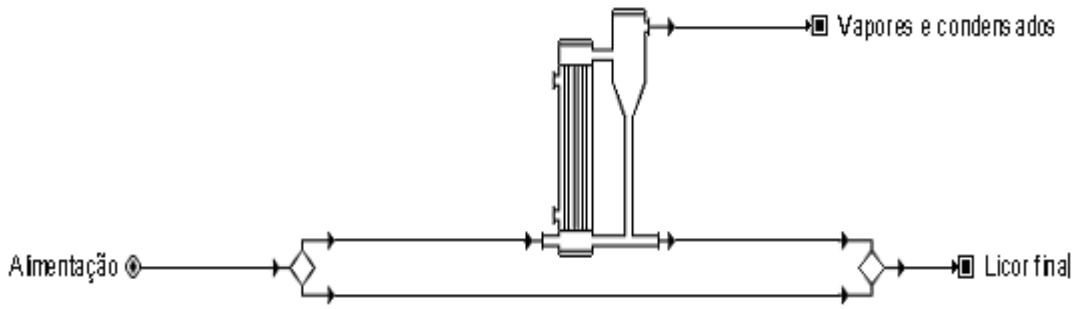

Figura 2. Simulação do evaporador múltiplo efeito para concentração do licor hidrolisado.

Considerou-se que somente uma fração do licor é concentrada, até um valor que varia entre 50 e 65 %; o licor não concentrado é misturado ao licor concentrado, produzindo o licor final.

A corrente de alimentação possui vazão de 10000 kg/h e concentração de 1 a 8 % em massa, e está disponível a 50 °C. Foi realizado um planejamento fatorial considerando-se os seguintes fatores: temperatura do vapor no primeiro efeito, temperatura da solução no último efeito, concentração do licor no licor concentrado. Os níveis dos fatores considerados no planejamento são apresentados na Tabela 4.

Tabela 4. Exemplo de fatores e níveis empregados no planejamento fatorial.

Fatores	**-1**	**0**	**1**
Temperatura no primeiro efeito – T1 (°C)	105	110	115
Temperatura último efeito – T5 (°C)	52	58	64
Teor de glicose no licor concentrado (% massa)	50	57,5	65

Um planejamento do tipo 2^n + ponto central (9 simulações) foi conduzido para as diferentes concentrações da alimentação, de modo a produzir um licor final com teor de 15 % de glicose (massa). Na Tabela 5 é apresentado como exemplo a matriz de planejamento para a simulação da concentração do licor alimentado com 8 % glicose:

Tabela 5. Condições e resultados da simulação da concentração do licor com 8 % glicose (massa).

	T1 (°C)	**T5 (°C)**	**Teor de glicose – licor concentrado (% massa)**	**Consumo de vapor (kg/h)**	**Área de troca por efeito (m²)**	**Concentração do licor final (% m glicose)**
Caso 1	115	64	65	1414,9	56,901	15,0009
Caso 2	115	64	50	1431,2	56,919	15,0011
Caso 3	115	52	65	1387,4	46,143	15,0009
Caso 4	115	52	50	1401,4	46,128	15,0011
Caso 5	105	64	65	1340,2	70,977	15,0009
Caso 6	105	64	50	1354,3	71,005	15,0011
Caso 7	105	52	65	1313,1	54,994	15,0009
Caso 8	105	52	50	1324,9	54,985	15,0011
Caso 9	110	58	57,5	1369,5	55,934	15,0003

O procedimento foi repetido para as diferentes concentrações de alimentação, e os casos que apresentam o menor consumo de vapor associado à menor área de troca térmica para cada uma delas foram selecionados como ótimos. Os resultados são apresentados na Figura 3.

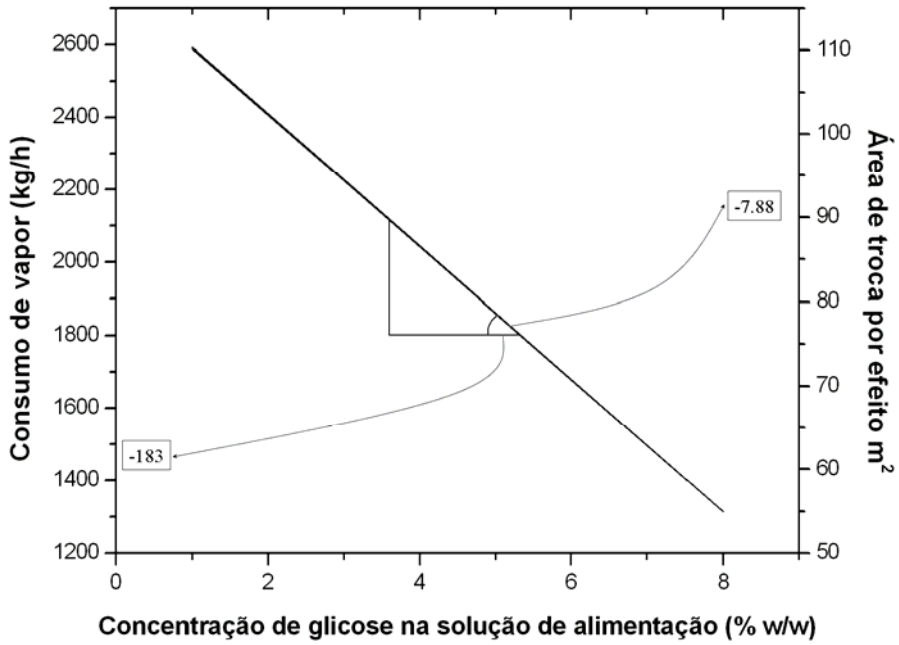

Figura 3. Resultados (consumo de vapor e área de troca térmica por efeito) obtidos para os melhores casos, para as soluções de alimentação com teor de glicose de 1 a 8 % em massa.

8.4 Conclusões

Neste capítulo foram apresentados cálculos preliminares para o volume de reatores contínuos de hidrólise enzimática de bagaço de cana. O procedimento de cálculo não leva em conta considerações sobre agitação e mistura principalmente pela carência de informação acerca da reología do sistema de reação. As concentrações de substrato e as diferentes configurações de reatores contínuos e formas de alimentação foram pensadas para garantir que o sistema pode operar em reatores de tanque agitado convencionais e reatores tubulares com defletores angulares internos. A alimentação distribuída de substrato (livre de água) nos primeiros 3 reatores da serie permite incrementar a produtividade volumetria dos reatores (g glicose/m^3, g xilose/m^3) por um fator de 2.5 aproximadamente quando comparado com a operação convencional. Mas o acumulo de material insolúvel (celulose e xilana não solubilizada, lignina, extrativos, etc.) ao longo da serie com

alimentação distribuída também se incrementa por um fator de 3.8 aproximadamente no terceiro reator da serie e diminui lentamente nos reatores restantes, seja um reator tubular ou uma serie de reatores de tanque agitado. Para uma serie de 6 reatores de tanque agitado com alimentação distribuída de substrato nos primeiros três reatores, o uso de um reator tubular depois dos três reatores de tanque agitado com alimentação distribuída diminui o tempo de residência requerido para atingir uma conversão determinada por um fator 0.96, 0.92 e 0.89 para tempos de residência por reator de 10 h, 30 h e 50 h, respectivamente. Quando considerada a concentração de glicose na corrente que sai dos reatores em evaporadores de múltiplo efeito, é evidente a importância de aumentar a produtividade volumétrica do reator. O consumo de vapor requerido (kg/h) para concentrar a uma corrente de glicose até 15% w/w, diminui num fator de 183 na medida em que a concentração de glicose numa corrente de 10000 kg/h é incrementada em 1% w/w. Para a mesma corrente, a área de troca por efeito diminui num fator de 8 na medida em que a concentração de glicose numa corrente de 10000 kg/h é incrementada em 1% w/w. Dentre os sistemas de reação estudados nesta dissertação, o que apresenta maiores vantagens em termos de produtividade volumétrica e operabilidade em reatores convencionais é uma serie de três reatores de tanque agitado com alimentação distribuída de substrato e enzima seguidos de um reator tubular com defletores angulares internos.

Referências

Aden A, Rith M, Ibsen K, et al. 2002. Lignocellulosic biomass to ethanol process design and economic utilizing co-current dilute acid prehydrolysis and enzymatic hydrolysis for corn stover: NREL, Golden, Co, USA.

Higa, M. 2003. Co-geração e integração térmica em usinas de açúcar e álcool. Universidade Estadual de Campinas, Faculdade de Engenharia Mecânica. Tese de Doutorado.

Hugot E. 1986. Handbook of Cane Sugar Engineering, 3nd Ed. Elsevier Publishing Company, Amsterdam.

Shao X, Lynd L, Wyman C, Bakker A. 2009. Kinetic modeling of cellulosic biomass to ethanol via simultaneous saccharification and fermentation: Part I. Accomodation of intermittent feeding and analysis of staged reactors. Biotechnol Bioeng 102:59-69.

Wen CY, Fan LT. 1975. Models for flow systems and chemical reactors, Marcel Dekker Inc, New York.

Wooley R, Ruth M, Sheehan J, Ibsen K, Majdeski H, Galvez A. 1999. Lignocellulosic biomass to ethanol process design and economic utilizing co-current dilute acid prehydrolysis and enzymatic hydrolysis current and futuristic scenarios: NREL, Golden, Co, USA.

Zheng Y, Zhongli P, Zhang R, Jenkins BM. 2009. Kinetic modeling for enzymatic hydrolysis of pretreated creeping wild ryegrass. Biotechnol Bioeng 102(6):1558-1569.

Capítulo 9 – Sugestões Para Trabalhos Futuros

9.1 Introdução

Na discussão sobre trabalhos futuros o sistema de reação é dividido em duas partes: numa primeira chamada de "zona de alimentação e reação rápida" onde substrato é alimentado e a fração celulósica e de hemiceluloses convertida ao redor de 50% aproximadamente, e uma segunda parte chamada "zona de reação lenta" onde o substrato é convertido até a conversão desejada. Os desafios técnicos e de modelagem na "zona de alimentação e reação rápida" estão relacionados intimamente com a operação à maior concentração de substrato possível, enquanto na zona de "reação lenta" os desafios técnicos e de modelagem estão relacionados com a diminuição do volume de reação e minimização do efeito inibitório dos produtos sobre as enzimas (Figura 1).

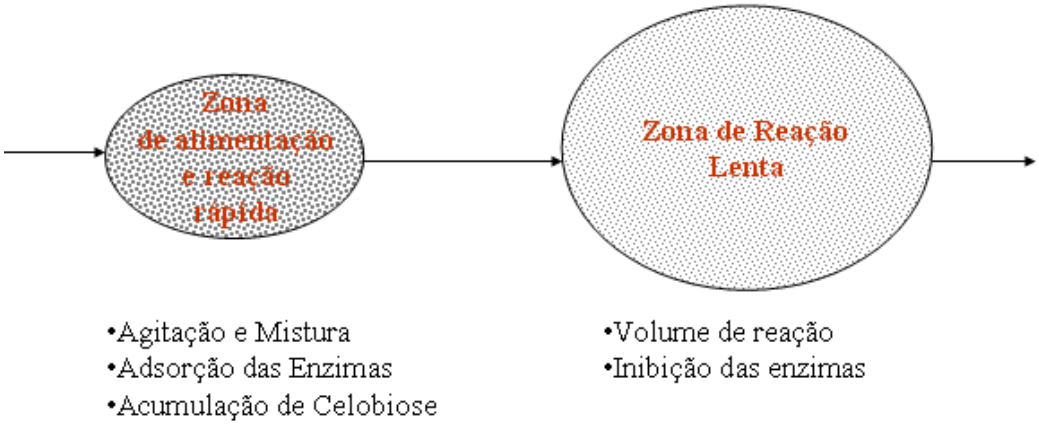

Figura 1. Sistema de reação para a hidrólise enzimática ressaltando as principais barreiras atuais.

Quando o sistema é esquematizado desta maneira, é claro que se devem propor soluções de acordo com os requerimentos de cada uma das etapas. A agitação e a mistura na primeira etapa de reação tem sido foco de vários trabalhos recentes, e algumas propostas encontram-se na literatura. O acúmulo de celobiose, prejudicial para as enzimas celulase, pode ser evitado manipulando a relação celulase/β-glicosidase no sistema e com modos

diferentes de alimentação de enzima. Na zona de reação lenta, embora se tenha uma concentração considerável de sólidos insolúveis, o material pode ser homogeneizado em reatores convencionais com algumas modificações. Em seguida, são resumidos alguns trabalhos relevantes da literatura que mostram opções para o desenvolvimento da tecnologia.

9.2 Zona de alimentação e reação rápida

Reator com retenção de sólidos (South e Lynd, 1994): Foi descrita a modelagem de uma serie de reatores de tanque agitado com retenção de enzima e sólidos. Para uma serie de reatores com retenção de sólidos (tempo de residência dos sólidos = 1.5 vezes tempo de residência do líquido) a modelagem prediz uma diminuição de até 47% no volume de reação quando comparado com um sistema batelada convencional para uma conversão de celulose de 90%. Para um reator de tanque agitado, a distribuição de tempos de residência foi determinada como sendo um reator perfeitamente agitado. Considerou-se que a retenção dos sólidos é uniforme, ou seja, a distribuição de tempos de residência dos sólidos é idêntica para todos os sólidos dentro do reator. O tamanho, forma, e composição das partículas de substrato na corrente que entra no reator de hidrólise definem o tempo de retenção de cada fração devido a que na prática a retenção baseia-se no tamanho de partícula. Não há trabalhos posteriores de modelagem e experimentação desta opção de reatores tanto na modelagem como na experimentação.

Reator tubular com parafuso sem-fim (Borchert e Buchholz, 1987): O autor sugere o uso de reatores tubulares com a maior concentração de substrato possível que evite retro-mistura e não ocasione muito efeito inibitório dos produtos. Foram realizados experimentos com um reator tubular com parafuso sem-fim para o transporte do substrato.

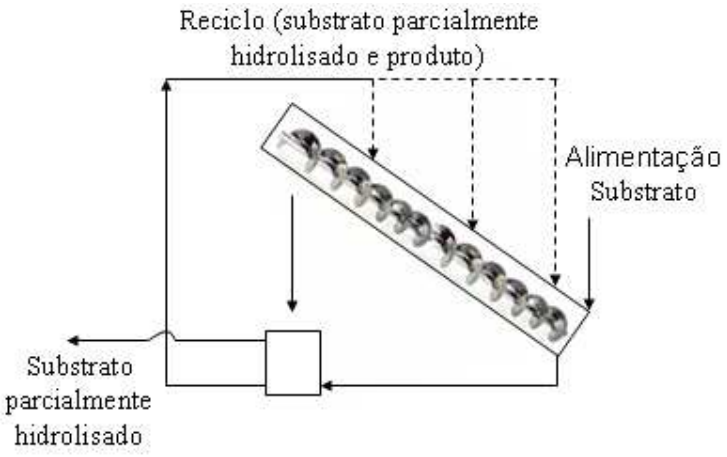

Figura 2. Diagrama do reator tubular com parafuso sem-fim. Modificado de Borchert e Buchhholz, (1987).

<u>*Reator liquefator*</u> *(Mohagheghi et al., 1992)***:** Os experimentos foram realizados num fermentador de frasco rotatório horizontal. Foi testada a hidrólise enzimática da palha de trigo (pré-tratada com ácido diluído) com concentrações de iniciais de celulose no substrato pré-tratado entre 7.5% e 20% w/w. Os resultados da sacarificação e fermentação simultâneas indicaram que a fermentação da celulose em palha de trigo pré-tratada pode ser eficazmente fermentada em etanol para até uma concentração de 15% de celulose (24,4% de concentração de palha pré-tratada).

*Jørgensen et al. (2007)***:** A tecnologia baseia-se em queda livre de mistura empregando um tambor horizontalmente colocado com um eixo horizontal rotativo montado com remadores para a mistura. Foi testada a liquefação e sacarificação enzimática da palha de trigo (pré-tratada com explosão a vapor) com até 40% (w / w) de matéria seca inicial. Em menos de 10 h, a estrutura do material foi alterada a partir de partículas de palha intacta em uma pasta / líquido que pode ser bombeado. Experimentos conduzidos em 2%-40% (w / w) de matéria seca inicial mostraram que a conversão da celulose e hemicelulose diminuem quase linearmente com o aumento da concentração de substrato. Experimentos realizados com sacarificação e fermentação simultâneas também revelaram uma queda na produção de etanol com o aumento da concentração de substrato.

Roche et al. (2009): Experimentos de hidrólise enzimática foram realizados com resíduos de milho (talhos e folhas pré-tratadas com ácido diluído), com uma carga inicial de sólidos insolúveis de 20% (w / w). Os experimentos foram realizados em fermentadores de frasco rotatório horizontal, similares àqueles reportados por Mohagheghi et al. (1992) e

num tambor horizontalmente colocado com um eixo horizontal rotativo montado com remadores para mistura. O esquema é similar ao reportado por Jørgensen et al. (2007). Os sólidos sacarificados liquefazem a ponto de fluir continuamente (Tensão de cisalhamento ≤10 Pa) numa conversão de aproximadamente 20%, após cerca de 2 dias de sacarificação com uma carga enzimática de 2,45-9,8 FPU/g-celulose.

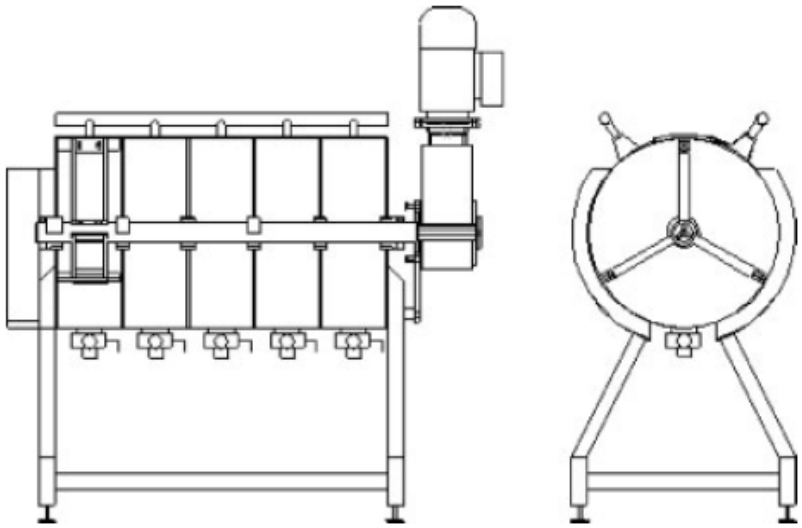

Figura 3. Esquema de um reator liquefator de 5 câmeras (Jørgensen et al., 2007).

Reator semicontínuo (Fan et al., 2003): Conversão de lamas de papel para o etanol via fermentação e sacarificação simultânea foi investigada. A alimentação de substrato e feita em intervalos de 12 h, um tempo de residência de 4 dias e cargas enzimáticas de 15 a 20 FPU / g-celulose. Dois projetos de bioreator foram investigados. O primeiro deles, chamado de "original" deu lugar a considerações adicionais para o projeto de outro, chamado de "adaptado". O projeto adaptado foi operado duas vezes durante um tempo de um mês, os balanços de massa foram fechados com sucesso e se atingiu estado estacionário. Os detalhes do projeto deste reator podem ser consultados na referencia correspondente.

Reatores de tanque agitado com alimentação distribuída de substrato e enzima (discorridos nos capítulos 5 e 8 desta dissertação): Este tipo de operação foi descrito em detalhe neste trabalho. É importante ressaltar que a alimentação distribuída de substrato e enzima pode ser complementada com a retenção dos sólidos. Uma alternativa que não foi

estudada nesta dissertação é uma série de 3 reatores continuous de tanque agitado com alimentação distribuída de substrato e enzima com reciclo do material parcialmente hidrolizado que sai no terceiro reator. Este sistema permite obter altas produtividades volumétricas, embora as conversões finais de substrato sejam baixas.

9.3 Zona de reação lenta

Nesta parte do sistema de reação a maior preocupação é com o excessivo volume de reação como resultado da cinética de reação lenta, e com o efeito inibitório inevitável dos produtos sobre as enzimas. Os dois itens anteriores sugerem que o reator mais conveniente é o tubular ou uma serie de reatores de tanque agitado. O reator tubular assim como uma variante do mesmo (reator tubular com defletores internos) foi estudado em detalhe neste trabalho nos capítulos 4, 5, 6, 7 e 8 desta dissertação e a serie de reatores de tanque agitado foi estudada nos capítulos 4, 5 e 8 desta dissertação.

Com base nas considerações anteriores e nos resultados obtidos ao longo deste trabalho, sugere-se em seguida trabalhos que poderiam ser feitos.

9.4 Sugestões para próximos trabalhos

Como discorrido no capítulo 2 desta dissertação, a modelagem cinética da reação de hidrólise tem sido estudada amplamente e têm sido propostos modelos cinéticos com diverso grau de complexidade os quais podem ser ajustados dependendo da disponibilidade de dados experimentais. O nível de detalhe e domínio de aplicabilidade (concentrações de substrato e enzima) do modelo cinético determina o grau de detalhe no projeto do reator. São necessários estudos na adsorção das enzimas sobre a fração celulósica do substrato e sobre a lignina a fim de estudar estratégias de alimentação e reciclo das enzimas no projeto do reator. Devido à heterogeneidade do sistema de reação, a velocidade inicial de hidrólise é proporcional à enzima adsorvida e não à enzima em solução, o que ratifica a importância dos estudos de adsorção. Zhen et al. (2009) apresentam uma metodologia para incorporar a informação da adsorção num modelo cinético a fim de avaliar o efeito da concentração e distribuição de lignina. O estudo de Zhen et al. (2009) é uma referência importante a ser consultada para iniciar estudos experimentais na adsorção visando a incorporação desta informação num modelo cinético. Outro fator a ser evaluado é a desativação das enzimas,

tanto adsorvidas como em solução, por efeitos térmicos e mecânicos ao fim de determinar um perfil de adição de enzima baseado num modelo cinético. No capítulo 2 foram discorridas varias alternativas para incorporar a desativação das enzimas, tanto adsorvidas como em solução, no modelo cinético.

Um dos aportes deste trabalho é a alimentação distribuída de substrato e enzima em reatores contínuos. A cinética para este tipo de operação é estudada a través de experimentos de batelada alimentada. Mas, o que acontece com a enzima ativa, adsorvida e em solução, e com a reatividade do substrato quando quantidades adicionais de substrato fresco são adicionadas no sistema? É factível minimizar o consumo de enzima por re-adsorção de enzima ativa em substrato fresco durante a batelada alimentada? Como incorporar o efeito de substrato adicional adicionado durante a hidrólise no modelo cinético? Muito mais dúvidas surgem que só podem ser esclarecidas com experimentos de hidrólise enzimática em batelada alimentada, e hidrólise de substrato parcialmente hidrolisado. Metodologias experimentais nessa área foram apresentadas por Kadam et al. (2004), Drissen et al. (2007), Roosgaard et al. (20070 e Zhen et al. (2009).

O modelo cinético usado no projeto de reatores no capítulo 5 e que foi ajustado no capítulo 3 deste trabalho agrupa a concentração de enzima e uma constante de velocidade num parâmetro só chamado de v_m (Capítulo 3, Equação 1). Informação experimental de enzima adsorvida a diferentes cargas enzimáticas é necessária para ajustar o valor da constante de velocidade de forma independente e estudar o efeito da carga enzimática na cinética e no sistema de reação. Como a carga enzimática influencia significativamente o tempo de residência para atingir uma conversão determinada, mas o custo de enzima é um fator limitante da tecnologia, a incorporação do efeito da carga enzimática no modelo permite obter conclusões valiosas acerca da carga enzimática que deve ser utilizada. A desativação das enzimas por efeitos térmicos, efeitos mecânicos, perdida de mobilidade, adsorção irreversible na lignina, etc., deve ser incluída no modelo cinético através de uma taxa global de desativação dependente do tempo de reação ou da conversão de substrato.

Hodge et al. (2009) e Roche et al. (2009) mostraram que além de quantificar a conversão de celulose e hemicelulose é importante considerar as propriedades físicas e reológicas da lama para desenvolver estratégias de alimentação para uma batelada alimentada. A alimentação distribuída apresentada neste trabalho pode ser baseada num modelo que considere as propriedades físicas e reológicas da lama ao invés de uma

estratégia "*ad hoc*". Para tal fim, requer-se o uso de uma expressão para a densidade da fase líquida em função da concentração dos principais açúcares liberados como a apresentada por Weast (1985). Requer-se também da medição da fração de volume ocupada pelos sólidos em suspensão, a qual depende em grande parte da quantidade de líquido associado à partícula sólida assim como da composição do substrato. Roche et al. (2009) apresenta relações empíricas para este parâmetro o que pode ser um ponto de partida para próximos trabalhos. Diferentes modelos têm sido usados para correlacionar a taxa de cisalhamento e a tensão de cisalhamento durante a hidrólise enzimática de substratos lignocelulósicos. Entre eles podemos citar o modelo de Wildemuth-Williams (Roche et al., 2009), o modelo da potencia (Pimenova Hanley, 2003) e o modelo de Casson (Viamajala et al., 2009). Stickel et al. (2009) apresenta um estudo atualizado e detalhado de técnicas de medição de propriedades reológicas de lamas de biomassa. Os estúdios mencionados são imprescindíveis no projeto de reatores para a hidrólise enzimática de bagaço de cana e ainda não se tem esta informação experimental.

Um outro aspecto a ser estudado é o efeito do tamanho de partícula na reação de hidrólise e nas propriedades reológicas da lama. Dasari e Bérgson, (2007) mostraram que a redução do tamanho de partícula diminui os tempos de residência requeridos para atingir uma conversão determinada, e que permitem operar os reatores a maiores cargas de sólidos. Num trabalho mais recente, (Rezania e Bérgson, 2009) mostraram que quando o tamanho de partícula é reduzido abaixo dum determinado valor, a viscosidade aparente do material aumenta ao invés de diminuir como eles esperavam. Viamajala et al. (2009) sugerem que a disponibilidade de água livre (não presa dentro da estrutura do sólido) e consequentemente as propriedades reológicas da lama durante a hidrólise enzimática dependem principalmente da composição química do substrato, da porosidade e do tamanho de partícula.

A fluidodinâmica computacional (CFD) tem sido uma ferramenta de rápida aceitação e amplo uso no projeto de sistemas de reação, como descrito por Ranade (2002). O sistema de reação da hidrólise enzimática pode ser estudado desde dois pontos de vista usando fluidodinâmica computacional: (*i*) como um sistema pseudo-homogêneo onde propriedades físicas como densidade e o modelo reológico são "aparentes", ou seja, refletem o comportamento da mistura sólido líquido e (*ii*) visualizando o sistema como multifásico onde a fração sólida pode ser tratada como partículas o fibras que intercambiam

momento e massa com outras partículas. Estudos recentes aplicam a primeira aproximação a suspensões de biomassa seja em reação (Bérgson et al., 2006, Um e Hanley, 2009) ou transporte (Ventura et al., 2008) e demonstram o potencial do uso da CFD no projeto de equipamentos. A aproximação tomada neste trabalho (Capítulo 7) que assume o sistema como sendo multifásico é mais exigente do ponto de vista computacional e experimental, mas também pode trazer maior informação para o projeto. Este último enfoque exige a medição de coeficientes de arraste em função do tamanho de partícula e da incorporação de um termo no calculo de intercambio de momento entre as fases que leve em conta o efeito de altas concentrações de sólidos na velocidade de sedimentação das partículas como ressaltado por Camenen (2003).

Os campos de velocidade obtidos a partir de fluidodinâmica computacional podem ser usados numa estratégia híbrida que divide o reator em compartimentos interconectados a fim de incorporar a cinética e a transferência de massa no projeto do reator. O modelo de compartimentos é derivado e explicado amplamente por Wen e Fan (1975) e seu possível uso no projeto numa estratégia híbrida que faça uso da informação obtida a través da aplicação de CFD é discutido por Ranade, (2002), Bezzo et al (2000) e Rigopoulos e Jones (2003). Estes estudos possibilitariam o estudo do grau de segregação da mistura e das limitações de transferência e representariam um grande avanço ao respeito dos modelos de macrofluido e microfluido que foram usado no projeto de reatores nos capítulos 4 e 5 desta dissertação.

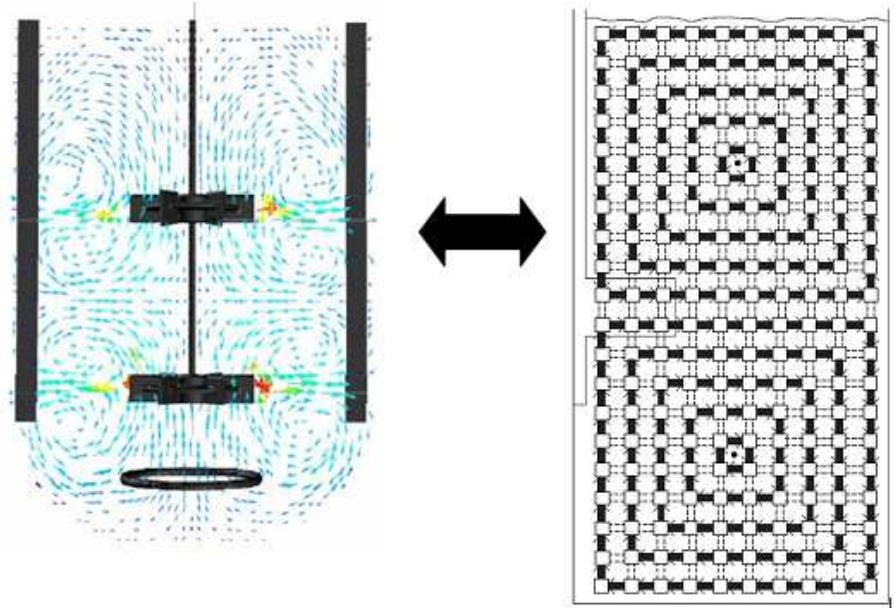

Figura 4. Esquema geral do modelo de compartimentos para integrar CFD, transferência de massa e o modelo cinético no projeto de reatores de hidrólise.

Referencias

Bezzo F, Macchietto S, Pantelides CC. 2000. A general framework for the integration of computational fluid dynamics and process simulation. Comput Chem Eng 24:653-658.

Borchert A, Buchholz K. 1987. Enzymatic hydrolysis of cellulosic materials. Process Biochem 22:173-180.

Berson RE, Dasari RK, Hanley TR. 2006. Modeling of a continuous pretreatment reactor using computational fluid dynamics. Appl Biochem Biotechnol. 129-132:621-630.

Camenen B. 2005. Settling velocity of sediments at high concentrations, in Sediment and Ecohydraulics: INTERCOH 2005.

Dasari RK, Berson RE. 2007. The effect of particle size on hydrolysis reaction rates and rheological properties in cellulosic slurries. Appl Biochem Biotechnol 136-140:289-299.

Drissen R, Maas R, Van-Der-Maarel M, Kabel M, Schols H, Tramper J, Beeftink H. 2007. A generic model for glucose production from various cellulose sources by a commercial cellulase complex. Biocatal Biotransform 25:419-429.

Fan ZL, South C, Lyford K, Munsie J, van Walsum P, Lynd LR. 2003. Conversion of paper sludge to ethanol in a semicontinuous solid-fed reactor. Bioprocess Biosyst Eng. 26:93-101.

Hodge DB, Karim MN, Schell DJ, McMillan JD. 2009. Model-based fed-batch for high-solids enzymatic cellulose hydrolysis. Appl Biochem Biotechnol. 152:88-107Jørgensen H, Vibe-Pedersen J, Larsen J, Felby C. 2007. Liquefaction of lignocellulose at high-solids concentrations. Biotechnol Bioeng. 96:862-870.

Kadam KL, Rydholm EC, McMillan JD. 2004. Development and validation of a kinetic model for enzymatic saccharification of lignocellulosic biomass. Biotechnol prog 20:698-705.

Mohagheghi A, Tucker M, Grohmann K, Wyman C. 1992. High solids simultaneous saccharification and fermentation of pretreated wheat straw to ethanol. Appl Biochem Biotechnol. 33:67-81.

Pimenova NV, Hanley TR. 2003. Measurement of rheological properties of corn stover suspensions. Applied Biochemistry and Biotechnology 105-108:383-392.

Ranade VV, 2002. Computational flow modeling for chemical reactor engineering, 1ª ed., Academic Press, London UK.

Rezania S, ye Z, Berson RE. 2009. Enzymatic saccharification of sawdust slurries following ultrasonic particle size reduction. Appl Biochem Biotechnol. DOI 10.1007/s12010-008-8467-x.

Rigopoulos S, Jones. 2003. A hybrid CFD-reaction engineering framework for multiphase reactor modeling: basic concept and application to bubble column reactors. Chem Eng Sci 58: 3077-3089.

Roche CM, Dibble CJ, Knutsen JS, Stickel JJ. 2009. Particle concentration and yields stress of biomass slurries during enzymatic hydrolysis at high-solids loadings. Biotechnol Bioeng. DOI 10.1002/bit.22381.

Rosgaard L, Andric P, Dam-Johansen K, Pedersen S, Meyer AS. 2007. Effects of substrate loading on enzymatic hydrolysis and viscosity of pretreated barley straw. Appl Biochem Biotechnol. 143:27-40.

South CR, Lynd LR. 1994. Analysis of conversion of particulate biomass to ethanol in continuous solid retaining and cascade bioreactors, Appl Biochem Biotechnol. 45-46: 467-481.

Stickel JJ, Knutsen JS, Liberatore MW, Luu W, Bousfield DW, Klingenberg DJ, Scott CT, Root TW, Ehrhardt MR, Monz TO. 2009. Rheological measurements of a biomass slurry: an inter-laboratory study. Rheol Acta. DOI 10.1007/s00397-009-0382-8.

Um B, Hanley TR. 2007. A comparison of simple rheological parameters and simulation data for *Zymomonas mobilis* fermentation broths with high substrate loading in a 3-L bioreactor. Appl Biochem Biotechnol 145:29-38.

Ventura CAF, Garcia FAP, Ferreira PJ, Rasteiro MG. 2008. CFD simulation of the turbulent flow of pulp suspensions, in Aiche, The 2008 annual meeting.

Viamajala S, McMillan JD, Schell DJ, Elander RT. 2009. Rheology of corn stover slurries at high solids concentrations – Effects of saccharifications and particle size. Bioresour Technol. 100:925-934.

Wen CY, Fan LT. 1975. Models for flow systems and chemical reactors, Marcel Dekker Inc, New York.

Zheng Y, Zhongli P, Zhang R, Jenkins BM. 2009. Kinetic modeling for enzymatic hydrolysis of pretreated creeping wild ryegrass, Biotechnol Bioeng 102(6):1558-1569

Apêndice A – Modelamento e Simulação de Reatores Continuos Para a Hidrólise Enzimática de Biomassa Lignocelulósica com um Modelo Cinético de Três Reações

1. Kinetic Model

The semimechanistic three-reaction kinetic model developed, fitted and validated by Zheng et al. (2009) was used in this work. This kinetic model incorporates adsorption of cellulase and β-glucosidase enzymes on cellulose and lignin, competitive inhibition of cellulase and β-glucosidase enzymes by glucose and cellobiose, and substrate reactivity. The substrate, creeping wild ryegrass pretreated with dilute sulfuric acid, was composed of 53% w/w cellulose and 38% w/w lignin (dry basis). The kinetic model was fitted and validated under an initial substrate concentration ranged from 4%-12% w/w, enzyme loading ranged from 15-150 FPU/g-cellulose (cellulase), and 15-150 CBU/g-cellulose (β-glucosidase), background glucose 30 and 60 g/L, and background cellobiose 10 g/L. Cellulase and β-glucosidase enzymes had respective activities of 90 FPU/mL and 490 CBU/mL, corresponding to 54 and 65 mg protein/mL. A simplified reaction scheme of the kinetic model is depicted in Figure 1.

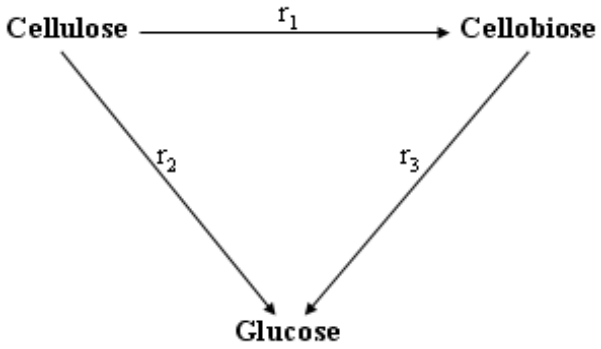

Figure 1. Simplified reaction scheme for modeling cellulose hydrolysis. Modified from Zhen et al. (2009).

Mass balances on cellulose, cellobiose and glucose, Equations 1, 2 and 3, respectively, were established as follow:

$$\frac{dC}{dt} = -r_1 - r_2 \tag{1}$$

$$\frac{dG_2}{dt} = 1.056r_1 - r_3 \tag{2}$$

$$\frac{dG}{dt} = 1.1116r_2 + 1.053r_3 \tag{3}$$

The kinetic rate equations r_1, r_2 and r_3, along with the estimated kinetic parameters, are reported in Appendix A.

2. Accommodation of distributed feeding

Four "*ad hoc*" operation strategies with continuous distributed feeding of substrate and enzyme in a series of CSTR's were modeled, simulated and compared in terms of cellulose conversion and, cellobiose and glucose yields with two operations with continuous feeding of substrate and enzyme only at the first reactor of the series. It was considered that cellulase and β-glucosidase enzymes are supplemented at each substrate addition to maintain the initial enzyme loading. Substrate fed along the series of CSTR's was assumed as free of water, however the modeling approach presented here remains useful even if wet substrate is fed. The cumulative substrate concentration along the series of CSTR's in the operation strategies with distributed feeding was calculated by taking the basis of calculation (mass flow) at the outlet of the last reactor with distributed feeding, and assuming that the mass of substrate fed in each reactor is the same. Figure 2 depicts a scheme of the series of reactors with continuous distributed feeding, and Table 1 summarizes the cumulative substrate concentration at the first three reactors of the series for each feeding strategy.

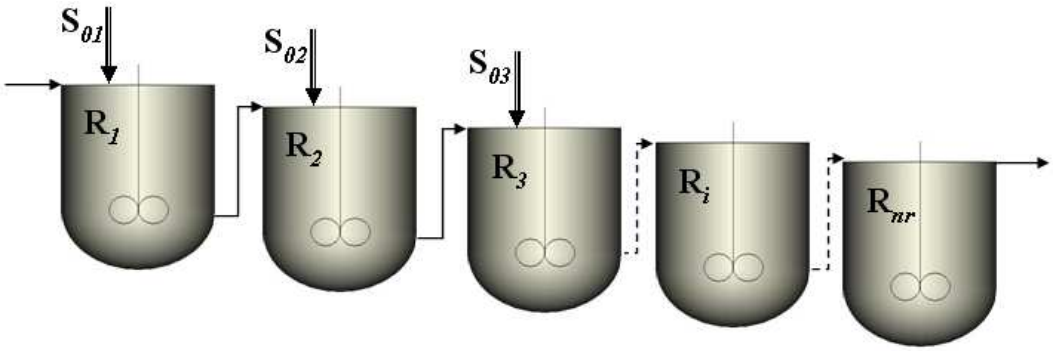

Figure 2. Schematic diagram of the configuration of reactors proposed (double lines represent points of continuous feeding of substrate and enzymes).

Table 1. Cumulative substrate concentration at the first three reactors of the series for different operating strategies

Feeding Strategy	**Cumulative substrate concentration (% w/w, dry basis)**		
	R_1	R_2	R_3
1	5	5	5
2	5.26	10	10
3	10	10	10
4	5.56	10.5	15
5	10.5	15	15
6	11.1	15.8	20

Each feed addition that takes place simultaneously at the first reactors of the series gives rise to a new substrate population *j* (*j* varies from 1 to 3). Mass balances on cellulose, cellobiose and glucose adapted to include the effects of distributed feeding, are represented by Equations 4, 5 and 6, respectively.

$$\frac{dC_j}{dt} = -r_{1j} - r_{2j} \tag{4}$$

$$\frac{dG_2}{dt} = 1.056\sum_{j=1}^{np} r_{1j} - r_3 \tag{5}$$

$$\frac{dG}{dt} = 1.1116\sum_{j=1}^{np} r_{2j} + 1.053 r_3 \tag{6}$$

were *np* is the number of substrate populations in each reactor which depends on the feeding strategy and the location of the reactor in the series. The system of differential equations solved to find the concentration of cellulose, cellobiose and glucose along the series is made up of *j* equations similar to equation 4 that correspond to the disappearing of each substrate population present, and Equations 5 and 6 that correspond to the cellobiose and glucose production rates, respectively.

3. Reactor modeling

The following assumptions were necessaries for modeling: isothermal and steady state operation, the mean residence time of the suspension in each reactor (τ) is the same and reactors are well mixed in the macroscopic sense. An important issue to be addressed here is the implications of the classic assumption of well mixed reactors. 12 to 15% w/w is often considered the upper value of initial substrate concentrations at which lignocellulosic biomass can be mixed and hydrolyzed in conventional stirred tank reactors (Kistensen et al., 2009). In addition, it is usually feasible to achieve well-mixed conditions in turbulent stirred vessels unless the reactions are very fast such as acid-base neutralizations. If the blend time is small compared to the residence time in the reactor, the reactor can be considered well-mixed (Paul et al., 2004). The maximal initial substrate concentration at the first reactor considered here was 10% w/w and the mean residence time by reactor (τ) considered was ranged from 10 h to 50 h.

Flowing material is in some state of aggregation, depending on its nature. A single-phase system lies between the extremes of microfluid and macrofluid. A stream of

solids always behaves as a macrofluid (Levenspiel, 1999). At the beginning of the enzymatic hydrolysis of lignocellulosic biomass, the volume of the reactor is occupied by liquid-swollen particles which collapse and release continuous phase as cellulose is hydrolyzed. So, at the beginning of the reaction the material behaves as a macrofluid (South et al., 1995) and a gradual evolution to microfluid is expected with the progress of the reaction. Çakal et al. (2007) studied a solid-liquid reaction in a series of 4-CSTR's and found out that the conversion predicted by the macrofluid model was closed to experimental values for the first reactor of the series, whereas the conversion predicted by the microfluid model was closed to experimental values for the third and fourth reactors. The prediction of cellulose conversion for the limiting situations of macrofluid and microfluid constitute an initial frame for initial calculations in the performance of CSTR's for the enzymatic hydrolysis of lignocellulosic biomass and are presented below.

3.1 Macrofluid model

For a well mixed series of *n*-CSTR's the RTD function is given below (Levenspiel, 1999):

$$E = \frac{t^{nr-1}}{(nr-1)!}\exp(-\frac{t}{\tau}) \tag{7}$$

where t is the reaction time and nr the number of reactors of the series.

The RTD function of substrate population j at the outlet of reactor i is given by Equation 8:

$$E_{i,j} = \frac{t^{nr_j-1}}{(nr_j-1)!}\exp(-\frac{t}{\tau}) \tag{8}$$

were nr_j is the number of reactors between the feeding point of substrate population j and reactor i.

The cellulose concentration of substrate population *j* at the outlet of reactor *i* ($C_{i,j}$) was expressed in terms of the kinetic model modified to include the effects of continuous distributed feeding (Equations 4, 5 and 6) and its RTD function (Equation 8) as follow:

$$C_{i,j} = \int_{t=0}^{t\to\infty} C_j E_{i,j} dt \tag{9}$$

where C_j is the cellulose concentration of substrate population *j*. To ensure an adequate range of residence times, the time-integral of each RTD function (Equation 8) was numerically evaluated, and the maximal value of Δt ($\Delta t \approx dt$) that guarantees a minimal value of 0.999 for each time-integral was used for the numerical evaluation of Equation 9.

3.2 Microfluid model

For reactor *i* in the series, the mass balances of cellulose for substrate population *j* and the mass balances of cellobiose and glucose were expressed respectively as follow:

$$C_{i-1,j} - C_{i,j} - \tau(r_{1j} + r_{2j}) = 0 \tag{10}$$

$$G_{2i-1} - G_{2i} + \tau(\sum_{j=1}^{np} 1.056 r_{1j} - r_3) = 0 \tag{11}$$

$$G_{i-1} - G_i + \tau(\sum_{j=1}^{np} 1.1116 r_{2j} + 1.053 r_3) = 0 \tag{12}$$

4. Results and discussion

An An economical number of reactors in a series of CSTR's is often 3 to 6 since the benefits of reduced volume may be out-weighed by the increased cost of multiple agitators, pumps and controls if a large number of reactors is used (Perry, 1999). In this

work, a series of 10-CSTR's was considered to be an appropriate number of reactors to study the operation with continuous distributed feeding of substrate and enzyme.

A model-based feeding profile of substrate and a feeding profile of enzyme other than supplementation to maintain the initial enzyme loading were not considered. A model-based feeding profile of substrate requires relating the progress of the reaction with solids concentration and yield stress. Significant advances in this area have been recently published (Roche et al., 2009), however the semi-empirical relations obtained cannot be applied to any substrate. On the other hand, the catalytic action of enzymes in this solid-liquid system is mediated by various factors such as adsorption and desorption, deactivation by thermal and mechanical effects, inhibition by cellobiose and glucose, accumulation of lignin, changes in the accessibility of cellulose, etc. As a consequence, it is not possible to calculate a feeding profile of enzyme based on mass balances of enzymes and the kinetic model used in this work.

Figure 3 illustrates the predicted cellulose conversion along the series when substrate and enzyme are continuously is added only at the first reactor. For each vertical line, the top indicates the prediction of the macrofluid model, the bottom indicates the prediction of the microfluid model and the central symbol indicates the mean. Results show that for a given residence time by reactor (τ) cellulose conversion along the series predicted by the macrofluid model is greater than the conversion predicted by the microfluid model. But, the predictions of both models get closer to each other as the number of reactors and the residence time by reactor are increased. Cellulose conversion along the series exhibits an upward trend, but tends toward a constant value at the end of the series. When the conversion profile along the series for an initial substrate concentration of 5% w/w is compared with the conversion profile for an initial substrate concentration of 10% w/w, is manifest that a higher cellulose conversion is reached with a less number of reactors to the extent that the initial substrate concentration diminish. Glucose concentration at the outlet of the series of 10-CSTR's for residence times by reactor of 10, 30 and 50 h reach values up to 26.4, 28.2 and 28.6 g/L for an initial substrate concentration of 5% w/w, and 51.3, 55.6 and 56.8 g/L for an initial substrate concentration of 10%, respectively. So, continuous distributed feeding of substrate and enzyme would be an option to be explored to increase

the initial substrate concentration that can be handled in continuous reactors, and consequently the volumetric productivity of the reaction system.

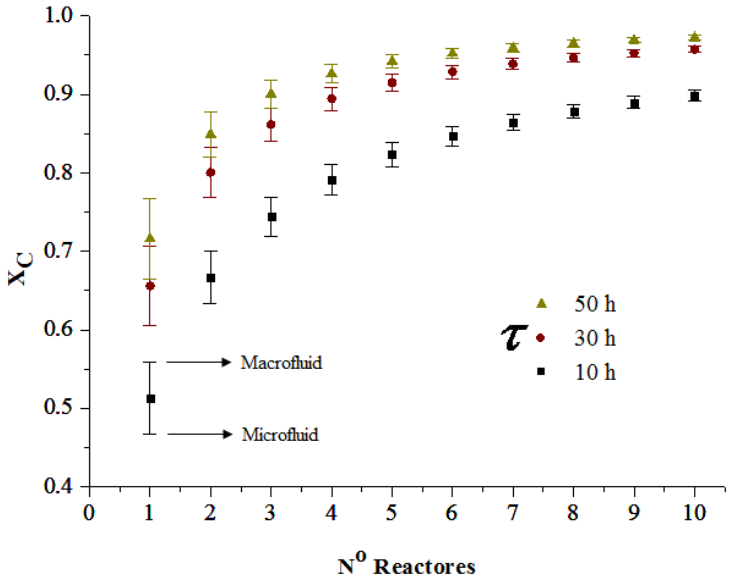

a)

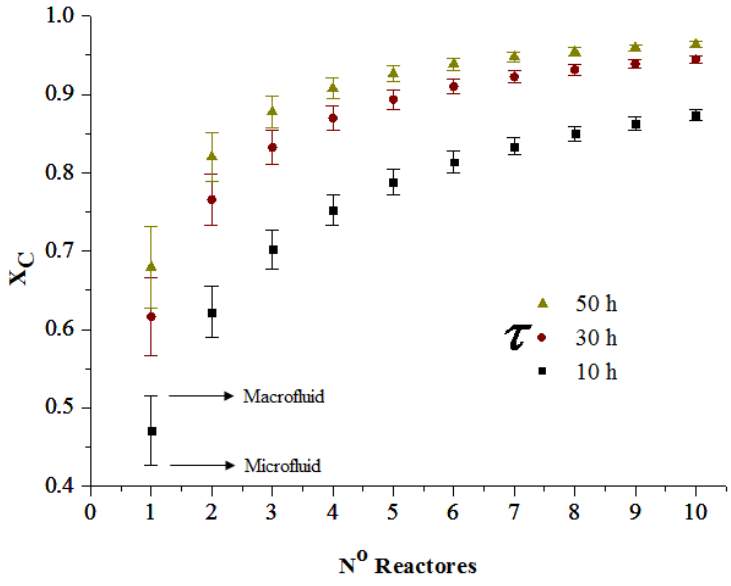

b)

Figure 3. Cellulose conversion profiles along the series of CSTR's for the operation with continuous feeding at the first reactor of the series. Initial substrate concentration a) 5%, b) 10% w/w (dry basis)

Figure 4 shows cellulose conversion along the series when substrate is continuously fed at the first two reactors to reach a cumulative substrate concentration of 10% w/w. Cellulose conversion exhibits a decrease at the second reactor due to the addition of substrate at this reactor, and in subsequent reactors is lower than the conversion reached when an equivalent concentration of substrate is added at the first reactor (Figure 3b). Nevertheless, for a series of five or more than five reactor the series with continuous distributed feeding reaches cellulose conversions similar to those achieved when an equivalent concentration of substrate is added at the first reactor. Results indicate that the operation with continuous distributed feeding does not offer advantages in terms of cellulose conversion when compared with the operation with continuous feeding only at the first reactor of the series. The main reason for this result is that for the operation with continuous distributed feeding cellobiose concentration reaches higher values in the second and third reactor (Figure 6a) and as a consequence the inhibitory effect in these reactors is higher. It is important to highlight that the kinetic model adapted to include the effects of distributed feeding does not consider the effects of additional populations of substrate on enzyme adsorption and substrate reactivity at subsequent reactors. These factors can be evaluated by fed-batch experiments to improve the kinetic model.

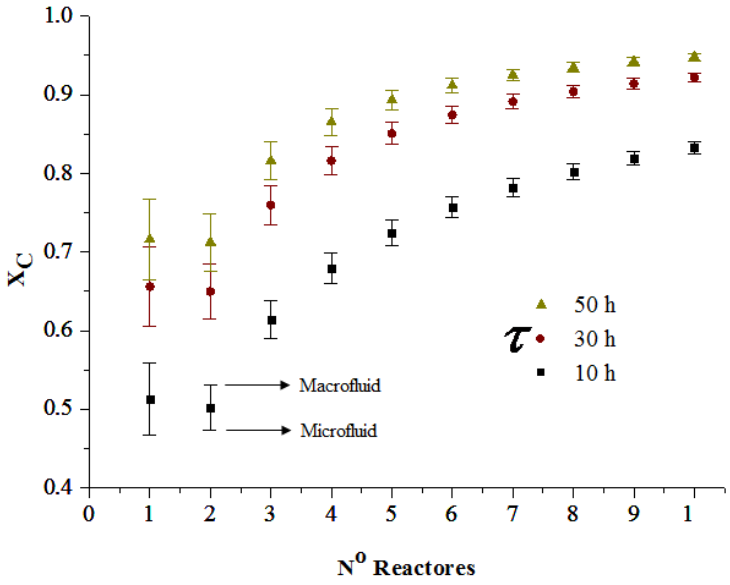

Figure 4. Cellulose conversion profiles along the series of CSTR's for the operation with continuous distributed feeding at the first two reactors of the series. Cumulative substrate concentration 10% w/w (dry basis)

Figure 5 shows cellulose conversion along the series when substrate is continuously fed at the first two reactors (Figure 5a) and at the first three reactors (Figure 5b) of the series to reach a cumulative substrate concentration of 15% w/w. As in the previous cases, distributed feeding of substrate in more reactors does not increase cellulose conversion. However, the operation with continuous distributed feeding has the potential to increase substrate concentrations beyond the concentrations that can be handled in the operation with continuous feeding only at the first reactor, without significant detriment on cellulose conversion. This issue has important implications in the economy of the process as was already discussed in the introduction. An alternative configuration of reactors to reduced the required reaction volume to achieve a given cellulose conversion would be a tubular reactor from the outlet of the last CSTR with continuous distributed feeding. However, must be considered that there is a portion of the substrate that remains as insoluble solids and accumulates along the series, which can lead to mixing difficulties in tubular reactors.

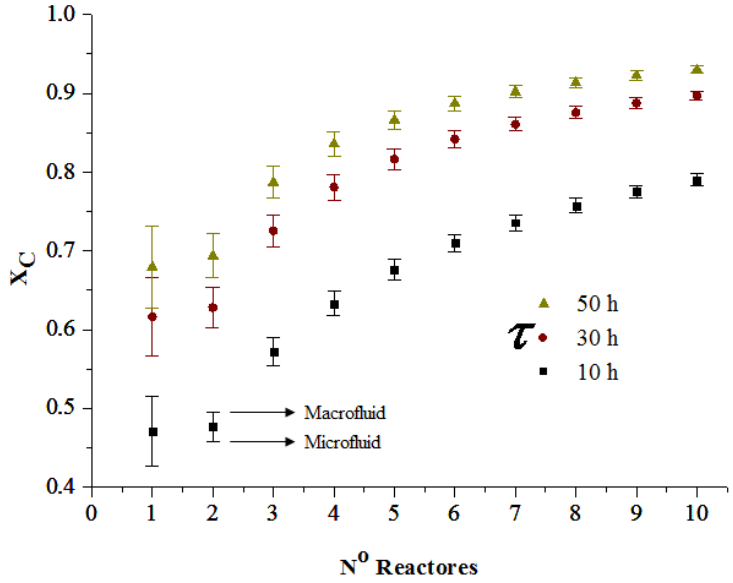

a)

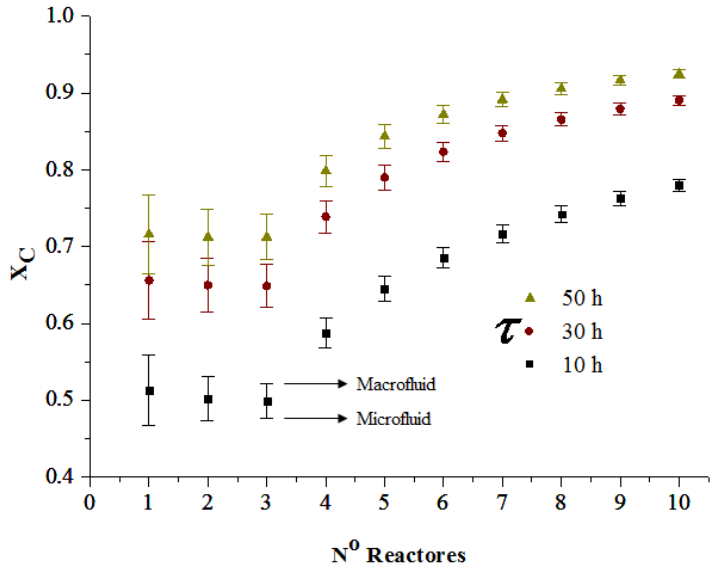

b)

Figure 5. Cellulose conversion profiles along the series of CSTR's for the operation with continuous distributed feeding, a) at the first two reactors, b) at the first three reactors. Cumulative substrate concentration 15% w/w (dry basis)

According to Kristensen et al. (2009), event in the absent of mixing constraints, the conversion linearly decreases with increased initial substrate concentration and

inhibition of enzyme adsorption by final products appears to be the main cause. For the series of CSTR's, the decreasing conversion at increasing initial substrate concentration is evident when analyzing cellulose conversion in a point of the series for the different strategies for continuous feeding proposed here. Figure 6a shows the mean cellulose conversion (calculated from predictions of the macrofluid and microfluid model) at the outlet of the sixth reactor of the series for cumulative substrate concentrations ranged from 5% to 15% w/w, corresponding to the feeding strategies 1, 2 and 4 in Table 1, which have initial substrate concentrations at the first reactor of the series around 5% w/w, and a similar mass of substrate entering in the subsequent reactors. On the other hand, Figure 6b shows the same results for cumulative substrate concentrations ranged from 10% to 20% w/w, corresponding to the feeding strategies 3, 5 and 6 in Table 1, which have initial substrate concentration around 10% w/w at the first reactor, and around a half of this mass entering in subsequent reactors. Despite the difference in insoluble solids, cellulose conversion shows a similar downward trend at increased cumulative substrate concentration. This decrease in yield is undesirable as it offsets the advantages of working at high solid levels. However, adsorption of enzyme and consequently conversion would be increased in the operation with continuous distributed feeding due to the lower instantaneous substrate concentration along the series.

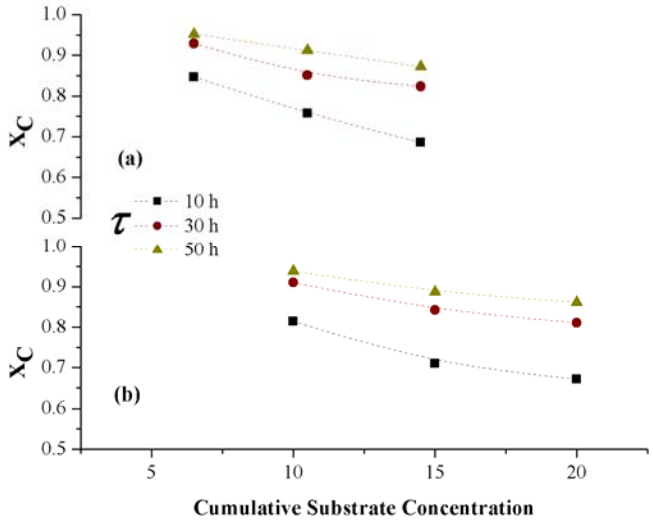

Figure 6. Decreasing conversion at increasing cumulative substrate concentration at the sixth reactor of the series for the feeding strategies of Table 1.

The mean concentration of cellobiose (calculated from predictions of the macrofluid and microfluid models) at the first three reactors of the series and the mean glucose concentration at the sixth and tenth reactors of the series, are depicted in Figure 7. When substrate is continuously added only at the first reactor of the series, the cellobiose concentration profile along the series exhibits a downward trend. For the operations with continuous distributed feeding, cellobiose concentration increases up to the last reactor with distributed feeding, and decreases along the remaining reactors. Cellobiose has been implicated as a strong inhibitor of β-glucosidase activity (Bezerra et al., 2006) therefore its concentration along the series should be kept as lower as possible. Cellobiose accumulation along the series of CSTR's with continuous distributed feeding could be minimized by adjusting cellulase and β-glucosidase loadings in reactors with continuous distributed feeding. It is worth noticing in Figure 6b that glucose concentration at the sixth reactor of the series is 90%, 94% and 96% of the concentration achieved at the tenth reactor of the series for residence times by reactor of 10 h, 30 h and 50 h, respectively.

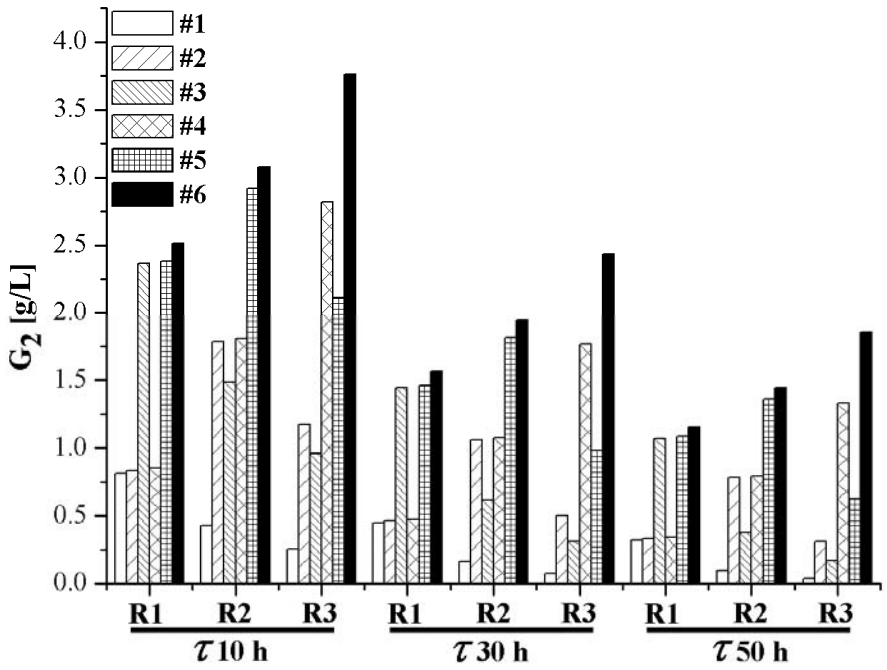

a)

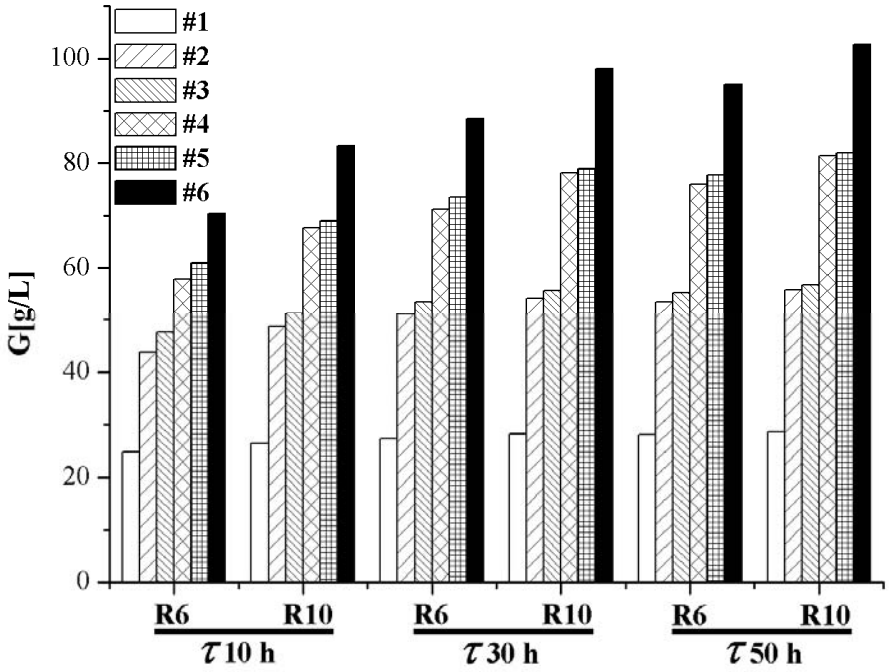

b)

Figure 7. Mean concentration of a) cellobiose in the first three reactors of the series and b) glucose at sixth and tenth reactors (Symbol # indicate the feeding strategy as enumerated in Table 2)

Compared to a batch or fed-batch operation, an operation with continuous distributed feeding of substrate and enzymes offers important potential advantages as reduced labor costs and heat exchanger demands due to greater automation, reduced vessels down time for cleaning and filling and improve the effectiveness of utilizing expensive enzymes (for instance, β-glucosidase loading could be reduced in a continuous system because cellobiose production slows with conversion). Also, separate saccharification and fermentation might be advantageous because of the ability to operate the continuous system at the respective optimal temperatures of each process. Despite the study of south et al. (1995) there are no experimental results for continuous conversion of lignocellulosic biomass to ethanol to be compared with batch or fed-batch studies, however a recent review

presents current knowledge of continuous processes for enzymatic hydrolysis of lignocellulosic biomass (Brethauer and wyman, 2009) and the base case scenarios for large scale lignocellulosic ethanol production consist of continuous multiples stages (Aden et al., 2002; Wooley et al., 1999). It is important to highlight that fed-batch simultaneous enzymatic hydrolysis and fermentation has allowed to increase ethanol concentration above 4% w/w (Lu et al., 2007; Tomás-Pejó et al., 2009, Li et al., 2009; Zhang et al., 2009), the lower limit on ethanol concentration suggested in the literature to make and economically feasible process (Fan et al., 2003; Wingren et al., 2003). Assuming and ethanol yield of 0.5 g/g-glucose (Jørgensen et al., 2007), the continuous feeding strategy 6 in Table 2 fits this requirement. However, the required total residence time and enzyme loading to reach this glucose concentration can vary for other pretreated substrates.

5. Conclusions

The kinetic model of the enzymatic hydrolysis of lignocellulosic biomass developed, fitted and validated by Zheng et al. (2009) was extended to accommodate continuous distributed feeding of substrate and enzymes. This model was used for a modeling and simulation study considering the micromixing limiting situations of macrofluid and microfluid in a series of CSTR's. The macrofluid and microfluid models allowed to obtain the upper and lower limits of cellulose conversion along the series assuming the reactors like well mixed in a macroscopic sense. Cellulose conversion predicted by the macrofluid model is greater than the predicted by the microfluid model and shows significant differences for the first three reactors of the series, but the predicted cellulose conversions get closer to each other as the number of reactors and the residence time by reactor are increased. According to published experimental results (South et al., 1995; Çakal et al., 2007) a gradual evolution from macrofluid to microfluid is expected to the extent that the material flows throughout the series of CSTR's.

Despite continuous distributed feeding does not show advantages in terms of conversion when compared with an operation where an equivalent mass of substrate is fed at the first reactor of the series, it has the potential to increases substrate concentration beyond those concentrations that can be handled in a conventional series of CSTR's and as

a consequence the volumetric productivity of the reaction system. While these results are encouraging, experimental work is essential to elucidate relevant aspects such as reutilization of enzymes by readsorption on fresh substrate, feeding strategies of enzymes to minimize cellobiose accumulation, the influence of additional population of substrate on enzyme adsorption, and the effect of substrate particle size and composition on the rheological properties of biomass slurries. To further exploit the modeling approach proposed here, semi-empirical relations that connect the progress of enzymatic hydrolysis of lignocellulosic biomass with insoluble solid concentration and yield stress must be developed and used along with the kinetic model to obtain a model-based continuous distributed feeding.

6. Appendix A1

The Langmuir isotherm for endoglucanase/cellobiohydrolase adsorption on pretreated substrate which contains cellulose and lignin is given below:

$$\frac{E_{1b}}{S} = \frac{E_{1\max} K_{1ad} E_{1f}}{1 + K_{1ad} E_{1f}} \tag{13}$$

The Langmuir isotherm for endoglucanase/cellobiohydrolase and β-glucosidase adsorption on lignin was expressed as follow:

$$\frac{E_{1bL}}{L} = \frac{E_{1\max L} K_{1adL} E_{1fL}}{1 + K_{1adL} E_{1fL}} \tag{14}$$

$$\frac{E_{2bL}}{L} = \frac{E_{2\max L} K_{2adL} E_{2fL}}{1 + K_{2adL} E_{2fL}} \tag{15}$$

The amount of endoglucanase/cellobiohydrolase adsorbed on lignin was calculated as follow:

$$E_{1bC} = E_{1b} - E_{1bL} \tag{16}$$

Cellulose-to-cellobiose reaction:

$$r_1 = \frac{k_{1r} E_{1bC} C}{1 + \left(G_2 / K_{1IG_2}\right) + \left(G / K_{1IG}\right)} R_S \tag{17}$$

$$R_S = \alpha \frac{C}{C_0} \tag{18}$$

Cellulose-to-glucose reaction:

$$r_2 = \frac{k_{2r} E_{1bC} C}{1 + \left(G_2 / K_{2IG_2}\right) + \left(G / K_{2IG}\right)} R_S \tag{19}$$

Cellobiose-to-glucose reaction:

$$r_3 = \frac{k_{2r} E_{2fL} G_2}{K_{3M}\left[1 + \left(G / K_{3IG}\right)\right] + G_2} \tag{20}$$

Table 2. Estimated kinetic parameters of the reaction rate equations (Zheng et al., 2009)

E_{1max}	42.55 (mg protein/g substrate)
E_{1maxL}	86.07 (mg protein/g lignin)
E_{2maxL}	173.5 (mg protein/g lignin)
K_{1ad}	0.6 (L/g protein)
K_{1adL}	0.51 (L/g protein)
K_{2adL}	0.75 (L/g protein)
k_{1r}	16.5 (L/gh)
K_{1IG2}	0.04 (g/L)
K_{1IG}	0.1 (g/L)
k_{2r}	7.1 (L/gh)

K_{2IG2}	132.5 (g/L)
K_{2IG}	0.01 (g/L)
k_{3r}	267.6 (h^{-1})
K_{3M}	25.5 (g/L)
K_{3IG}	2.1 (g/L)
A	1.007

Nomenclature

C	cellulose concentration at a given time (g/L)
C_0	cellulose concentration in pretreated substrate (g/L)
E	residence time distribution function (dimensionless)
E_{1b}	bound concentration of endoglucanase/cellobiohydrolase (EG/CBH) on substrate (g protein/L)
E_{1bC}	bound concentration of EG/CBH on cellulose content in substrate (g protein/L)
E_{1bL}	bound concentration of EG/CBH on lignin (g protein/L)
E_{2bL}	bound concentration of β-glucosidase on lignin (g protein/L)
E_{2fL}	concentration of free β-glucosidase in solution when lignin is contained in substrate
E_{1max}	maximum mass of EG/CBH that can adsorb on a unit mass of substrate (mg protein/g substrate)
E_{1maxL}	maximum mass of EG/CBH that can adsorb on a unit mass of lignin (mg protein/g lignin)
E_{2maxL}	maximum mass of β-glucosidase that can adsorb on a unit mass of lignin (mg protein/g lignin)
G	glucose concentration (g/L)
G_2	cellobiose concentration (g/L)
i	Subscript that indicates a reactor in a series of CSTR's
j	Subscript that indicates a population of substrate
K_{1ad}	dissociation constant for EB/CBH adsorption/desorption reaction with substrate (L/g protein)
K_{1adL}	dissociation constant for EB/CBH adsorption/desorption reaction with lignin (L/g protein)
K_{2adL}	dissociation constant for β-glucosidase adsorption/desorption reaction with lignin (L/g protein)
k_{1r}	reaction rate constant for cellulose-to-cellobiose (L/gh)
k_{2r}	reaction rate constant for cellulose-to-glucose (L/gh)
k_{3r}	reaction rate constant for cellobiose-to-glucose (h^{-1})
K_{1IG}	inhibition constant of glucose on enzymes for cellulose-to-cellobiose (g/L)
K_{2IG}	inhibition constant of glucose on enzymes for cellulose-to-glucose (g/L)
K_{3IG}	inhibition constant of glucose on enzymes for cellobiose-to-glucose (g/L)
K_{1IG2}	inhibition constant of cellobiose on enzymes for cellulose-to-cellobiose (g/L)
K_{2IG2}	inhibition constant of cellobiose on enzymes for cellulose-to-glucose (g/L)
K_{3M}	substrate (cellobiose) saturation constant (g/L)
L	lignin content concentration (g/L)

nr	number of reactors
np	number of substrate populations
r_1	cellulose-to-cellobiose reaction (g/Lh)
r_2	cellulose-to-glucose reaction (g/Lh)
R_3	cellobiose-to-glucose reaction (g/Lh)
SR	substrate reactivity (dimensionless)
T	elapse time during enzymatic hydrolysis (h)
X_C	cellulose conversion
α	a constant (dimensionless)
τ	residence time by reactor (h)

References

Aden A, Ruth M, Ibsen K, Jechura J, Sheehan J, Wallace K, Montague L, Slayton A, Lukas J (2002) Lignocellulosic biomass to ethanol process design and economics utilizing co-current dilute acid pre-hydrolysis and enzymatic hydrolysis of corn stover. National Renewable Energy Laboratory, Golden CO, NRTL/TP-510-32438

Ballesteros I, Oliva JM, Saez F, Ballesteros M (2001) Ethanol production from lignocellulosic byproducts of olive oil extraction. Appl Biochem Biotechnol. 91-93:237-252

Ballesteros M, Oliva JM, Manzanares P, Negro MJ, Ballesteros I (2002) Ethanol production from paper material using a simultaneous saccharification and fermentation in a fed-batch basis. World J Microbiol Biotechnol. 18:559-561

Bezerra RMF, Dias AA, Fraga I, Pereira AN (2006) Simultaneous ethanol and cellobiose inhibition of cellulose hydrolysis studied with integrated equations assuming constant or variable substrate concentration. Appl Biochem Biotechnol. 134:27-38

Brethauer S, Wyman Charles (2009) Review: Continuous hydrolysis and fermentation for cellulosic ethanol production. Bioresour Technol. Doi:10.1016/j.biortech.2009.11.009

Çacal GO, Eroğlu I, Özkar S (2007) Simulation of continuous boric acid slurry reactors in series by microfluid and macrofluid models. J Crystal Growth. 306:240-247

Cara C, Moya M, Ballesteros I, Negro MJ, González A, Ruiz E (2007) Influence of solid loading on enzymatic hydrolysis of steam exploded or liquid hot water pretreated olive tree biomass. Process Biochem. 42:1003-1009

Fan ZL, South C, Lyford K, Munsie J, van Walsum P, Lynd LR (2003) Conversion of paper sludge to ethanol in a semicontinuous solid-fed reactor. Bioprocess Biosyst Eng. 26:93-101

Jørgensen H, Vibe-Pedersen J, Larsen J, Felby C (2007) Liquefaction of lignocellulose at high-solids concentrations. Biotechnol Bioeng. 96:862-870

Kristensen JB, Felby C, Jørgensen H (2009) Yield-determining factors in high-solids hydrolysis of lignocellulose. Biotechnol Biofuels. Doi 10.1186/1754-6834-2-11

Levenspiel O (1999) Chemical Reaction Engineering. New York: John Wiley & Sons Inc.

Li H, Kim N, Jiang J, Wong Kang J, Nam Chang H (2009) Simultaneous saccharification and fermentation of lignocellulosic residues pretreated with phosphoric acid-acetone for bioethanol production. Bioresource Technol 100: 3245-3251

Lu Y, Wang Y, Xu G, Chu J, Zhuang Y, Zhang S (2008) Influence of high solid concentration on enzymatic hydrolysis and fermentation of steam-exploded corn stover biomass. Appl Biochem Biotechnol. DOI: 10.1007/s12010-008-8306-0

Perry RH, Green DW, Maloney JO (1999) Chemical Engineering Handbook. New York. McGraw Hill. 7-17p

Paul LE, Atiemo-Obeng VA, Kresta SM (2004) Handbook of industrial mixing Science and Practice. John Wiley & Sons Inc, New Jersey

Roche CM, Dibble CJ, Knutsen JS, Stickel JJ (2009) Particle concentration and yields stress of biomass slurries during enzymatic hydrolysis at high-solids loadings. Biotechnol Bioeng. DOI 10.1002/bit.22381

Rosgaard L, Andric P, Dam-Johansen K, Pedersen S, Meyer AS (2007) Effects of substrate loading on enzymatic hydrolysis and viscosity of pretreated barley straw. Appl Biochem Biotechnol. 143:27-40

South CR, Hogsett DAL, Lynd LR (1995) Modeling simultaneous saccharification and fermentation of lignocellulose to ethanol in batch and continuous reactors. Enzyme Microb Technol. 17:797-803

Tomás-Pejó E, Oliva JM, González A, Ballesteros I, Ballesteros M (2009) Bioethanol production from wheat Straw by the thermotolerant yeast Kluyveromyces marxianus CECT 10875 in a simultaneous saccharification and fermentation fed-batch process. Fuel 88:2142-2147

Viamajala S, McMillan JD, Schell DJ, Elander RT (2009) Rheology of corn stover slurries at high solids concentrations – Effects of saccharifications and particle size. Bioresour Technol. 100:925-934

Wald S, Wilke CR, Blanch HW (1984) Kinetic of enzymatic hydrolysis of cellulose. Biotechnol Bioeng. 26:221-230

Wingren A, Galbe M, Zacchi G (2003) Techno-economic evaluation of producing ethanol from softwood: Comparisson of SSF and SHF and identification of bottlenecks. Biotechnol Prog. 19:1109-1117

Wooley R, Ruth M, Sheehan J, Ibsen K, Majdeski H, Galvez A (1999) Lignocellulosic biomass to ethanol process design and economics utilizing co-current dilute acid pre-hydrolysis and enzymatic hydrolysis: current and futuristic scenarios. National Renewable Energy Laboratory, Golden CO, NRTL/TP-580-26157

Zhang M, Wang F, Su R, Qi W, He Z (2009) Ethanol production from high dry matter corncob using fed-batch saccharification and fermentation after combined pretreatment. Bioresour Technol. Doi 10.1016/j.biortech2009.11.010

Zheng Y, Zhongli P, Zhang R, Jenkins BM (2009) Kinetic modeling foer enzymatic hydrolysis of pretreated creeping wild ryegrass. Biotechnol Bioeng. 102:1558-1569

Zwietering, T (1959) The degree of mixing in continuous flow systems. Chem Eng Sci 11:1-15